Comparison of High- and Low-LET Radioimmunotherapy

in

HER-2 positive Carcinomas

By

Nasir Abbas

Department of Radiation Biology

Institute of Cancer Research-The Norwegian Radium Hospital,

Oslo University Hospital

Oslo University Hospital

HELSE SØR-ØST

Radiumhospitalet
Comprehensive Cancer Center

Series of dissertations submitted to the
Faculty of Medicine, University of Oslo
No. 1478

ISBN 978-82-8264-210-1

Cover: Inger Sandved Anfinsen.
Printed in Norway: AIT Oslo AS.

Produced in co-operation with Akademika publishing.
The thesis is produced by Akademika publishing merely in connection with the thesis defence. Kindly direct all inquiries regarding the thesis to the copyright holder or the unit which grants the doctorate.

Acknowledgements

Thanks to God who has created (everything) and proportionated it.

The work of this thesis was carried out at the Department of Radiation Biology, The Norwegian Radium Hospital, Oslo university Hospital, Oslo, Norway, between 25-3-2008 to 31-08-2012. This study was financially supported by the South-Eastern Norway Regional Health Authority from March 2008 to March 2012 and by Radiumhospitalets Legater from April to August 2012. I am deeply grateful for this financial support.

I would like to express my gratitude and thanks to my principle supervisor Dr. Jostein Dahle, for letting me work in the exciting field of Radioimmunotherapy. Many of the ideas to the experiments were his. As a medical doctor, jumping into the field of Radiation Biology was not an easy task. But, Jostein, your positive attitude and invaluable help in every part of my work, from experimental to data analysis and in writing manuscripts and thesis, is unforgettable. It was impossible for me to complete my PhD without your help. In addition, attending international conferences and having dinners with you was not only learning but was also a fun. Thank you Jostein!

I am also deeply thankful to my co-supervisor Professor Dr. Øyvind Sverre Bruland for always being inspiring and helpful. I particularly appreciate his kindness for giving me time for discussions and ideas despite a busy schedule. Your critical comments especially in writing manuscripts and thesis were always helpful. You have inspired me to seek a future career in oncology.

My thanks further extend to Algeta ASA, for preparing and providing me with ^{227}Th-trastuzumab. My work could not be carried out without their participation. I would also like to say thanks to the people working at Algeta for dinner parties in international conferences. Special thanks to Lars Abrahamsen for comments to the manuscripts.

Also thanks to my co-authors, Jan Nesland, Helen Heyerdahl, Ellen Brevik and Jørgen Borrebæk. It was a good experience to work with you guys. Thanks also to Roy H. Larsen for being not only a co-author in a review article but also sharing some interesting ideas at social gatherings.

I am also very thankful to Anne Kristine Hjelmerud, Katrine B. Melhus, and Camilla Mollatt for their technical assistance in the lab and animal department. Thanks also to my group members Erta Kalanxhi and Ada Repetto for a nice company.

In the last, i want to pay my regards to my mother Ghulam Fatima and father Abdul Hameed for their love, care and prayers which strengthen me. Thanks also to my little family, my son Shawez, daughter Alina, and my wife Sadaf, for understanding my work and not complaining for my duty hours. Thanks also to my brothers and sister back home and all my friends for their love and support.

Oslo, August 2012
Nasir Abbas

1 Abbreviations

α	**Alpha particle radiation**
β	**Beta particle radiation**
Ab	**Antibody**
ADCC	**Antibody dependent cellular toxicity**
ALT	**Alanine Aminotransferase**
ALP	**Alkaline Phosphatase**
AST	**Aspartate Aminotransferase**
AUC	**Area under the curve**
BUL	**Blood Urea level**
CDC	**Complement dependent cytotoxicity**
CDR	**Complementarity determining regions**
^{60}Co	**Cobalt 60**
Fab	**Fragment antigen-binding**
Fc	**Fragment crystallisable**
FDA	**Food and Drug Administration**
HAMA	**Human anti-mouse antibody**
HER2	**Human epidermal growth factor receptor**
IgG	**Immunoglobulin type G**
I.P.	**Intraperitoneal**
I.V.	**Intravenous**
LET	**Linear Energy Transfer**
MAb	**Monoclonal antibody**
MTA	**Maximum Tolerated Activity**
MTD	**Maximum Tolerated Dose**
NK-Cells	**Natural killer cells**
OC	**Ovarian carcinoma**
RIC	**Radioimmunoconjugate**
RIT	**Radioimmunotherapy**
RBE	**Relative biological effectiveness**
S.C.	**Subcutaneous**
x-ray	**X -radiation**

2 List of publications

This thesis is based on the following papers

Paper 1. Experimental α-particle radioimmunotherapy of breast cancer using ^{227}Th-labeled p-benzyl-DOTA-trastuzumab. Nasir Abbas · Helen Heyerdahl · Øyvind S. Bruland · Jørgen Borrebæk · Jahn Nesland · Jostein Dahle. EJNMMI Research 2011, 1:18 (24 August 2011)

Paper 2. Preclinical evaluation of ^{227}Th- and ^{177}Lu-labeled-trastuzumab in mice with HER-2 Positive Ovarian Cancer Xenografts. Nasir Abbas · Øyvind S. Bruland· Ellen Mengshoel Brevik · Jostein Dahle. Nucl Med Commun. 2012 Aug; 33(8):838-4

Paper 3. Comparison of ^{227}Th- and ^{177}Lu-labeled-trastuzumab in mice with HER-2 Positive Breast cancer Xenografts. Nasir Abbas · Helen Heyerdahl[1] · Øyvind S. Bruland · Ellen Mengshoel Brevik · Jostein Dahle.
Submitted to PLoS ONE (PONE-D-12-20637).

3 Introduction

Surgery and external radiation therapy (ERT) are the main treatment modalities for primary (localized) tumors. No curative treatment is available for a large number of patients with metastatic adenocarcinomas (e.g. breast and ovarian carcinoma) and squamous cell carcinomas. Chemotherapy is often the only option when overt metastases are evident. Treatment aim is prolongation of symptom free survival. When micrometastases are present, adjuvant chemotherapies are in several cases shown to improve overall survival and are used either alone or as a part of combined treatment regimens. Despite dose limiting toxicity and low specificity of chemotherapy, prolonged survival can be achieved in a subset of patients. Hence, new treatment modalities (e.g. molecularly targeted therapies, immunotherapy, radioimmunotherapy (RIT), or gene therapy) are being developed to selectively target the tumor tissue cells and stromal components with lower normal tissue injury.

The aim of RIT is specific tumor cell killing with less collateral damage to the surrounding tissue. The aim of this thesis is to test RIT in the form of ^{227}Th-DOTA-trastuzumab in mouse models of human breast and ovarian cancers.

3.1 Radioimmunotherapy (RIT)

RIT can simply be defined as antibody guided radiation therapy. This is an administration of monoclonal antibodies or their derived constructs after chemical conjugation to therapeutic radioisotopes. In this way, either alpha- or beta-particle emitting radionuclides are predominantly delivered to tissues bearing the target antigen.

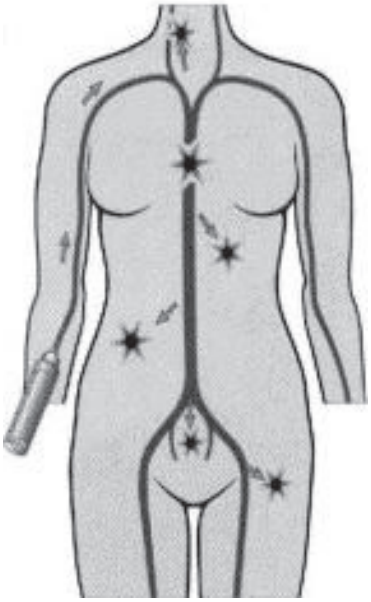

Figure 1: Principles of RIT. Systemic injection of radionuclides attached to antibodies that bind to tumor cell and selectively irradiates these cells. A radionuclide can either be an alpha or beta emitter.

3.1.1 Monoclonal antibodies

Monoclonal antibody is a Y shaped structure with two Fab domains and one Fc domain. The two Fab domains, the variable regions of antibody, are responsible for the specific binding to the target antigen. The Fc domain, the constant region, is responsible for the activation of various component of the immune system.

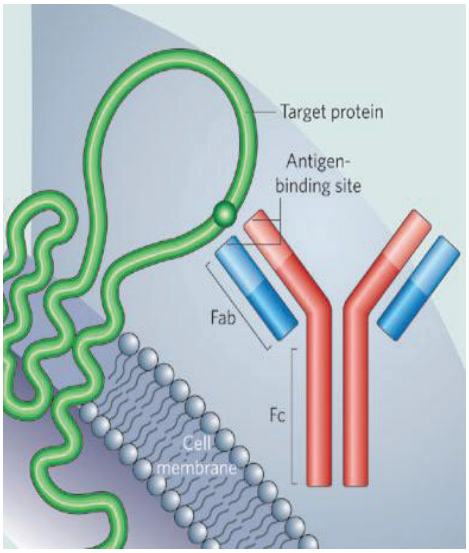

Figure 2: Y shaped structure of antibody. The Fc domain consists of the constant part of the two heavy chains (dark red), while the Fab domains consists of the variable part of the heavy chain (red) and the light chain (blue). The antibody binds to the specific epitope of the target protein.

3.1.1.1 Development of monoclonal antibodies

Paul Ehrlich (1854-1915), Nobel Prize holding German scientist, along with Emil Behring proposed a magic bullet as the treatment of infections [1]. Their ideas not only revolutionized the fields of immunology and histology but eventually also led to the invention of chemotherapy and radioimmunotherapy. Georges Kohler (1946-1995) and Cesar Milstein (1927-2002) shared the Nobel Prize in 1984 on their work of developing the hybridoma

technology for producing antibodies of a single specificity. However, patients treated with mouse antibodies developed human anti-mouse antibody (HAMA) response. This is a hypersensitivity reaction due to the production of human antibody against the administered murine antibody. In order to reduce HAMA, chimeric antibodies were designed through fusion of the variable region of the mouse antibody with the constant region of a human antibody. HAMA response was further decreased by developing humanized antibodies, retaining only the complementarity-determining region (CDRs) of the murine Ab, while more recent methods have generated fully human monoclonal antibodies (Figure 3) [2-5].

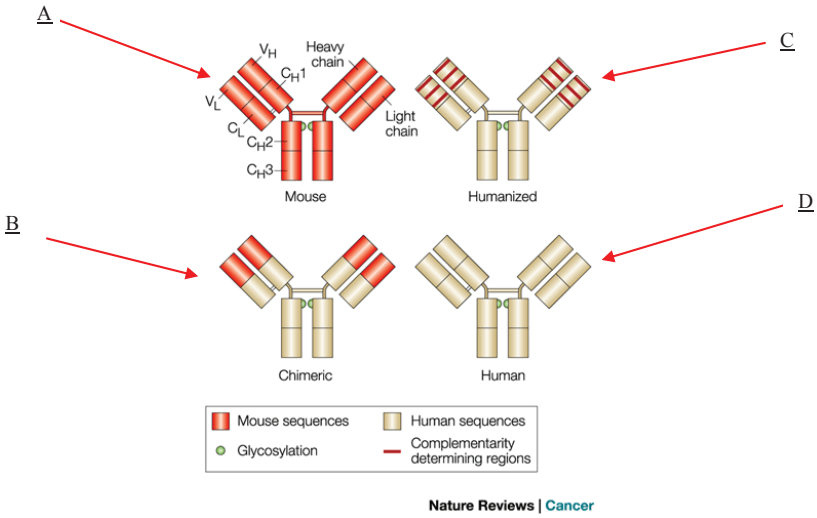

Figure 3: Most important types of antibodies used in radioimmunotherapy and immunotherapy. A) Mouse antibody with heavy chains and light chains and constant region. B) Chimeric antibody with replaced constant regions of mouse antibody by their human analogous. C) Humanized antibody with 90 to 95 % human. D) Fully human antibody (IgG) [6].

Clinical research based on monoclonal antibody therapy as a single agent or as a delivery vehicle for radionuclides was triggered due to development of humanized monoclonal antibodies. Many pharmaceutical companies are intensely involved in to improve the production of human monoclonal antibodies. The first humanized monoclonal antibody, trastuzumab (Herceptin), gained FDA approval in 1998 and recently reviewed [7].

3.1.1.2 Mechanism of action of therapeutic antibodies

Monoclonal antibodies as a single agent can exert cytotoxic effects on tumor cells after binding to their corresponding antigen. Antigen antibody complex leads to the stimulation of two major pathways, immune mediated cell killing and inhibition of intracellular growth signals. Immune mediated pathway involves effector cells like the natural killer (NK) cells or macrophages or the complement system. Effector cells bind to the Fc domain of the antibody, which is attached to its corresponding antigen, kill the tumor cell either via lysis or phagocytosis (Figure 4). This mechanism is called antibody dependent cellular cytotoxicity (ADCC). The activation of the complement cascade triggers the release of chemotactic factors which ultimately form the membrane attack complex and lyse the tumor cells (Figure 4). This mechanism is called complement dependent cytotoxicity (CDC). Growth inhibitory action of an antibody results when the antibody blocks the binding of a ligand to a growth factor receptor.

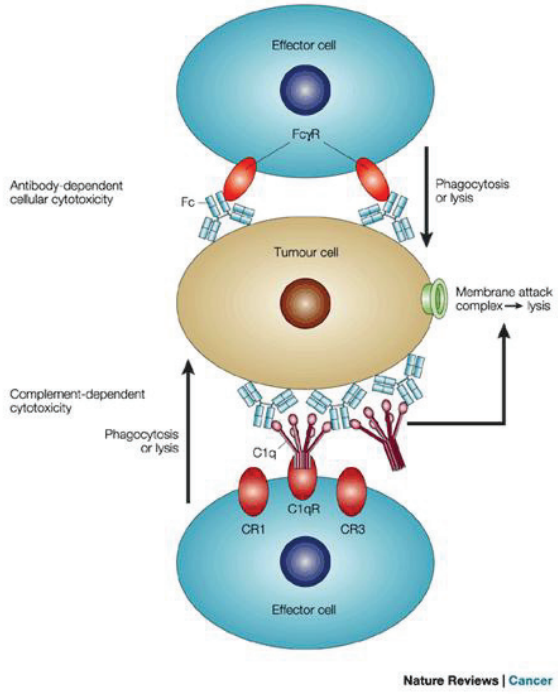

Figure 4: Mechanism of action of therapeutic monoclonal antibodies. The binding of mAb to the tumor cell results in immune effector cell migration to their binding site and initiation of complement cascade. Tumor cell death occurs either via phagocytosis or lysis [6].

3.1.1.3 Trastuzumab (Herceptin®)

Trastuzumab (Herceptin®, Hoffmann-La Roche) binds to the HER2 (Human Epidermal Growth Factor Receptor) receptor blocks the HER2 mediated down-stream signals, which are responsible for cell proliferation and growth, as shown in figure 5. As mentioned above, trastuzumab also initiate immune mediated cell killing (Figure 4).

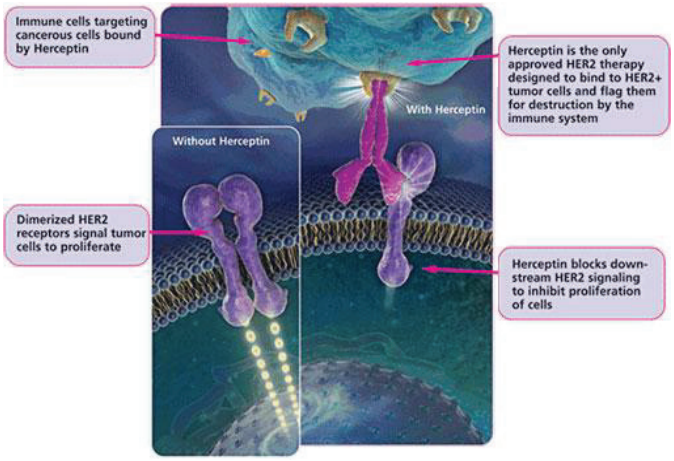

Figure 5: Mechanism of action of trastuzumab (Herceptin). HER-2 receptors on the tumor cell send proliferative signals from the plasma membrane to the nucleus of the cell and are responsible for the growth and proliferation of tumor cells. Trastuzumab not only blocks the HER2 signals but also flag the cells for destruction by the immune system [6].

Trastuzumab, as a single agent or with chemotherapy, is approved for the patients with HER-2 expressing metastatic breast cancer. In these patients, trastuzumab treatment resulted in a response rate of 12-35 % and in combination with paclitaxel or anthracyclines, the response rate increased to 40 % - 60 % [7, 8]. Trastuzumab is also showing clinical activity as monotherapy in phase I/II trial in women with HER-2 positive metastatic ovarian cancer [9, 10].

HER2 is a membrane of the human epidermal growth factor receptor family that consist EGFR (ErbB-1/HER1), HER2 (ErbB-2) HER3 (ErbB-3) and HER4 (ErbB-4). They comprise of an extracellular cellular ligand binding domain and an intracellular domain which is responsible for protein-tyrosine kinase activity. These receptors mediate cell growth, differentiation and survival. Overexpression of EGFR and HER2 has often been associated with malignant transformation and therefore can be considered as potential targets for targeted therapies [11, 12].

Trastuzumab temporarily stops the tumor growth, when given alone, and the tumor continues to grow if the delivery of the drug is stopped. This suggests that HER2 expressing tumors could probably be treated in a much better way if trastuzumab carries toxic material like radionuclides or if used along with chemotherapy [11, 12].

One of the necessities of a successful targeted therapy (RIT or Immunotherapy) is that the metastatic or disseminated tumors express the target antigen to a similar extent as the corresponding primary tumor. It has been seen that in growth factor receptor family, the receptor expression at primary tumor are similar to the receptor expression at their corresponding metastatic tumor sites [11, 12].

It has also been documented that the HER2 receptors are weekly expressed in critical normal organs, like liver and various epithelial tissue, and therefore has become a favorable target for RIT and immunotherapy. Use of trastuzumab as a carrier for either alpha- or beta-emitting radionuclides may enhance the effect of the treatment and thus may also allow treatment of patients with lower HER-2 overexpression [11, 13].

3.1.2 Structure of radioimmunoconjugates

A radioimmunoconjugate is typically made by attaching a metallic radionuclide to an antibody with the help of a bi-specific chelating agent. The chelator can be covalently linked to lysine residue of the antibody (Figure 6). For halogen radionuclides like 131-I, 125-I and 211-At, other chemical linkers are used. Halogens can also be directly bound to tyrosine residues on the antibody after first being oxidized.

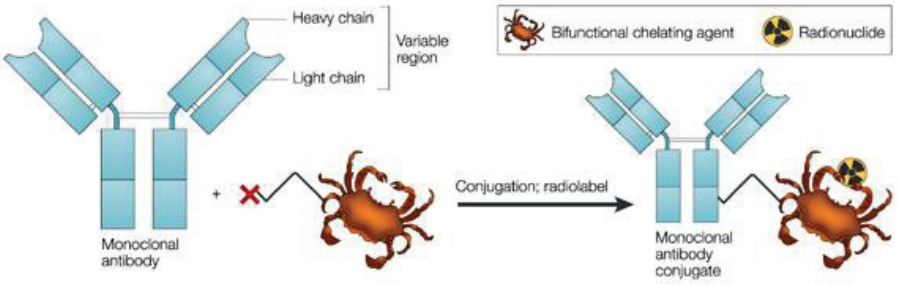

Figure 6: Formation of radioimmunoconjugate. Using a chelating linker, first a chelating agent is covalently bound to the antibody. Then the chelator binds (chelates) a radionuclide, making a complete radioimmunoconjugate [14].

The chelators are used by two different approaches in RIT; pre-labeling and post-labeling. In post labeling approach, a chelating agent is first conjugated to the antibodies before its radiolabeling. In pre-labeling approach, a chelator is first labeled with the radionuclides and then conjugated to antibodies. We have used both methods for ^{227}Th, but post labeling turned out to give the best labeling yields and stability [15].

Due to diverse properties and coordination chemistry of radionuclides, it is difficult to design a chelating agent which can bind to all radionuclides. Bifunctional chelating agent development is dependent on making different derivatives from three well defined inorganic chemistry chelating agents; EDTA, DOTA and DTPA. The most common form of chelators that are being used in RIT is either DOTA or DTPA derivatives and their structures have shown

in figure 7. EDTA derivatives were first developed as bifunctional chelating agent for ^{131}I and ^{90}Y, but their limited stability led to the development of bifunctional DTPA derivatives. Refinements of these DTPA derivatives led to the creation of CHX-A DTPA which has been reported to form stable complexes with ^{131}I, ^{177}Lu and ^{213}Bi. This bifunctional chelating agent was used in first clinical trial of using ^{213}Bi and ^{90}Y is now part of the commercially available radioimmunoconjugate Zevalin.

However, CHX-A DTPA complex with ^{111}In, ^{177}Lu and ^{213}Bi was less stable than for ^{90}Y. Therefore, DOTA derivatives were developed for complexing ^{111}In, ^{86}Y, ^{90}Y, ^{177}Lu, ^{213}Bi, ^{212}Pb and ^{225}Ac. DOTA complexes are generally more stable than DTPA. However, limitation of DOTA use is related to its slow complex formation rates which compromise radiolabeling yields, efficiency and specific activity. This problem can be overcome by increasing temperature provided the conjugate product is heat tolerant.

The field of bifunctional chelating agent development from DTPA, DOTA and as well from others chemical agents is still advancing but it seem little chance of further advancement in the stability of DTPA and DOTA [16].

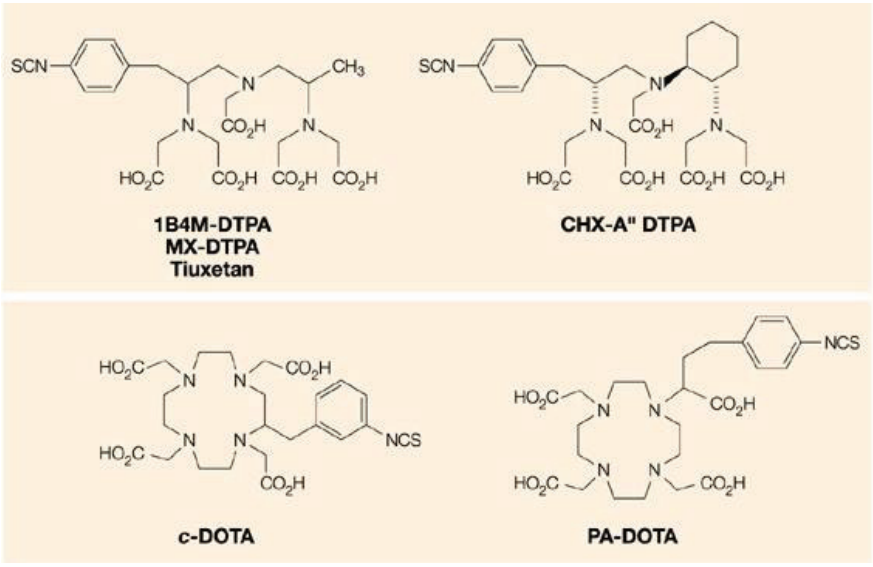

Figure 7 Structure of bi-functional chelating agents [14].

3.1.3 Mechanisms of action in RIT

The binding of antibody alone to antigen starts multiple mechanisms of tumor cell killing, including ADCC and complement system activation, as explained above (see 3.1.1.2). Radiolabeled antibody has two advantages over antibody as single agent; 1) Tumor cells not expressing the antigen or with unreachable antigen can still be targeted by the radiation emitted by the radionuclides (Figure 8 and 9). 2) Antibody -or drug -resistant tumor cells may be sensitive to radiation.

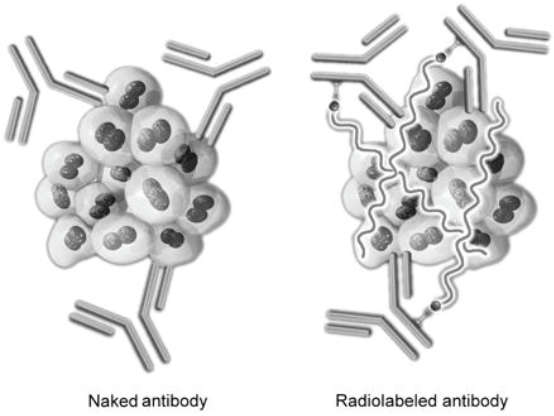

Figure 8: Mechanism of action of radioimmunotherapy
Radiolabeled antibody therapy has an advantage (right) " with crossed fire" over naked or single agent antibody therapy (left) due to killing of cells without binding to their corresponding antigen [17].

The efficacy of RIT depends on number of factors, including the properties of targeted antigen (specificity, density, availability, shedding and heterogeneity of expression) tumor vasculature (degree of vascularization, blood flow and permeability) the monoclonal antibody (specificity, immunoreactivity, stability and affinity) and the properties of chosen radioisotopes (emission characteristics and half life) [18].

Type of emission is an important physical property of a radionuclide which determines the severity of biological effects. Before describing the mechanism of interaction of radionuclides with absorbent or medium through which they pass, it is necessary to understand

the concept of ionization. When radiation energy is sufficient to eject one or more orbital electrons from atom or molecule of absorbing medium, the process is called ionization and the radiation is called ionizing. The process of ionization is produced either directly or indirectly. Charged particles are directly ionizing radiation [19].

Radiobiology is the study of action of ionizing radiation on living things. Directly ionizing radiation, in the form of radionuclide (RIT), principally damages the DNA. In addition to DNA, mitochondria, lipid membrane and some death receptor in the cell membrane can also be targeted by radionuclides. Two major types of DNA damage are produced in RIT; 1) single strand DNA breaks (SSB), 2) double strands DNA breaks (DSB). Grossly, radiation induced biological changes can be divided into lethal, sublethal and potentially lethal with different out comes. Lethal changes are always irreversible and results always in cell death. Sublethal changes can be repaired and are not deadly for the cells, but more than one sub-lethal damage in a short time can be transformed into a lethal damage. Potentially lethal damage to DNA will normally lead to cell death but if the cell gets enough time, the damage can be repaired. RIT may also kill tumor cells by bystander effects, the killing of cells not hit by direct radiation but by signals from irradiated cells. Further more particulate radiations can hit different regions of cell which may give different out come (Figure 9) [20-22].

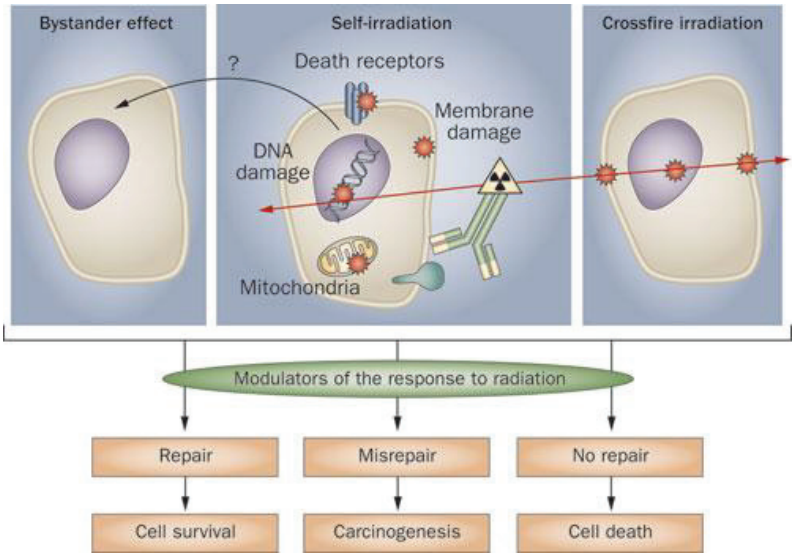

Figure 9: Radiobiology of radioimmunotherapy. Radioimmunotherapeutic agents not only irradiate the cells they attached but can also exert cross- irradiation effects and bystander effects. The radiation response also depends on the type of target being hit. Radiation-sensitive targets in cells include DNA, mitochondria and the lipid membrane. Some membrane receptors, including death receptors, can be stimulated by radiation and thereby starting downstream cellular signaling pathways [22].

Charged particles are directly ionizing radiation. This means that charged particles have sufficient kinetic energy to disrupt the atomic structure of absorbing material through which they pass. This interaction generates different kinds of biochemical process. In brief, when a charged particle passes through absorbent material, in tissue or cells, two kinds of collisions take place; hard collisions and soft collisions [23]. Due to this interaction, the charged particles slow down and release its energy along its track. After light collision, the loss of energy takes place in a long distance while after hard collision most of the energy is lost at a very short distance. This energy loss is determined by the stopping power of medium which indirectly determined by charge and velocity of particles [23, 24].

Heavy, charged particles (alpha particles) have short range and loose their energy in a very short distance while, lighter, charged particles have longer range and loose their energy at longer distance. The Bragg curve shows that the energy lost by an alpha particle per unit length increases dramatically before it stops. This peak of energy loss is known as the Bragg-peak and is characteristic of alpha particles (Figure 10). Figure 10 shows the appearance of the Bragg-peak along the particle track length which is less than 100 µm in water for alpha particles. Thus, when an alpha-particle hits a nucleus and deposits its Bragg peak inside the nucleus the chance of cell death is very high. In comparison, several hundred beta particles are necessary to give the same amount of damage.

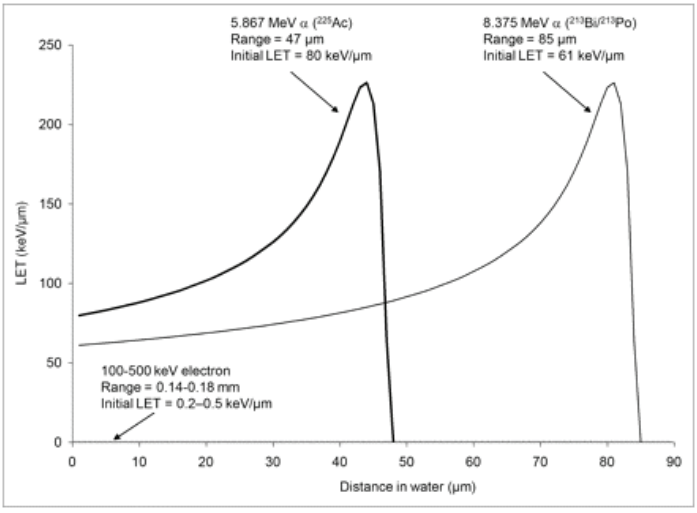

Figure 10: Energy depositions along the path of an α-particle per unit path. LET vs. distance travelled in tissue for α-particles with 2 different initial kinetic energies. α-particles emitted with lower initial energy are closer to their Bragg peak and, therefore, start out with higher LET. LET of electrons with initial energy of 100–500 keV is also shown at bottom of plot for comparison [24].

The term Linear Energy Transfer (LET) is used to describe the density of ionization in particle tracks. LET is the average energy deposited by a particle per unit track length traversed and is expressed in keV/µm [21].

Radionuclides are classified as low and high LET emitters depending upon the amount of energy released by the emitted particle in tissue (Table 1). Low LET beta-particles produce sparse ionization events and individual DNA lesions. However, high LET alpha-particles produce densely localized ionizations along a linear track resulting in multiple and severe damage of the DNA double strand (Figure 11) [22, 24].

A B

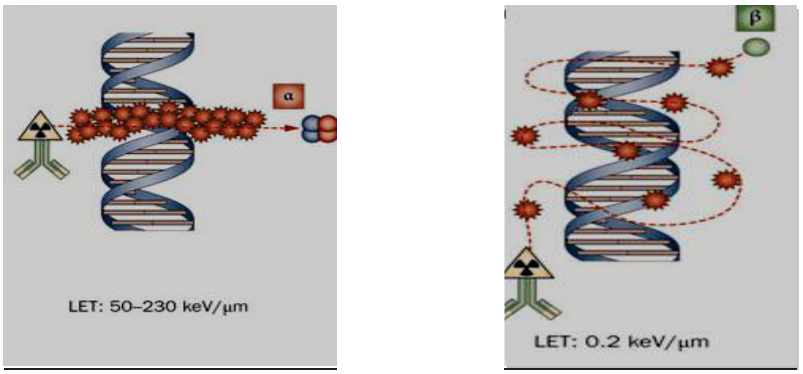

Figure 11: Patterns of DNA damage caused by different LET radiation. Low LET beta particle radiation, due to sparse or random ionization, produces reparable DNA damage (B). On the other hand, high LET alpha particle radiation, due to their dense ionization, produces multiple local damaging sites that are poorly reparable (A) [22].

Toxicity of high LET emitters is independent of oxygen and toxic effects are due to direct ionization of DNA. On the other hand, oxygen related free radicals play an important role in low LET mediated cellular toxicity [21, 24, 25].

Different radiation types produce different magnitude of biological response. As the LET increases, the probability of radiation induced biological damage also increases. Therefore, a term relative biological effectiveness (RBE) was introduced to determine the therapeutic

advantages and disadvantages among different radiation therapies (see. material and methods) [24].

Biological response of tissues does not only depend on the quality of radiation and total absorbed dose but also depends on dose rate. Radiation dose delivers at high rate decrease repair time of tissues. As the dose rate is lowered, time of dose delivery is increased and it becomes possible for repair mechanism to take place due to proliferation and possible DNA repair. This is an advantage for normal tissue but may be a disadvantage for tumor tissue. However, repair mechanism of tumor tissue is not working as normal tissue and therefore, repair is less likely since alpha radiation causes mainly irreparable DNA double strand breaks. Moreover, the dose rate effect is different from one tissue to another and therefore, it can be difficult to assess the efficacy of RIT solely on the basis of dose rates [26]. However, dose rate effect in RIT is very significant when compared with external beam radiation therapy. Clinically administered dose (X radiation) can be delivered in a very short time by RIT with minimum normal tissue toxicity [26, 27]. Therefore, continuous low dose rate give maximum normal tissue sparing and decrease tumor cell proliferation [27].

.

3.2 High and low LET emitting radionuclides used in RIT

The selection of radionuclides for RIT must be based on their physical and chemical properties, including their half-life, LET, gamma emissions for imaging and chemistry for binding to antibody. In addition, economic considerations, including cost of production and availability of radionuclides plays also an important role during radionuclide selection [28].

Table 1 High and Low LET emitting radionuclides used in RIT

Isotopes	Half -life	Maximum Energy (keV)	Maximum Range (mm)	Emission
Low linear energy transfer (LET 0.2 keV/µm) emitters				
^{90}Y	2.67 days	2.284	12	Beta
^{131}I	8.4 days	606	2-3	Beta, gamma, X ray
^{177}Lu	6.7 days	497	< 2	Beta, gamma, X ray
^{67}Cu	2.5 days	575	2.3	Beta, gamma, X ray
^{186}Re	3.7 days	1.077	4.8	Beta, gamma, X ray
^{188}Re	17.0 h	2.120	10.4	Beta, gamma, X ray
High linear energy transfer (LET 50–230 keV/µm) emitters				
^{225}Ac	10 days	6-883	<1	Alpha, gamma, X ray
^{211}At	7.2 h	6.867	<1	Alpha, gamma, X ray
^{213}Bi	46 min	8.377	<1	Alpha, gamma, X ray
^{227}Th	18.7 days	5.900	<1	Alpha, gamma

3.2.1 Low LET emitting radionuclides

Beta emitters, including ^{131}I, ^{90}Y, ^{177}Lu, ^{188}Re, ^{186}Re, and ^{67}Cu, have been in great focus from the last few decades and some of them have been approved for radioimmunotherapy (Zevalin and Bexxar) and the rest are in clinical trials. Their physical half-life ranges from 17 hours to 193 hours and the amount of energy released by particle ranges 575 keV to 2.284 keV. All the most commonly used beta emitters also emit gamma radiation, except ^{90}Y. Gamma rays allow external imaging (Table 1) [14, 22].

The availability and long experience with radiolabeling chemistry of beta emitters play an important role in their wide use. Iodine -131 has a half life of almost 8 days and emits 606 keV energy beta particles with a range of 2-3 mm. Its high gamma radiation yield result in isolation of the patient for about a week after treatment.

Yttrium-90 has a short half life of almost 2.6 days and emits 2.284 keV energy within a range of 12 mm. It has a high energy emission and prolonged tumor retention compared to ^{131}I. However, bone marrow toxicity due to the long range is a disadvantage.

Lutetium -177 and copper-67 have shown some advantages over other beta emitters due to deposition of high energy in a considerably short range. Lutetium -177 emits 497 keV energy in a range of less than 2 mm and in almost same range (2.3 mm), copper-67 (has half life of 2.5 days) emits 575 keV energy. Both radionuclides have been tested recently in both clinical and preclinical research and showed quite promising results [14, 29, 30]. Rhenium-186 has a half life of 3.7 days and emits 1.077 keV energy in a range of 4.8 mm is commonly used against bone metastasis of breast and ovarian cancers and arthritis [31]. Rhenium-188 has a half life of 17 hours and emits 2.120 keV energy in a range of 10.4 mm and showed considerably good results in leukemic patients [32].

3.2.2 High LET emitting radionuclides

Currently, only four alpha particle emitting radionuclides are being widely studied in both clinical and/or preclinical trials of RIT (Table 1) [22]. Actinium-225 has a half life of 10 days with alpha energy emission 6.883 keV, ^{211}At has a half life of 7.2 hours with alpha energy emission of 6.867 keV, ^{213}Bi has a half of 46 min with alpha energy emission of 8.377 keV and ^{227}Th has a half life of 18.7 days and emits with minimum energy of 5.900 keV alpha particles. Both the ^{227}Th and the ^{225}Ac nuclides, however, have a relatively large number of α-emitting daughter nuclides, which will detach from the radioimmunoconjugate and redistribute in the body after the first α-emission [28].

The progress towards clinical application of α-emitters has been halted by the low availability of radionuclides with proper physical and chemical characteristics. Also, because of short half-lives and/or limited chemical yields, the production of a final product in clinically useful quantities has been challenging. Therefore, attention has been brought to alpha-emitters that can be prepared in large quantities from long term operating generators such as ^{227}Th generated from ^{227}Ac [22, 28].

3.2.2.1 Thorium-227

Thorium-227 can be produced in clinically relevant amounts from ^{227}Ac, which is generated by thermal neutron irradiation of ^{226}Ra. The yield of ^{227}Th purification by anion exchange chromatography is almost quantitative [15]. ^{227}Th decays via its alpha- and beta-emitting daughters (5 α particles and 2 β particles) including, ^{223}Ra ($t_{½}$=11.4 d), ^{219}Rn ($t_{½}$= 4.0 s), ^{215}Po ($t_{½}$= 1.8 ms), ^{211}Pb ($t_{½}$= 36.1 m), ^{211}Bi ($t_{½}$= 2.2 m) and ^{207}Tl ($t_{½}$= 4.8 m) to stable ^{207}Pb (Figure 12 and Table 1) [33].

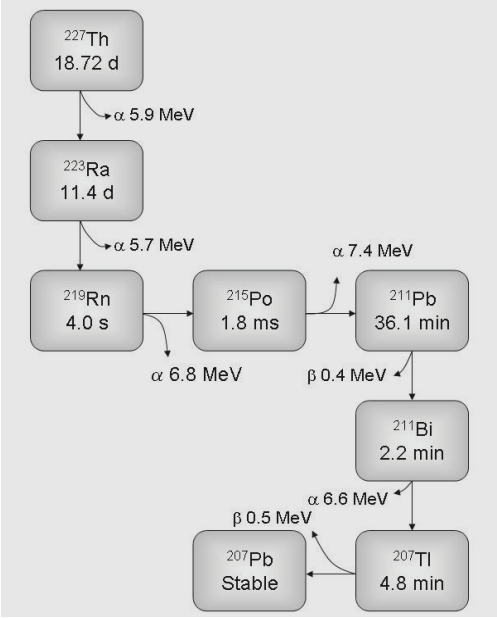

Figure 12: Decay scheme of ^{227}Th. Thorium-227 decays via its alpha and beta emitting daughters, including 5-alpha and 2- beta. Most of the ^{227}Th- daughters have short half-lives except ^{223}Ra.

It should be noted that the half-life of ^{223}Ra is much longer than that of ^{221}Fr, the daughter for ^{225}Ac, and allowing more than sufficient time for blood elimination before decay. ^{227}Th can be stably conjugated to antibodies with the p-SCN-benzyl–DOTA chelator in a two step procedure [15]. In vivo testing of ^{227}Th started in 2004 [34]. Although ^{227}Th can be produced in clinically relevant amounts and have been shown to be an efficient and safe nuclide in lymphoma, breast cancer and ovarian cancer preclinical models, no clinical studies have yet been started [33-40].

3.3 Pre clinical experience of high and low LET RIT targeting HER2 positive carcinomas

^{177}Lu has been tested in HER2 positive tumor models [41-43]. ^{177}Lu-labeled trastuzumab or pertuzumab has shown growth inhibition of HER2 positive breast and ovarian cancers and improved the survival of mice [41, 42, 44].

The efficacy of ^{225}Ac was compared with ^{213}Bi and ^{90}Y after conjugating to the anti-HER2 antibody (7.16.4) in a mouse model HER2 positive (NT2.5 cell lines). ^{225}Ac was much more effective than ^{213}Bi and ^{90}Y labeled anti-HER2 antibodies in tumor eradication and prolongation of survival mouse [45].

The efficacy of ^{211}At-labeled trastuzumab was evaluated in a rat model of breast carcinomatous meningitis (CM) (MCF7 cells). The median survival increased significantly after ^{211}At-labeled trastuzumab in comparison to the control. For animal receiving 33 and 66 μCi of ^{211}At-trastuzumab, the median survival was 45 and 48 days, while for animal receiving saline and cold trastuzumab groups, the median survival was 21 days [46]. The effect of ^{211}At-trastuzumab as a single therapy and fractionated therapy was compared with different dosages of cold trastuzumab in mice bearing (SKOV-3 xenografts). The combination of 500 μg trastuzumab and 400 kBq ^{211}At-trastuzumab had the greatest effect, with complete eradication of the tumors [47]. The efficacy of ^{213}Bi-conugates (trastuzumab and CC49 mAb antibody) was determined in a rat bearing (LS-174 T cells). The results showed that the maximum tolerated dose was 500 μCi/mice and prolonged the median survival to 41 days as compared to 28 days of control. The dual targeting effect of ^{213}Bi after conjugated to trastuzumab and CC49 mAb against the tumor associated glycoprotein was tested. The administration of ^{213}Bi-trastuzumab followed by the injection of ^{213}Bi-antiglycoprotein antibody resulted in greater therapeutic effects (therapeutic index of 9.8), as compared to single injection, and prolonged the survival of mice [48].

Our group has evaluated the therapeutic efficacy of ^{227}Th-trastuzumab on SKBR-3 and SKOV-3 both in vitro and in vivo [35, 36, 39, 40]. In addition, ^{227}Th-rituximab against CD20 on NHL has been evaluated both in vitro and in vivo [33, 34, 38, 49, 50].

3.4 Clinical experience of high and low LET RIT

3.4.1 Clinical experience of high and low LET RIT in haematological cancers

Non Hodgkin lymphoma (NHL)

The first clinical trial of NHL patients was performed with anti-HLA-DR mAb after labeling with Iodine-131 in 1988. Complete or partial remission in 4 out of 10 patients with minimal toxicity was seen in most of the patients [51]. Anti-CD20 antibodies labeled with ^{131}I were used in patients for the first time in 1993. After treatment and bone marrow reinfusion, the complete remission was seen in 16 patients and partial response was seen in 2 out of 19 patients with bone marrow toxicity [52]. Anti-CD37 phase I clinical trials investigating the biodistribution, therapeutic efficacy and toxicity of ^{131}I-MB-1 were reported in 1989 [53] and in 1992 [54] for NHL patients. 40 % of the patients experienced complete remission after ^{131}I- MB-1 with mild bone marrow suppression. ^{90}Y-hLL2 has been used against CD22 positive NHL [55]. A multicenter trial performed by Morschhauser et al showed that fractionated anti-CD22 therapy with ^{90}Y-hLL2 resulted in durable complete response and suggested a recommended dose of 22 mCi/m^2 in every second week for future studies [55]. A study performed by Linden et al. concluded that weekly fractionated RIT with ^{90}Y-hLL2 (5 mCi/m^2 or 185 MBq/m^2) showed highest response of 62 % with complete remission, with minor bone marrow toxicity [56].

In 2002 and 2003, ^{90}Y-ibritumomab tiuxetan (Zevalin) and ^{131}I-tositumomab (Bexxar), were approved by FDA for the treatment of relapsed and refractory low grade, follicular or transformed B-cell lymphoma (NHL) [57]. A complete response rate of 20-49 % and overall response rate of 60–80 % with mild toxicity was observed with Zevalin [58]. Zevalin was approved as first line therapy in Europe in 2008 [57, 59]. Promising complete response rates of 50 to 75 % were observed with Bexxar in NHL patients [60, 61]. RIT against lymphoma is considered as combination therapy with chemotherapy or as consolidation therapy.

Myeloid leukemia

The efficacy of anti- CD45, CD66 and CD33 RIT have been evaluated in combination with chemotherapy in these patients AML and CML patients [32, 62-65]. Advanced AML patients treated with (122-437 mCi/m^2) ^{131}I-labeleld M195 and Hum195, against CD33, in combination

with chemotherapy resulted in median survival of 4.9 (range 0.3-90 months) [62]. Pagel et al in his first clinical trial estimated that 3 year disease free survival was between 21 % to 61 % and in his second trial estimated 1 year survival was more than 41 % [63, 64]. In other study, 20 patients treated with ^{131}I-labeled anti CD45 along with chemotherapy showed median disease free survival of 17 months after bone marrow toxicity [66]. CD66 antigens in myeloid leukemic patients were also used as target antigen and ^{188}Re and ^{90}Y-labeled anti-CD66 antibodies were used in phase I and II clinical trials. The probability of survival was estimated to be 70 % at 1 year and 52 % at 2 years [32, 65].

Clinical trials with high LET alpha emitting ^{213}Bi- labelled HUM195 anti-CD33 showed quite promising results, especially due to decrease bone marrow toxicity [67, 68]. A study performed by Jurcic et al in 2002 included 18 patients with relapsed and refractory AML and CML and treated with ^{213}Bi-HuM195. All developed myelosuppression with a median time recovery of 14 days and 93 of patients showed reduction in circulating blast [67]. In a recent phase 1 and II trials, maximum tolerated dose and anti-leukemic effects of ^{213}Bi-HuM195 were determined in patients after partial cytoreductive chemotherapy. In these studies MTD was 37 MB/kg along with median response duration of 6 months (range, 2-12 months). Dose limiting myelosuppression was last for 35 days [68].

3.4.2 Clinical experience of high and low LET RIT in carcinomas

The first clinical trial of RIT in solid tumor was performed by Welt et al in 1990. In this study, biodistribution and imaging characteristics of ^{131}I were studied after binding to anti-A33 antibodies in colorectal carcinoma patients. Selective localization to tumor tissue was seen in 19 of 20 patients [69]. According to a recent review, a total of 58 clinical trials have been preformed to evaluate the efficacy of RIT against 15 different tumor targeting antigens in gliomas, colon, ovarian, gastric, liver, lungs, renal, breast, brain and in some gastrointestinal malignancies [22]. Tumor-associated glycoprotein 72 (TAG) and carcinoembryonic antigen (CEA) were the main target antigens in these studies and are widely expressed in all the above mentioned tumor types [22]. Only few clinical trials for RIT went beyond phase II showing that RIT for patients with solid tumors are more challenging than patients with haematological cancers [22].

However, in 2005, a phase II clinical study was performed to target CEA antigen with ^{131}I-labetuzumab in patients with metastatic colorectal carcinoma. Study showed quite promising results with median overall survival of 68 months and median disease free survival of 18 months. The 5 year survival rate was 51.3 % [70]. One year later a phase III clinical trial was reported by Verheijen et al with ^{90}Y-labeled HMFG1 murine monoclonal antibody in ovarian cancer patients. This study was a multi-central trial with the aim to compare the standard treatment plus RIT with standard treatment alone. The end points were survival and relapse and safety and no difference was found between standard treatments and RIT treatment [71].

Limited numbers of clinical trials have evaluated the alpha-particle based RIT in solid tumors. Zalutsky et al. investigated the efficacy and safety of ^{211}At-labeled ch81C6 in patients with recurrent malignant brain tumors. This study demonstrated that the regional administration of ^{211}At-labeled ch81C6 was safe, 96.7 % decay was localized, and was therapeutically beneficial with pronged survival of 1-3 years [72]. Anderson and co-workers at university of Gothenburg, Sweden, investigated ^{211}At-MX35 F $(ab)_2$ in ovarian cancer patients. This phase I study demonstrated that intraperitoneal administration of ^{211}At-MX35 F $(ab)_2$ was feasible to achieve therapeutic doses to microscopic tumor cluster without significance toxicity [73].

The limited success of RIT for solid tumors in clinical trials can be explained by the fact that radiation dose delivery by RIT to the tumor is not enough to overcome the radioresistance of solid tumor mass [22, 74, 75]. Tumors treated with external beam radiation therapy showed clinical response with radiation absorbed dose of 50 Gy to the tumor [22]. However, in clinical studies with ^{90}Y-CC49, ^{131}I -CC49 or ^{131}I-MN14 the maximum dose to tumor was between 1.8 and 33 Gy [76, 77]. Radiation dose to the tumor by RIT is very variable and can in some cases be too low to eradicate the tumor.

Different strategies have been considered or are being developed to find a way to improve radiation dose delivery to the solid tumors or their eradication. These strategies include; finding ways to improve antibody uptake into the tumor and its uniform distribution, and choosing antibodies which themselves can affect the growth of tumor. Tumor uptake of radiolabeled antibodies can be improved either by modifying its route of administration (locoregional administration in RIT enhances tumor uptake) or by modifying vascular

properties of tumors through hyperthermia, radiation and biologically active compounds. In addition, it has been found that radioimmunotherapy of solid tumors can be more effective if it is combined with chemotherapy. Recently, few clinical trials combining RIT with chemotherapy have shown considerably good results [75, 78-81].

3.5 Breast Carcinomas

Breast cancer is the most frequent malignancy and the leading cause of cancer related death in women all over the world, with an estimated 23 % of the total new cancer cases and 14 % of the total deaths in 2011 or 2010 [82]. In Norway, the incidence of breast cancer has increased over the last few decades [83]. However, breast cancer mortality in Norway has been declining in the last 15 years are so.

The treatment options are determined by the multiple factors, including patient age, disease stage, histological type of tumor and presence and absence of tumor markers [84-86]. Therefore, therapy often is a multi-modal approach, including surgery, chemotherapy, hormonal therapy, radiation therapy and targeted therapy [87, 88].

Surgery is the best option if the disease is localized or has spread to regional lymph node and the options are lumpectomy or mastectomy [89]. Chemotherapy and external beam radiation therapies can be used adjuvant treatment along with surgery or as single approach, depending on the stage and extent of disease [90].

Hormonal therapy is based on patient age and sex and its intention is to block the effects of estrogen and progesterone receptors on the tumor cells, which are known to accelerate cancer growth. Hormonal therapy considerably improves the survival and quality of life in patients with metastatic breast carcinomas [90, 91]. Targeted therapy is available in the form of trastuzumab (Herceptin®); see (3.1.1.3, trastuzumab). HER2/neu overexpression is linked with bad prognosis and poor survival [92]. One quarter of breast cancer patients overexpresses human epidermal growth factor receptor-2 (HER-2/neu) at their primary and distant tumor sites [12].

3.6 Ovarian carcinomas

Ovarian cancer is the sixth most common cancer world wide with estimated new cases of 225,500 [82]. More than 140.000 women died and approximately 230.555 cases were diagnosed in 2007 [93].

In Norway, a total of 4570 new cases of ovarian cancer were reported from 1999 to 2008 and the age adjusted incidence rates ranged from 10.8 to 13.8 per 100,000 person-years [83].

Ovarian cancer is mostly sporadic. Due to lack of specific symptoms, 67 % of the patients in USA were diagnosed at the stage III and IV. Therefore, surgery followed by adjuvant chemotherapy is the standard method of treatment.

Chemotherapy is always indicated after surgery in the form of paclitaxel. The routine treatment includes paclitaxel in combination with a platinum-based compound or platinum based therapy alone. Platinum-based chemotherapy alone or in combination with paclitaxel has been conformed to significantly improve the survival of OC patients [9, 94-96]. However, despite most of the patients have shown response to these above mentioned treatment strategies, relapse is still a big problem [9, 97].

Herceptin® (see 3.1.1.3) have shown clinical activity as monotherapy in phase I/II trial in women with HER-2 positive metastatic ovarian cancer [10].

Patients with early-stage OC had five year survival rates in the range of 71-93 %, whereas in patients with advanced ovarian cancers, survival rate was around 31% [98].

Overexpression of HER-2 has been reported to be a bad prognostic factor in both early and advanced stage disease [99, 100]. Human epidermal growth factor receptor (HER-2, also called ErbB-2) is overexpressed in 10 % of ovarian cancer patients [100].

4 Aims of the study

The purpose of this study was to investigate the in vivo stability, therapeutic and toxic effects of DOTA-trastuzumab labeled with thorium-227 and to compare this high-LET RIC with the low-LET beta-emitting ^{177}Lu-RIC using both ovarian and breast cancer tumor models.

This study investigated the following questions:

1. Is the administration of the alpha-particle emitting radioimmunoconjugate ^{227}Th-trastuzumab safe and therapeutically effective in mice with HER2-overexpressing breast and ovarian cancer xenografts?
2. Is the administration of the high-LET alpha-particle emitting radioimmunoconjugate ^{227}Th-trastuzumab therapeutically more effective and less toxic than low –LET beta particle emitting ^{177}Lu-trastuzumab in HER2-overexpressing breast and ovarian cancer xenografts?

5 Experimental methods

5.1 Radioimmunoconjugates preparation

Alpha radioimmunoconjugates (^{227}Th-DOTA-trastuzumab and ^{227}Th-DOTA -rituximab) were prepared at Algeta ASA and transported to the Norwegian Radium Hospital. Radiolabeling of freeze dried DOTA-trastuzumab, delivered by Algeta ASA, with beta-radionuclide ^{177}Lu conjugate was performed at our institute.

5.2 Animal and tumor model

Female Balb/C nu/nu (NCR) mice, with an average weight of 19 to 25 g at the start of study, were used in all experiments. Mice were provided by the Department of Comparative Medicine Radium Hospital, Oslo University Hospital, Oslo, Norway. All procedures and experiments involving animals in this study were approved by the National Animal Research Authority and carried out according to the European Convention for the Protection of Vertebrates used for Scientific Purposes. The animals were maintained under pathogen-free conditions, and food and water were supplied ad libitum.

Mice were anaesthetized before tumor implantation. A mixture of 2.4 mg/ ml and 2.4 mg (Zoletil® vet, Virbac, Carros Cedex, France) was used for anaesthesia of mice. The dose used was between 0.05-0.1 ml/animal (Paper 1, 2 and 3). Breast and ovarian cancer tumor xenografts were implanted in mice 2 to 3 weeks before the start of experiments. The xenografted tumor line originated from HER-2 positive breast and ovarian cancer (SKBR-3 and SKOV-3) cells from American Type Culture Collection (ATCC, Manassas, VA). All animals were euthanized by cervical dislocation at the end of experiment.

5.3 Biodistribution and dosimetry

The conjugates ^{227}Th-trastuzumab, ^{227}Th-rituximab and ^{177}Lu-trastuzumab were administrated by tail vein injection in 100µL solution to each tumor bearing animal. Different time points were decided for each conjugate and a total of four to six animals were autopsied at each time points.

Tumors and organs were collected, weighted and measured for radioactivity content. The cumulated activity in various organs, from the time of injection of preparation until no activity was left in the body, was estimated by calculation of the area under the activity concentration versus time curves (AUC) (Paper 1, 2 and 3).

Absorbed radiation dose was estimated using cumulated activity calculated from biodistribution data, assuming a complete absorption within the source tissue of the emitted particle. For ^{227}Th, no cross radiation was taken into count and it was assumed that there is 100 % and uniform dose distribution into the tissue. While, for ^{177}Lu cross radiation was taken into count as a tissue factor. This is a reliable method used in the animal research. However, this method can be improved by including tissue autoradiography to obtain more information about tissue activity distribution. Some centres used SPECT to determine the actual tissue activity concentration and associated total volume over which the activity is distributed [101, 102].

5.4 Therapy and toxicity

Tumor (SKBR-3 and SKOV-3) bearing mice were injected with a single dose of NaCl and different dosages of cold trastuzumab and ^{227}Th-trastuzumab, ^{227}Th-rituximab and ^{177}Lu-trastuzumab in100µL solution. Therapeutic effects were determined by tumor growth and survival assessment of mice after treatment. Tumor growth and survival of mice were assessed 3 times a week for three weeks after injection and thereafter, growth and survival were assessed twice a week. Mice with tumor volume larger than 20 mm were killed (Paper 1, 2 and 3).

Toxicity was evaluated by measuring weight changes in mice after treatment, including 3 times a week for first three weeks after treatment and thereafter 2 times a week. Blood cell counts, white blood cell and platelet counts were measured before and at three different time points after treatment, including at the time of autopsy, to assess the therapeutic toxicity. In addition, liver enzymes and kidney functions were assessed to evaluate the therapy related toxicity (Paper 1, 2 and 3).

5.5 Relative biological effects and therapeutic index

Relative biological effects (RBE) compare the dose of test radiation to the dose of standard radiation to produce the same effects.

RBE = Dose from standard radiation to produce a given biological effect/ Dose from test radiation to produce the same biological effect

Type of radiation used for reference radiation is usually X or ^{60}Co-γ-radiation. In this study, however, the low LET RIT was used as reference for the high LET RIT. RBE was calculated by dividing the dose for ^{227}Th-trastuzumab by the dose for ^{177}Lu-trastuzumab to reach the same end point, which was the difference in the therapeutic efficacy after administration of both RICs. Therapeutic efficacy was estimated by plotting the treatment–induced percent increase in number of days to grow to 500 mm^3 and/or 1000 mm^3 against the cumulative absorbed radiation dose. Anti-tumor effects and bone marrow toxicity are the two most commonly used end points to determine RBE in most in-vivo studies [28]. RBE is useful preclinical information that can be taken into consideration when designing clinical trials of a RIC [28]. However, RBE depends on the quality of radiation, end point and dose rate. Therefore, it is some times challenging to compare the various treatments with respect to RBE.

Therapeutic index is the percent of tumor control that can be achieved for a given level of normal tissue damage [19] and might be a more clinically relevant parameter to compare different RITs. In this study a 50 % decrease of WBC was used as a parameter for normal tissue damage. The therapeutic index also varies with dose rate, LET and the design of experiments. Therefore, therapeutic index in clinical studies will be different from preclinical studies.

6 Summary of papers

6.1 Paper 1

This study was designed to investigate biodistribution, normal tissue toxicity and therapeutic efficacy of low dose rate alpha particle emitting radioimmunoconjugate ^{227}Th-trastuzumab in mice with HER2 positive breast cancer xenografts. For comparison purpose, the mice bearing SKBR xenografts were injected with anti-HER2 antibody trastuzumab alone, ^{227}Th-rituximab (non-targeted) and normal saline.

A significant dose dependent tumor growth inhibition was observed with different dosage of ^{227}Th-trastuzumab (200, 400 and 600 kBq/kg) but anti-tumor effects were not seen with non-targeted ^{227}Th-rituximab (400 and 600 kBq/kg) and trastuzumab alone. Absorbed radiation dose to the tumor was approximately 3 Gy after administration of 400 kBq/kg ^{227}Th-trastuzumab. No serious bone marrow and normal organ toxicity was seen after the administration of ^{227}Th-trastuzumab except a transit reduction of leukocyte count in highest dose-group. This study came up with the conclusion that the ^{227}Th-trastuzumab therapy not only was effective and well tolerated in mice bearing breast cancer xenografts but also warrant the further preclinical studies aiming at a clinical trail in breast cancer patients with bone metastasis.

6.2 Paper 2

In this study, HER2 positive ovarian carcinomas bearing mice were injected with low dose alpha particle emitting ^{227}Th-trastuzumab and beta-particle emitting ^{177}Lu-trastuzumab and evaluated for their biodistribution (specific and non specific distribution), therapeutic efficacy along with bone marrow and normal organ toxicity.

The absorbed radiation dose to the tumor was 4 Gy after the administration of 400 kBq/kg of ^{227}Th-trastuzumab and 72 MBq/kg ^{177}Lu-trastuzumab, respectively. The therapeutic efficacy, as growth inhibition and growth delay, was better after ^{227}Th-trastuzumab therapy as compared to the control, trastuzumab alone, non- tumor binding ^{227}Th-rituximab and ^{177}Lu-

trastuzumab therapies. Mean survival of mice after treatment with ^{227}Th-trastuzumab was significantly improved compared to control and other radioimmunoconjugates ($p < 0.05$, Kaplan Meier). Treatment related bone marrow and normal organ toxicities were not observed except for a transient decrease of leukocyte count between 3 to 9 weeks after highest administrated dosages of ^{227}Th-trastuzumab. The study showed that alpha emitting RIC ^{227}Th-trastuzumab therapy improved the survival of mice and effectively inhibited the tumor growth as compared to ^{177}Lu-trastuzumab. These results suggest further clinical testing of this RIC (^{227}Th-trastuzumab) in patients with micro-metastatic ovarian carcinoma.

6.3 Paper 3

This study was designed to compare the invivo investigations, including biodistribution, therapeutic efficacy and toxicity, of a low dose alpha particle RIT (^{227}Th-trastuzumab) with beta particle RIT (^{177}Lu-trastuzumab) in mice bearing breast carcinoma xenografts.

The absorbed radiation dose to the tumor was approximately 3 Gy after the administration of 400 kBq/kg of ^{227}Th-trastuzumab and 40 MBq/kg ^{177}Lu-trastuzumab, respectively. Tumor growth was significantly controlled with improved survival at injected dosage of 400-1000 kBq/kg ^{227}Th-trastuzumab and 200 MBq/kg of ^{177}Lu-trastuzumab as compared to control. Relative biological effectiveness was also calculated to compare the therapeutic efficacy of ^{227}Th-trastuzumab with ^{177}Lu-trastuzumab. When compared at same therapeutic effect (100 % increases in growth delay) ^{227}Th-trastuzumab was 3 times more effective than ^{177}Lu-trastuzumab. On the basis of temporary decrease of WBC, therapeutic index of ^{177}Lu-trastuzumab was superior to that of ^{227}Th-trastuzumab.

7 Discussion

This study of high LET alpha-particle emitting ^{227}Th- trastuzumab and low LET beta-particle emitting ^{177}Lu-trastuzumab includes biodistribution, tumor targeting and normal tissue toxicity in mice with HER 2 positive breast and ovarian cancer xenografts. The concentration of ^{227}Th- and ^{177}Lu-labeled-trastuzumab followed a bell shaped curve in tumor tissue as a function of time, and the concentration in tumor tissue was significantly higher than in normal tissue. The daughter nuclide of ^{227}Th, ^{223}Ra, partly relocated after decay of ^{227}Th to bone tissue, was partly internalized by the tumor cells or trapped in the tumor tissue and was partly excreted. Therapeutic effect of ^{227}Th-trastuzumab was observed as dose dependent growth inhibition with improvement in survival for both tumor models. Beta emitting ^{177}Lu-trastuzumab was also effective; however at the same absorbed radiation dose to the tumor, ^{227}Th-trastuzumab efficacy was superior to ^{177}Lu-trastuzumab, for both models. On the contrary, when compared at doses giving the same temporary decrease of WBC, the therapeutic index of ^{177}Lu-trastuzumab was superior to that of ^{227}Th-trastuzumab in the breast cancer model. Mild bone marrow toxicity (transient decrease of WBC count) was the only side effect observed with the highest doses of both RICs except 1000 kBq/kg of ^{227}Th-trastuzumab where weight loss was observed in few animals.

7.1 Treatment of mice with breast cancer and ovarian cancer xenografts with ^{227}Th-trastuzumab

Dose dependent growth inhibition of breast and ovarian tumors was seen after ^{227}Th-trastuzumab. ^{227}Th-trastuzumab at dosage of 400-600 kBq/kg in both tumor models and 1000 kBq/kg in SKBR-tumor model showed improved anti-tumor effects. The lowest administered dose of 200 kBq/kg gave variable results against breast cancers and was not effective against ovarian cancers, even though absorbed radiation dose to breast tumors was lower (1.5 Gy) than ovarian (2 Gy) (Table 2). Higher dosages (400-600 kBq/kg, ^{227}Th-trastuzumab) demonstrated relatively better anti-tumor effects against breast carcinomas as compared to ovarian carcinomas. However, absorbed radiation doses to the breast tumors (3 Gy and 4 Gy) were lower than the ovarian tumor (4 Gy and 6 Gy) as shown in Table 2. Similar methods used for

the calculation of absorbed radiation dose to both tumors but cell geometry was not taken into consideration. From in vitro microscopy we know that SKOV-3 cells are larger than SKBR-3 cells and that can have an impact on the absorbed radiation dose since the probability of hitting the nucleus will be lower in larger cells than a small cell if the nucleus is of the same size [39]. In addition, SKOV-3 cells in culture had a weaker expression of HER2 as compared the SKBR-3 cells. This does not fit well with the higher dose calculated for the SKOV-3 tumors. We observed that the ovarian tumors were more resistant to the ^{227}Th-trastuzumab than breast tumors. Inherent difference in radiosensitivity between breast and ovarian malignancies could be an explanation for variability (breast more radiosensitive than ovarian) [103]. Moreover, it has been shown that the proliferation rate in cell culture of SKOV-3 cells was higher than of SKBR-3 cells [39] while it was opposite for tumor xenografts. Absorbed radiation dose rate to the ovarian tumors was lower than breast after ^{227}Th-trastuzumab, which fits well with the in vitro studies described above. This low dose rate could be due to weaker expression of HER2 because this leads to fewer binding sites available for ^{227}Th-trastuzumab binding. The growth inhibitory effect of 200 kBq/kg ^{227}Th-rituximab against mice with Raji, NHL xenografts [37] was better than for 200 kBq/kg ^{227}Th-trastuzumab. However, higher dosages ^{227}Th-trastuzumab demonstrated relatively better anti-tumor effects than higher dosages of ^{227}Th-rituximab (Table 2). Tumor growth delay after administration of higher dosages ^{227}Th-trastuzumab was superior as compared to the higher dosages of ^{227}Th-rituximab. This difference might be due to the variation in the optimal dose delivery to tumors which may be achieved at higher dosages for ^{227}Th-trastuzumab and at lower dosages for ^{227}Th-rituximab. ^{227}Th-RIT resulted in transient decrease of white blood cells (Table 2). The extent of white blood cell reduction increased with increasing dosage of ^{227}Th-trastuzumab. Therapeutic effects of 400 kBq/kg ^{227}Th-trastuzumab was also considerably good. Therefore, we consider that the optimal therapeutic effects, i.e. low toxicity and good treatment efficacy, was achieved with 400 kBq/kg of ^{227}Th-trastuzumab.

Table 2: Summary of therapeutic and toxic effects of ^{227}Th-RICs

^{227}Th-trastuzumab against breast carcinomas			
Tumor dose (injected activity)	Delay to grow to a volume of 500 mm^3	1000 mm^3	Toxicity (WBC count)
1.5 Gy (200 kBq/kg)	4 days	9 days	Reversible decrease upto 5 weeks
3 Gy (400 kBq/kg)	23 days	46 days	Reversible decrease upto 5 weeks
4.5 Gy (600 kBq/kg)	45 days	57 days	Reversible decrease upto 9 weeks
7.5 Gy (1000 kBq/kg)	38 days	170 days	Reversible decrease upto 9 weeks
^{227}Th-trastuzumab against ovarian carcinomas			
2 Gy (200 kBq/kg)	0 days	0 days	No
4 Gy (400 kBq/kg)	8 days	27 days	Reversible decrease upto 6 week
6 Gy (600 kBq/kg)	30 days	34 days	Reversible decrease upto 6 week
^{227}Th-rituximab against Non-Hodgkin's lymphoma			
2 Gy (200 kBq/kg)	N.E	17 days	Reversible decrease upto 4 weeks
4 Gy (400 kBq/kg)	N.E	15 days	Reversible decrease upto 7 weeks
10 Gy (1000 kBq/kg)	N.E	40 days	Reversible decrease upto 9 weeks

N.E: Not estimated

7.2 Treatment of mice with breast cancer and ovarian cancer xenografts with ^{177}Lu-trastuzumab

Administration of 200 MBq/kg ^{177}Lu-trastuzumab resulted in growth inhibition of breast carcinomas with improvement in survival. Lower dosages of ^{177}Lu-trastuzumab (40 MBq/kg vs breast and 72 MBq/kg vs ovarian) failed to exhibit anti-tumor effects. Slightly higher dosage (74 MBq/kg) of ^{177}Lu-d9MAb used for treatment of mice with intraperitoneal gastric carcinoma cells (HSC45-M2) improved the survival (Table 3) [104]. In previous studies, the dosages between 200 – 296 MBq/kg were reported to be the lowest dosages used for both ^{177}Lu-pertuzumab and ^{177}Lu-trastuzumab in HER2 positive ovarian and breast carcinoma,

respectively [41, 42]. It seems like the dosages used for the ovarian cancer model in this study were too low.

Table 3: Summary of therapeutic and toxic effects of ^{177}Lu-RICs

^{177}Lu-trastuzumab against breast carcinomas			
Tumor dose (injected activity)	Delay to grow to a volume of 500 mm^3	Survival	Toxicity (WBC count)
3 Gy (40 MBq/kg)	1 day	Failed to improve	No seen
16 Gy (200 MBq/kg)	74 days	Significantly Improved	Reversible decrease upto 5 weeks
^{177}Lu-trastuzumab against ovarian carcinomas			
4 Gy (72 MBq/kg)	-5 days	Failed to improve	No seen
^{177}Lu-pertuzumab against ovarian carcinomas			
32 Gy (200 MBq/kg)	75 days	Significantly Improved	N.E
50 Gy (280 MBq/kg)	> 90 days	Significantly Improved	N.E
^{177}Lu-d9MAb against gastric carcinoma (I.P)			
(74 MBq/kg)	N.E	Significantly Improved (> 200 days)	Reversible decrease upto 5 weeks
(296 MBq/kg)	N.E	Significantly Improved (> 200 days)	Reversible decrease upto 6weeks
(592 MBq/kg)	N.E	Significantly Improved (> 200 days)	Reversible decrease upto 6 weeks

N.E= Not estimated
I.P = Intraperitoneal administration

7.3 Comparison of ^{227}Th-trastuzumab and ^{177}Lu-trastuzumab in the breast cancer xenograft model

At the same therapeutic level (100 % prolonged growth delay as compared to control) the absorbed radiation dose of ^{227}Th-trastuzumab to the tumor was 3 times lower than for ^{177}Lu-trastuzumab. In other words, ^{227}Th-trastuzumab was 3 times more efficacious than ^{177}Lu-trastuzumab. In our previous study on NHL tumor xenografts, RBE of ^{227}Th-rituximab was between 2.5 and 7.2 and showed that administration of low dose ^{227}Th-rituximab was more effective per dose unit as compared to both low LET RIT (Zevalin) and X-radiation [38]. Using similar end point, RBE of ^{211}At-MX35 f $(ab)_2$ was found to be 3.6 - 6.3 compared to external radiation (60Co) in ovarian cancers [105]. In targeted therapy, end-points for RBE are efficacy or toxicity, for such end points, the RBE is in the range of 3 to 7 [24]. Thus, RBE for treatment of tumors with ^{227}Th-trastuzumab was almost similar to RBE of ^{227}Th-rituximab and of ^{211}At-MX35 f $(ab)_2$.

In contrast, at similar toxicity level (reversible 50 % decreased of WBC count), the increase in growth delay was 3 times longer with ^{177}Lu-trastuzumab than for ^{227}Th-trastuzumab which indicates that therapeutic index of ^{177}Lu-trastuzumab was superior to the ^{227}Th-trastuzumab. In tumor tissue, the absorbed radiation dose rate was lower for ^{227}Th-trastuzumab than for ^{177}Lu-trastuzumab. This difference may indicate that ^{177}Lu-trastuzumab is suitable for more rapidly growing tumors than ^{227}Th-trastuzumab. This may partly explain the difference in the therapeutic index. However, small sized metastatic spots in humans are more suitable for short range alpha than long range beta emitters. Therefore, it can be anticipated that therapeutic index would have been higher for ^{227}Th-trastuzumab than for ^{177}Lu-trastuzumab in clinical condition.

7.4 Comparison of ^{227}Th-trastuzumab and ^{177}Lu-trastuzumab in the ovarian cancer xenograft model.

The difference in the therapeutic efficacy of ^{227}Th-trastuzumab and ^{177}Lu-trastuzumab was determined at similar absorbed radiation dose to tumor. An absorbed radiation dose of 4 Gy in SKOV-3 tumor was achieved after 400 kBq/kg ^{227}Th-trastuzumab and 72 MBq/kg ^{177}Lu-trastuzumab. Therapeutic efficacy of ^{227}Th-trastuzumab (tumor growth inhibition and improved survival) was superior to ^{177}Lu-trastuzumab. In addition, normal organ toxicity was not seen

with ^{177}Lu-trastuzumab.The reason of the failure of ^{177}Lu-trastuzumab could be that the administered dose was too low to produce any effect, or inherently radioresistent behavior of ovarian tumors, as mentioned above. Administration of 200 MBq/kg ^{177}Lu-pertuzumab demonstrated anti-tumor effects against ovarian carcinomas [41]. Higher doses of ^{177}Lu-trastuzumab might have shown relatively better anti-tumor effects against ovarian cancers and should be tested in the same tumor model.

7.5 The ^{223}Ra daughter nuclide

Biodistribution experiments showed that ^{223}Ra was excreted either through intestine or ends up in the bone as hydroxyapatite crystals. Microautoradiography studies of ^{227}Th-rituximab have also indicated that ^{223}Ra and its daughters contribute to the absorbed radiation dose to the bone marrow [33]. Bone distribution of ^{223}Ra has also been reported in other studies [106]. Radium-223 has considerably longer half life (11.4 days) than its daughters (milliseconds to minutes). Therefore, absorbed radiation dose contribution of ^{223}Ra daughters was considered to occur as the same site as ^{223}Ra. One could suspect that uptake of ^{223}Ra distribution can lead to serious consequences. In the present studies, however, ^{223}Ra related effect appeared to be mild and short term due to no effect on platelets (remained unaffected). In addition, clinical studies have also shown how well the ^{223}Ra is tolerated without exerting serious toxic effects on bone marrow [106-109]. Low bone marrow toxic effects of ^{223}Ra could be due to its decreased localization to bone which could be caused by; 1) 1ong half-life of ^{227}Th may allow excretion of larger amount of ^{227}Th-trastuzumab before the ^{223}Ra is generated, 2) ^{223}Ra generated inside cells due to internalization of ^{227}Th-trastuzumab after binding to the HER2, resulting in decreased free ^{223}Ra, as mentioned above. In addition, the short range of alpha particles emitted by ^{223}Ra could be a potential reason for the low toxicity as shown previously [106]. Therefore, in the present study the role of ^{223}Ra may add a therapeutic effect with minimal toxicity, showing no worries for the selection of ^{227}Th in RIT.

7.6 Internalization of the radioimmunoconjugate

Target antigen internalization from cell surface after antibody binding is an important contributing factor in RIT [110]. HER2 antigen internalization after binding to^{227}Th-trastuzumab traps ^{227}Th–trastuzumab inside the cell and therefore some of the ^{223}Ra forms

inside the cell and thereby possibly contributed to total tumor absorbed dose instead of being taken up in bone. It has been shown that 50 to 75 % of total absorbed dose came from internalized activity after ^{227}Th-trastuzumab [39]. Internalization of ^{227}Th –trastuzumab could also result in a close proximity between the point of decay and the cell nucleus compared with decays from radionuclides at cell surface and thus a higher probability of hitting the nucleus with the alpha particle. Thus, trastuzumab internalization probably contributed to anti-tumor effects and low toxicity seen after both RICs.

7.7 Size of tumor vs range of alpha and beta particles

Tumor size is an important determinant for the choice of radionuclides [111]. The size of tumor xenografts used in this study was considerably larger (4-8 mm) than actual metastases (< 2 mm) and may be more ideal for beta particles than alpha particles. Therefore, higher doses (16 Gy) of long range (0.67 mm) ^{177}Lu-trastuzumab demonstrated considerable therapeutic effects. On comparison with alpha particle, anti-tumor effect caused by short ranged ^{227}Th- in this tumor model (solid, large and radioresistent tumors) is quite encouraging. Although, ^{227}Th- is able to deliver a tremendous amount of energy in a very short range, the probability to hit the cells in this tumor model was lower due to physical and physiological limitations, including short range, stochastic nature of alpha radiation, long half life vs growth rate of tumors, inhomogeneous HER2 distribution and tumor microvasculature. Therefore, this shows that the targeted delivery or internalization of ^{227}Th-trastuzumab may not only be the reason for growth inhibitory effects and some other mechanisms might have involved. Autoradiography images of ^{227}Th-trastuzumab have shown hot spots in perfused areas within the tumor indicating the destruction of blood vessels (paper 1). Lack of nutrient due to tumor vasculature destruction by high LET alpha particle ^{227}Th or ^{223}Ra could be a reason. It has also been shown that a positive therapeutic effect could be expected by targeting solid tumor vasculature with alpha particle emitting radionuclide therapy [112, 113]. Therefore, we assume that good therapeutic effects of ^{227}Th-trastuzumab in our model is due to combined effect of ^{227}Th-trastuzumab, internalization of HER2 after binding to trastuzumab, ^{223}Ra and destruction of blood vessels.

7.8 Therapeutic and toxic effect of non-targeted ^{227}Th-rituximab

Absorbed radiation dose to the tumor was higher compared to normal organs after injections of ^{227}Th-trastuzumab and ^{177}Lu-trastuzumab but not for non-targeted ^{227}Th-rituximab. Administration of different dosages of non-targeted ^{227}Th-rituximab, neither inhibited tumor growth nor improved the survival of mice with HER2 positive tumors. This emphasizes the importance of antibody binding to specific target antigen to achieve desired antitumor effects. Normal organ toxicity was not measured after ^{227}Th-rituximab treatment.

7.9 Therapeutic and toxic effect of trastuzumab

In the present study, trastuzumab therapy alone neither inhibited growth of HER-2 expressing carcinomas (SKBR-3 and SKOV-3) nor improved the survival. The administered doses were similar that is used in clinics (paper 1) [7]. The reason of this failure could be partly explained by the absence of immune mediated tumor cell killing in immunodefficient mice [114]. Moreover, as there is reduced vascularity and blood flow at the center of growing tumor, trastuzumab might not have reached or bound to all receptors [115]. However, when we labeled trastuzumab with ^{227}Th or ^{177}Lu, it demonstrated anti-tumor effects. Therefore, we believe that the clinical effects of trastuzumab can be enhanced when labelled with ^{227}Th-or ^{177}Lu.

7.10 Normal tissue toxicity

Normal tissue functions (liver, kidney and bone marrow) remained intact after administration of both RICs. Maximum tolerated activity reflects the tolerability of whole body functions after treatment. For ^{227}Th-conjugates maximum tolerated activity was 1000 kBq/kg (Table 2). In comparison to ^{225}Ac-conjugates (a radionuclide with long half life) [28] maximum tolerated activity was higher for ^{227}Th-trastuzumab than for ^{225}Ac-conjugates [116-118]. The reason for the lower MTA for ^{225}Ac-conjugates could be probably short half life of daughter nuclide of ^{225}Ac which produce higher immediate activity [28]. For ^{177}Lu-conjugates, maximum tolerated activity of 1000 MBq/kg of ^{177}Lu-1033-BR96 has been reported [119].

Although bone marrow toxicity is generally the dose limiting factor in RICs testing, renal toxicity has been also observed for ^{225}Ac and ^{213} Bi [28]. A transient decrease of WBC count was seen in first few weeks after the administration of highest dosages of ^{227}Th-

trastuzumab, which may partly was due to bone-relocalization of ^{223}Ra. Similar results were observed after ^{227}Th-rituximab in mice bearing NHL tumor [37] (Table 2). Maximum tolerated dose to the bone marrow was more than 2.1 Gy for ^{227}Th-rituximab [28]. Dosimetry methods used in preclinical studies to determine the maximum tolerated dose were different from each other and therefore also difficult to compare different treatment groups [28].

7.11 Conclusion

Regulatory authorities usually require toxicity data from at least one species before allowing studies in humans with a radiopharmaceutical. Administration of ^{227}Th-RICs, both in the present and previous studies, showed considerably good therapeutic effects with very low toxicity. Therefore, we believe that this radionuclide (^{227}Th) has a potential to be tested in clinics in patients with micrometastatic disease. While, low LET emitting ^{177}Lu-trastuzumab has also showed treatment potential at high dose. This shows that ^{177}Lu-trastuzumab needs more preclinical evaluations, including determination of maximum tolerated dose (MTD), in both solid (HER2 expressing tumors) and haematological tumors.

8 Conclusions and future prospects

8.1 Conclusions

1. Administration of high LET ^{227}Th-labeled and low LET ^{177}Lu-labeled trastuzumab was safe at the activity concentrations used.
2. ^{227}Th-trastuzumab inhibited growth of HER2 expressing carcinomas in a dose dependent manner and improved survival of treated mice.
3. RBE of ^{227}Th-trastuzumab was superior to ^{177}Lu-trastuzumab when compared at relatively low radiation dose to the tumor.
4. Therapeutic index of ^{177}Lu-trastuzumab was superior to that of ^{227}Th-trastuzumab.
5. A transient decrease of white blood cells (WBC) was the only toxicity observed with administration of higher dosages of both RICs except 1000 kBq/kg of ^{227}Th-trastuzumab where weight loss was also observed in few animals.

8.2 Future prospects

1. Comparison of ^{227}Th-trastuzumab and ^{177}Lu-trastuzumab in micrometastases or intraperitoneal mouse model can be started. In addition, maximum tolerated doses (MTD) should be determined for both RICs.
2. Xenografts sizes used were much larger than the size of the micrometastases in breast and ovarian cancer patients. Therefore, we suggest testing ^{227}Th-trastuzumab as an adjuvant treatment in breast and ovarian cancers patients with micrometastases.
3. Clinical trails of ^{227}Th-RICs in patients with a high risk of developing bone metastasis warrant further studies, due to ^{223}Ra affinity to bone.

9 References

1. Winau F, Westphal O, Winau R. Paul Ehrlich-in search of the magic bullet. Microbes Infect 2004;6:786-789.

2. Hargittai RbI. K, ÂhlerΓÇÖs Invention Klaus Eichmann (Max-Planck-Institut fur Immunbiologie, Freiburg, Germany), Birkhauser Verlag, Basel. 2005. 223 pp. USD 65.95; EUR 51.36. ISBN 3-7643-7173-0. Structural Chemistry 2006;17:161-162.

3. Steinitz M. Three decades of human monoclonal antibodies: past, present and future developments. Hum Antibodies 2009;18:1-10.

4. Boswell CA, Brechbiel MW. Development of radioimmunotherapeutic and diagnostic antibodies: an inside-out view. Nucl Med Biol 2007;34:757-778.

5. Winter G, Harris WJ. Humanized antibodies. Trends Pharmacol Sci 1993;14:139-143.

6. Carter P. Improving the efficacy of antibody-based cancer therapies. Nat Rev Cancer 2001;1:118-129.

7. Boekhout AH, Beijnen JH, Schellens JH. Trastuzumab. Oncologist 2011;16:800-810.

8. Shepard HM, Jin P, Slamon DJ, Pirot Z, Maneval DC. Herceptin. Handb Exp Pharmacol 2008;183-219.

9. Bookman MA. Standard treatment in advanced ovarian cancer in 2005: the state of the art. Int J Gynecol Cancer 2005;15 Suppl 3:212-220.

10. Bookman MA, Darcy KM, Clarke-Pearson D, Boothby RA, Horowitz IR. Evaluation of monoclonal humanized anti-HER2 antibody, trastuzumab, in patients with recurrent or refractory ovarian or primary peritoneal carcinoma with overexpression of HER2: a phase II trial of the Gynecologic Oncology Group. J Clin Oncol 2003;21:283-290.

11. Carlsson J. EGFR-Family Expression and Implications for Targeted Radionuclide Therapy Targeted Radionuclide Tumor Therapy. In: Stigbrand T, Carlsson J, Adams GP, editors. Springer Netherlands, 2008: 25-58.

12. Carlsson J, Nordgren H, Sjostrom J, Wester K, Villman K, Bengtsson NO, Ostenstad B, Lundqvist H, Blomqvist C. HER2 expression in breast cancer primary tumours and corresponding metastases. Original data and literature review. Br J Cancer 2004;90:2344-2348.

13. Milenic DE, Wong KJ, Baidoo KE, Nayak TK, Regino CA, Garmestani K, Brechbiel MW. Targeting HER2: a report on the in vitro and in vivo pre-clinical data supporting trastuzumab as a radioimmunoconjugate for clinical trials. MAbs 2010;2:550-564.

14. Milenic DE, Brady ED, Brechbiel MW. Antibody-targeted radiation cancer therapy. Nat Rev Drug Discov 2004;3:488-499.

15. Larsen RH, Borrebaek J, Dahle J, Melhus KB, Krogh C, Valan MH, Bruland OS. Preparation of TH227-labeled radioimmunoconjugates, assessment of serum stability and antigen binding ability. Cancer Biother Radiopharm 2007;22:431-437.

16. Brechbiel MW. Bifunctional chelates for metal nuclides. Q J Nucl Med Mol Imaging 2008;52:166-173.

17. Fink-Bennett DM, Thomas K. 90Y-Ibritumomab Tiuxetan in the Treatment of Relapsed or Refractory B-Cell Non-HodgkinΓÇÖs Lymphoma. Journal of Nuclear Medicine Technology 2003;31:61-68.

18. Knox SJ, Meredith RF. Clinical radioimmunotherapy. Semin Radiat Oncol 2000;10:73-93.

19. Hall EJ, Giaccia AJ. Radiobiology for the radiologist. 5 ed. Philadelphia: Lippincott Williams & Wilkins, 2006.

20. Boyd M, Ross SC, Dorrens J, Fullerton NE, Tan KW, Zalutsky MR, Mairs RJ. Radiation-induced biologic bystander effect elicited in vitro by targeted radiopharmaceuticals labeled with alpha-, beta-, and auger electron-emitting radionuclides. J Nucl Med 2006;47:1007-1015.

21. Michael Joiner and Albert Van der Kogel. Basic Clinical Radiobiology. 2012;Fourth edition

22. Pouget JP, Navarro-Teulon I, Bardies M, Chouin N, Cartron G, Pelegrin A, Azria D. Clinical radioimmunotherapy--the role of radiobiology. Nat Rev Clin Oncol 2011;8:720-734.

23. Attix F. Introduction to radiological physics and radiation dosimetry. WILEY-VCH W, editor. 2012;

24. Sgouros G, Roeske JC, McDevitt MR, Palm S, Allen BJ, Fisher DR, Brill AB, Song H, Howell RW, Akabani G, Bolch WE, Brill AB, Fisher DR, Howell RW, Meredith RF, Sgouros G, Wessels BW, Zanzonico PB. MIRD Pamphlet No. 22 (abridged): radiobiology and dosimetry of alpha-particle emitters for targeted radionuclide therapy. J Nucl Med 2010;51:311-328.

25. Pouget JP, Mather SJ. General aspects of the cellular response to low- and high-LET radiation. Eur J Nucl Med 2001;28:541-561.

26. Dale RG. Dose-rate effects in targeted radiotherapy. Phys Med Biol 1996;41:1871-1884.

27. Steel GG. Basic Clinical Radiobiology. 3 ed. New York: Arnold, 2002.

28. Dahle J, Abbas N, Bruland OS, Larsen RH. Toxicity and relative biological effectiveness of alpha emitting radioimmunoconjugates. Current Radiopharmaceuticals 2011;4:321-328.

29. McDevitt MR, Sgouros G, Finn RD, Humm JL, Jurcic JG, Larson SM, Scheinberg DA. Radioimmunotherapy with alpha-emitting nuclides. Eur J Nucl Med 1998;25:1341-1351.

30. O'Donnell RT, DeNardo GL, Kukis DL, Lamborn KR, Shen S, Yuan A, Goldstein DS, Carr CE, Mirick GR, DeNardo SJ. A clinical trial of radioimmunotherapy with 67Cu-2IT-BAT-Lym-1 for non-Hodgkin's lymphoma. J Nucl Med 1999;40:2014-2020.

31. Lam M, Klerk J, Rijk P. 186Re-HEDP for metastatic bone pain in breast cancer patients. European Journal of Nuclear Medicine and Molecular Imaging 2004;31:S162-S170.

32. Lauter A, Strumpf A, Platzbecker U, Schetelig J, Wermke M, Radke J, Kiani A, Wunderlich G, Thiede C, Ehninger G, Kotzerke J, Bornhauser M. 188Re anti-CD66 radioimmunotherapy combined with reduced-intensity conditioning and in-vivo T cell depletion in elderly patients undergoing allogeneic haematopoietic cell transplantation. Br J Haematol 2010;148:910-917.

33. Dahle J, Jonasdottir TJ, Heyerdahl H, Nesland JM, Borrebaek J, Hjelmerud AK, Larsen RH. Assessment of long-term radiotoxicity after treatment with the low-dose-rate alpha-particle-emitting radioimmunoconjugate (227)Th-rituximab. Eur J Nucl Med Mol Imaging 2010;37:93-102.

34. Dahle J, Borrebaek J, Melhus KB, Bruland OS, Salberg G, Olsen DR, Larsen RH. Initial evaluation of ^{227}Th-p-benzyl-DOTA-rituximab for low-dose rate alpha-particle radioimmunotherapy. Nucl Med Biol 2006;33:271-279.

35. Abbas N, Heyerdahl H, Bruland OS, Borrebaek J, Nesland J, Dahle J. Experimental alpha-particle radioimmunotherapy of breast cancer using 227Th-labeled p-benzyl-DOTA-trastuzumab. EJNMMI Res 2011;1:18.

36. Abbas N, Bruland ØS, Brevik EM, Dahle J. Preclinical evaluation of 227Th-labeled and 177Lu-labeled trastuzumab in mice with HER-2-positive ovarian cancer xenografts. Nuclear Medicine Communications 9000;Publish Ahead of Print

37. Dahle J, Borrebaek J, Jonasdottir TJ, Hjelmerud AK, Melhus KB, Bruland OS, Press OW, Larsen RH. Targeted cancer therapy with a novel low-dose rate alpha-emitting radioimmunoconjugate. Blood 2007;110:2049-2056.

38. Dahle J, Bruland OS, Larsen RH. Relative biologic effects of low-dose-rate alpha-emitting 227Th-rituximab and beta-emitting 90Y-tiuexetan-ibritumomab versus external beam X-radiation. Int J Radiat Oncol Biol Phys 2008;72:186-192.

39. Heyerdahl H, Krogh C, Borrebaek J, Larsen A, Dahle J. Treatment of HER2-expressing breast cancer and ovarian cancer cells with alpha particle-emitting 227Th-trastuzumab. Int J Radiat Oncol Biol Phys 2011;79:563-570.

40. Heyerdahl H, Abbas N, Brevik EM, Mollatt C, Dahle J. Fractionated Therapy of HER2-Expressing Breast and Ovarian Cancer Xenografts in Mice with Targeted Alpha Emitting 227Th-DOTA-p-benzyl-trastuzumab. PLoS ONE 2012;7:e42345.

41. Persson M, Gedda L, Lundqvist H, Tolmachev V, Nordgren H, Malmstrom PU, Carlsson J. [177Lu]pertuzumab: experimental therapy of HER-2-expressing xenografts. Cancer Res 2007;67:326-331.

42. Rasaneh S, Rajabi H, Babaei MH, Daha FJ. 177Lu labeling of Herceptin and preclinical validation as a new radiopharmaceutical for radioimmunotherapy of breast cancer. Nucl Med Biol 2010;37:949-955.

43. Wild D, Frischknecht M, Zhang H, Morgenstern A, Bruchertseifer F, Boisclair J, Provencher-Bolliger A, Reubi JC, Maecke HR. Alpha- versus beta-particle radiopeptide therapy in a human prostate cancer model (213Bi-DOTA-PESIN and 213Bi-AMBA versus 177Lu-DOTA-PESIN). Cancer Res 2011;71:1009-1018.

44. Chopra A. 177Lu-Labeled humanized monoclonal antibody against human epidermal growth factor receptor 2. 2004;

45. Song H, Hobbs RF, Vajravelu R, Huso DL, Esaias C, Apostolidis C, Morgenstern A, Sgouros G. Radioimmunotherapy of breast cancer metastases with alpha-particle emitter 225Ac: comparing efficacy with 213Bi and 90Y. Cancer Res 2009;69:8941-8948.

46. Boskovitz A, McLendon RE, Okamura T, Sampson JH, Bigner DD, Zalutsky MR. Treatment of HER2-positive breast carcinomatous meningitis with intrathecal administration of alpha-particle-emitting (211)At-labeled trastuzumab. Nucl Med Biol 2009;36:659-669.

47. Palm S, Back T, Claesson I, Danielsson A, Elgqvist J, Frost S, Hultborn R, Jensen H, Lindegren S, Jacobsson L. Therapeutic efficacy of astatine-211-labeled trastuzumab on radioresistant SKOV-3 tumors in nude mice. Int J Radiat Oncol Biol Phys 2007;69:572-579.

48. Milenic DE, Brady ED, Garmestani K, Albert PS, Abdulla A, Brechbiel MW. Improved efficacy of alpha-particle-targeted radiation therapy: dual targeting of human epidermal growth factor receptor-2 and tumor-associated glycoprotein 72. Cancer 2010;116:1059-1066.

49. Dahle J, Larsen RH. Targeted alpha-particle therapy with 227Th-labeled antibodies. Current Radiopharmaceuticals 2008;1:209-214.

50. Dahle J, Krogh C, Melhus KB, Borrebaek J, Larsen RH, Kvinnsland Y. In Vitro Cytotoxicity of Low-Dose-Rate Radioimmunotherapy by the Alpha-Emitting Radioimmunoconjugate Thorium-227-DOTA-Rituximab. Int J Radiat Oncol Biol Phys 2009;

51. DeNardo SJ, DeNardo GL, O'Grady LF, Hu E, Sytsma VM, Mills SL, Levy NB, Macey DJ, Miller CH, Epstein AL. Treatment of B cell malignancies with 131I Lym-1 monoclonal antibodies. Int J Cancer Suppl 1988;3:96-101.

52. Press OW, Eary JF, Appelbaum FR, Martin PJ, Badger CC, Nelp WB, Glenn S, Butchko G, Fisher D, Porter B, . Radiolabeled-antibody therapy of B-cell lymphoma with autologous bone marrow support. N Engl J Med 1993;329:1219-1224.

53. Press OW, Eary JF, Badger CC, Martin PJ, Appelbaum FR, Levy R, Miller R, Brown S, Nelp WB, Krohn KA, . Treatment of refractory non-Hodgkin's lymphoma with radiolabeled MB-1 (anti-CD37) antibody. J Clin Oncol 1989;7:1027-1038.

54. Kaminski MS, Fig LM, Zasadny KR, Koral KF, DelRosario RB, Francis IR, Hanson CA, Normolle DP, Mudgett E, Liu CP, . Imaging, dosimetry, and radioimmunotherapy with iodine 131-labeled anti-CD37 antibody in B-cell lymphoma. J Clin Oncol 1992;10:1696-1711.

55. Morschhauser F, Kraeber-Bodere F, Wegener WA, Harousseau JL, Petillon MO, Huglo D, Trumper LH, Meller J, Pfreundschuh M, Kirsch CM, Naumann R, Kropp J, Horne H, Teoh N, Le GS, Bodet-Milin C, Chatal JF, Goldenberg DM. High rates of durable responses with anti-CD22 fractionated radioimmunotherapy: results of a multicenter, phase I/II study in non-Hodgkin's lymphoma. J Clin Oncol 2010;28:3709-3716.

56. Linden O, Hindorf C, Cavallin-Stahl E, Wegener WA, Goldenberg DM, Horne H, Ohlsson T, Stenberg L, Strand SE, Tennvall J. Dose-fractionated radioimmunotherapy in non-Hodgkin's lymphoma using DOTA-conjugated, 90Y-radiolabeled, humanized anti-CD22 monoclonal antibody, epratuzumab. Clin Cancer Res 2005;11:5215-5222.

57. Steiner M, Neri D. Antibody-radionuclide conjugates for cancer therapy: historical considerations and new trends. Clin Cancer Res 2011;17:6406-6416.

58. Witzig TE, Gordon LI, Cabanillas F, Czuczman MS, Emmanouilides C, Joyce R, Pohlman BL, Bartlett NL, Wiseman GA, Padre N, Grillo-Lopez AJ, Multani P, White CA. Randomized controlled trial of yttrium-90-labeled ibritumomab tiuxetan radioimmunotherapy versus rituximab immunotherapy for patients with relapsed or refractory low-grade, follicular, or transformed B-cell non-Hodgkin's lymphoma. J Clin Oncol 2002;20:2453-2463.

59. Goldenberg DM, Sharkey RM. Recent progress in cancer therapy with radiolabeled monoclonal antibodies. Therapeutic Delivery 2011;2:675-679.

60. Kaminski MS, Tuck M, Estes J, Kolstad A, Ross CW, Zasadny K, Regan D, Kison P, Fisher S, Kroll S, Wahl RL. 131I-tositumomab therapy as initial treatment for follicular lymphoma. N Engl J Med 2005;352:441-449.

61. Leahy MF, Turner JH. Radioimmunotherapy of relapsed indolent non-Hodgkin lymphoma with 131I-rituximab in routine clinical practice: 10-year single-institution experience of 142 consecutive patients. Blood 2011;117:45-52.

62. Burke JM, Caron PC, Papadopoulos EB, Divgi CR, Sgouros G, Panageas KS, Finn RD, Larson SM, O'Reilly RJ, Scheinberg DA, Jurcic JG. Cytoreduction with iodine-131-anti-CD33 antibodies before bone marrow transplantation for advanced myeloid leukemias. Bone Marrow Transplant 2003;32:549-556.

63. Pagel JM, Appelbaum FR, Eary JF, Rajendran J, Fisher DR, Gooley T, Ruffner K, Nemecek E, Sickle E, Durack L, Carreras J, Horowitz MM, Press OW, Gopal AK, Martin PJ, Bernstein ID, Matthews DC. 131I-anti-CD45 antibody plus busulfan and cyclophosphamide before allogeneic hematopoietic cell transplantation for treatment of acute myeloid leukemia in first remission. Blood 2006;107:2184-2191.

64. Pagel JM, Gooley TA, Rajendran J, Fisher DR, Wilson WA, Sandmaier BM, Matthews DC, Deeg HJ, Gopal AK, Martin PJ, Storb RF, Press OW, Appelbaum FR. Allogeneic hematopoietic cell transplantation after conditioning with 131I-anti-CD45 antibody plus fludarabine and low-dose total body irradiation for elderly patients with advanced acute myeloid leukemia or high-risk myelodysplastic syndrome. Blood 2009;114:5444-5453.

65. Ringhoffer M, Blumstein N, Neumaier B, Glatting G, von HS, Buchmann I, Wiesneth M, Kotzerke J, Zenz T, Buck AK, Schauwecker P, Stilgenbauer S, Dohner H, Reske SN, Bunjes D. 188Re or 90Y-labelled anti-CD66 antibody as part of a dose-reduced conditioning regimen for patients with acute leukaemia or myelodysplastic syndrome over the age of 55: results of a phase I-II study. Br J Haematol 2005;130:604-613.

66. Matthews DC, Appelbaum FR, Eary JF, Fisher DR, Durack LD, Bush SA, Hui TE, Martin PJ, Mitchell D, Press OW, . Development of a marrow transplant regimen for acute leukemia using targeted hematopoietic irradiation delivered by 131I-labeled anti-CD45 antibody, combined with cyclophosphamide and total body irradiation. Blood 1995;85:1122-1131.

67. Jurcic JG, Larson SM, Sgouros G, McDevitt MR, Finn RD, Divgi CR, Ballangrud AM, Hamacher KA, Ma D, Humm JL, Brechbiel MW, Molinet R, Scheinberg DA. Targeted alpha particle immunotherapy for myeloid leukemia. Blood 2002;100:1233-1239.

68. Rosenblat TL, McDevitt MR, Mulford DA, Pandit-Taskar N, Divgi CR, Panageas KS, Heaney ML, Chanel S, Morgenstern A, Sgouros G, Larson SM, Scheinberg DA, Jurcic JG. Sequential cytarabine and alpha-particle immunotherapy with bismuth-213-lintuzumab (HuM195) for acute myeloid leukemia. Clin Cancer Res 2010;16:5303-5311.

69. Welt S, Divgi CR, Real FX, Yeh SD, Garin-Chesa P, Finstad CL, Sakamoto J, Cohen A, Sigurdson ER, Kemeny N, . Quantitative analysis of antibody localization in human metastatic colon cancer: a phase I study of monoclonal antibody A33. J Clin Oncol 1990;8:1894-1906.

70. Liersch T, Meller J, Kulle B, Behr TM, Markus P, Langer C, Ghadimi BM, Wegener WA, Kovacs J, Horak ID, Becker H, Goldenberg DM. Phase II trial of carcinoembryonic antigen radioimmunotherapy with 131I-labetuzumab after salvage resection of colorectal metastases in the liver: five-year safety and efficacy results. J Clin Oncol 2005;23:6763-6770.

71. Verheijen RH, Massuger LF, Benigno BB, Epenetos AA, Lopes A, Soper JT, Markowska J, Vyzula R, Jobling T, Stamp G, Spiegel G, Thurston D, Falke T, Lambert J, Seiden MV. Phase III trial of intraperitoneal therapy with yttrium-90-labeled HMFG1 murine monoclonal antibody in patients with epithelial ovarian cancer after a surgically defined complete remission. J Clin Oncol 2006;24:571-578.

72. Zalutsky MR, Reardon DA, Akabani G, Coleman RE, Friedman AH, Friedman HS, McLendon RE, Wong TZ, Bigner DD. Clinical experience with alpha-particle emitting 211At: treatment of recurrent

brain tumor patients with 211At-labeled chimeric antitenascin monoclonal antibody 81C6. J Nucl Med 2008;49:30-38.

73. Andersson H, Cederkrantz E, Back T, Divgi C, Elgqvist J, Himmelman J, Horvath G, Jacobsson L, Jensen H, Lindegren S, Palm S, Hultborn R. Intraperitoneal alpha-particle radioimmunotherapy of ovarian cancer patients: pharmacokinetics and dosimetry of (211)At-MX35 F(ab')2--a phase I study. J Nucl Med 2009;50:1153-1160.

74. Behr TM, Salib AL, Liersch T, Behe M, Angerstein C, Blumenthal RD, Fayyazi A, Sharkey RM, Ringe B, Becker H, Wormann B, Hiddemann W, Goldenberg DM, Becker W. Radioimmunotherapy of small volume disease of colorectal cancer metastatic to the liver: preclinical evaluation in comparison to standard chemotherapy and initial results of a phase I clinical study. Clin Cancer Res 1999;5:3232s-3242s.

75. Sharkey RM, Goldenberg DM. Cancer radioimmunotherapy. Immunotherapy 2011;3:349-370.

76. Tempero M, Leichner P, Baranowska-Kortylewicz J, Harrison K, Augustine S, Schlom J, Anderson J, Wisecarver J, Colcher D. High-dose therapy with 90Yttrium-labeled monoclonal antibody CC49: a phase I trial. Clin Cancer Res 2000;6:3095-3102.

77. Sharkey RM, Goldenberg DM, Murthy S, Pinsky H, Vagg R, Pawlyk D, Siegel JA, Wong GY, Gascon P, Izon DO, . Clinical evaluation of tumor targeting with a high-affinity, anticarcinoembryonic-antigen-specific, murine monoclonal antibody, MN-14. Cancer 1993;71:2082-2096.

78. Forero A, Meredith RF, Khazaeli MB, Shen S, Grizzle WE, Carey D, Busby E, Lobuglio AF, Robert F. Phase I study of 90Y-CC49 monoclonal antibody therapy in patients with advanced non-small cell lung cancer: effect of chelating agents and paclitaxel co-administration. Cancer Biother Radiopharm 2005;20:467-478.

79. Richman CM, DeNardo SJ, O'Donnell RT, Yuan A, Shen S, Goldstein DS, Tuscano JM, Wun T, Chew HK, Lara PN, Kukis DL, Natarajan A, Meares CF, Lamborn KR, DeNardo GL. High-dose radioimmunotherapy combined with fixed, low-dose paclitaxel in metastatic prostate and breast cancer by using a MUC-1 monoclonal antibody, m170, linked to indium-111/yttrium-90 via a cathepsin cleavable linker with cyclosporine to prevent human anti-mouse antibody. Clin Cancer Res 2005;11:5920-5927.

80. Sharkey RM, Hajjar G, Yeldell D, Brenner A, Burton J, Rubin A, Goldenberg DM. A phase I trial combining high-dose 90Y-labeled humanized anti-CEA monoclonal antibody with doxorubicin and peripheral blood stem cell rescue in advanced medullary thyroid cancer. J Nucl Med 2005;46:620-633.

81. Wong JY, Shibata S, Williams LE, Kwok CS, Liu A, Chu DZ, Yamauchi DM, Wilczynski S, Ikle DN, Wu AM, Yazaki PJ, Shively JE, Doroshow JH, Raubitschek AA. A Phase I trial of 90Y-anti-carcinoembryonic antigen chimeric T84.66 radioimmunotherapy with 5-fluorouracil in patients with metastatic colorectal cancer. Clin Cancer Res 2003;9:5842-5852.

82. Jemal A, Bray F, Center MM, Ferlay J, Ward E, Forman D. Global cancer statistics. CA Cancer J Clin 2011;61:69-90.

83. Cancer in Norway 2009.Cancer Incidence, Mortality,Survival and Prevalence in Norway. 2011; Oslo, Cancer Registry of Norway 2011.

84. Vodermaier A. Breast cancer treatment and cognitive function: the current state of evidence, underlying mechanisms and potential treatments. Womens Health (Lond Engl) 2009;5:503-516.

85. Aapro M, Monfardini S, Jirillo A, Basso U. Management of primary and advanced breast cancer in older unfit patients (medical treatment). Cancer Treatment Reviews 2009;35:503-508.

86. Marin AP, Sanchez AR, Arranz EE, Aunon PZ, Baron MG. Adjuvant chemotherapy for breast cancer and cognitive impairment. South Med J 2009;102:929-934.

87. Wolff AC, Davidson NE. Primary systemic therapy in operable breast cancer. J Clin Oncol 2000;18:1558-1569.

88. Wolff AC. Systemic therapy. Curr Opin Oncol 2002;14:600-608.

89. Ruiterkamp J, Ernst MF. The role of surgery in metastatic breast cancer. European Journal of Cancer 2011;47, Supplement 3:S6-S22.

90. Abeloff MD WAWBea. Cancer of the breast. Abeloff,s Clinical Oncology 4th ed.Edinburgh:Churchill Livingstone. 2008:.pp1875-943.

91. Guarneri V, Conte PF. The curability of breast cancer and the treatment of advanced disease. Eur J Nucl Med Mol Imaging 2004;31 Suppl 1:S149-S161.

92. Lonning PE, Knappskog S, Staalesen V, Chrisanthar R, Lillehaug JR. Breast cancer prognostication and prediction in the postgenomic era. Ann Oncol 2007;18:1293-1306.

93. American Cancer Society. Global cancer facts and figures 2007. Atlanta, GA: American Cancer Society,2008.

94. du BA, Luck HJ, Meier W, Adams HP, Mobus V, Costa S, Bauknecht T, Richter B, Warm M, Schroder W, Olbricht S, Nitz U, Jackisch C, Emons G, Wagner U, Kuhn W, Pfisterer J. A randomized clinical trial of cisplatin/paclitaxel versus carboplatin/paclitaxel as first-line treatment of ovarian cancer. J Natl Cancer Inst 2003;95:1320-1329.

95. Neijt JP, Engelholm SA, Tuxen MK, Sorensen PG, Hansen M, Sessa C, de Swart CA, Hirsch FR, Lund B, van Houwelingen HC. Exploratory phase III study of paclitaxel and cisplatin versus paclitaxel and carboplatin in advanced ovarian cancer. J Clin Oncol 2000;18:3084-3092.

96. Ozols RF, Bundy BN, Greer BE, Fowler JM, Clarke-Pearson D, Burger RA, Mannel RS, DeGeest K, Hartenbach EM, Baergen R. Phase III trial of carboplatin and paclitaxel compared with cisplatin and paclitaxel in patients with optimally resected stage III ovarian cancer: a Gynecologic Oncology Group study. J Clin Oncol 2003;21:3194-3200.

97. Aletti GD, Gallenberg MM, Cliby WA, Jatoi A, Hartmann LC. Current management strategies for ovarian cancer. Mayo Clin Proc 2007;82:751-770.

98. Heintz AP, Odicino F, Maisonneuve P, Quinn MA, Benedet JL, Creasman WT, Ngan HY, Pecorelli S, Beller U. Carcinoma of the ovary. FIGO 26th Annual Report on the Results of Treatment in Gynecological Cancer. Int J Gynaecol Obstet 2006;95 Suppl 1:S161-S192.

99. Berchuck A, Elbendary A, Havrilesky L, Rodriguez GC, Bast RC, Jr. Pathogenesis of ovarian cancers. J Soc Gynecol Investig 1994;1:181-190.

100. Camilleri-Broet S, Hardy-Bessard AC, Le TA, Paraiso D, Levrel O, Leduc B, Bain S, Orfeuvre H, Audouin J, Pujade-Lauraine E. HER-2 overexpression is an independent marker of poor prognosis of advanced primary ovarian carcinoma: a multicenter study of the GINECO group. Ann Oncol 2004;15:104-112.

101. Fisher DR. Radiation dosimetry for radioimmunotherapy. An overview of current capabilities and limitations. Cancer 1994;73:905-911.

102. Wessels BW, Syh JH, Meredith RF. Overview of dosimetry for Systemic Targeted Radionuclide Therapy (STaRT). Int J Radiat Oncol Biol Phys 2006;66:S39-S45.

103. Steffen AC, Gostring L, Tolmachev V, Palm S, Stenerlow B, Carlsson J. Differences in radiosensitivity between three HER2 overexpressing cell lines. Eur J Nucl Med Mol Imaging 2008;35:1179-1191.

104. Seidl C, Zockler C, Beck R, Quintanilla-Martinez L, Bruchertseifer F, Senekowitsch-Schmidtke R. 177Lu-immunotherapy of experimental peritoneal carcinomatosis shows comparable effectiveness to 213Bi-immunotherapy, but causes toxicity not observed with 213Bi. Eur J Nucl Med Mol Imaging 2011;38:312-322.

105. Back T, Andersson H, Divgi CR, Hultborn R, Jensen H, Lindegren S, Palm S, Jacobsson L. 211At Radioimmunotherapy of Subcutaneous Human Ovarian Cancer Xenografts: Evaluation of Relative Biologic Effectiveness of an {alpha}-Emitter In Vivo. J Nucl Med 2005;46:2061-2067.

106. Nilsson S, Larsen RH, Fossa SD, Balteskard L, Borch KW, Westlin JE, Salberg G, Bruland OS. First clinical experience with alpha-emitting radium-223 in the treatment of skeletal metastases. Clin Cancer Res 2005;11:4451-4459.

107. Nilsson S, Franzen L, Parker C, Tyrrell C, Blom R, Tennvall J, Lennernas B, Petersson U, Johannessen DC, Sokal M, Pigott K, Yachnin J, Garkavij M, Strang P, Harmenberg J, Bolstad B, Bruland OS. Bone-targeted radium-223 in symptomatic, hormone-refractory prostate cancer: a randomised, multicentre, placebo-controlled phase II study. Lancet Oncol 2007;8:587-594.

108. Parker C, Heinrich D, O'Sullivan JM, Fossa S, Chodacki A, Demkow T, Cross A, Bolstad B, Garcia-Vargas J, Sartor O. Overall Survival Benefit of Radium-223 Chloride (Alpharadin) in the Treatment of Patients with Symptomatic Bone Metastases in Castration-resistant Prostate Cancer (CRPC): a Phase III Randomized Trial (ALSYMPCA). European Journal of Cancer 2011;47, Supplement 2:3.

109. Sartor O, Hoskin P, Bruland OS. Targeted radio-nuclide therapy of skeletal metastases. Cancer Treat Rev 2012;

110. Scheinberg DA, Strand M. Radioimmunotherapy in experimental animal models: principles derived from models. Cancer Res 1990;50:962s-963s.

111. Karagiannis TC. Comparison of different classes of radionuclides for potential use in radioimmunotherapy. Hell J Nucl Med 2007;10:82-88.

112. Kennel SJ, Mirzadeh S, Eckelman WC, Waldmann TA, Garmestani K, Yordanov AT, Stabin MG, Brechbiel MW. Vascular-targeted radioimmunotherapy with the alpha-particle emitter 211At. Radiat Res 2002;157:633-641.

113. Kennel SJ, Chappell LL, Dadachova K, Brechbiel MW, Lankford TK, Davis IA, Stabin M, Mirzadeh S. Evaluation of 225Ac for vascular targeted radioimmunotherapy of lung tumors. Cancer Biother Radiopharm 2000;15:235-244.

114. Giovanella BC, Fogh J. The nude mouse in cancer research. Adv Cancer Res 1985;44:69-120.

115. Tannock IF. Tumor Physiology and Drug Resistance. Cancer and Metastasis Reviews 2001;20:123-132.

116. Jaggi JS, Seshan SV, McDevitt MR, Laperle K, Sgouros G, Scheinberg DA. Renal Tubulointerstitial Changes after Internal Irradiation with {alpha}-Particle-Emitting Actinium Daughters. J Am Soc Nephrol 2005;16:2677-2689.

117. McDevitt MR, Ma D, Lai LT, Simon J, Borchardt P, Frank RK, Wu K, Pellegrini V, Curcio MJ, Miederer M, Bander NH, Scheinberg DA. Tumor therapy with targeted atomic nanogenerators. Science 2001;294:1537-1540.

118. Miederer M, McDevitt MR, Sgouros G, Kramer K, Cheung NK, Scheinberg DA. Pharmacokinetics, dosimetry, and toxicity of the targetable atomic generator, 225Ac-HuM195, in nonhuman primates. J Nucl Med 2004;45:129-137.

119. Mårtensson L, Wang Z, Nilsson R, Ohlsson T, Senter P, Sjogren HO, Strand SE, Tennvall J. Determining Maximal Tolerable Dose of the Monoclonal Antibody BR96 Labeled with 90Y or 177Lu in Rats: Establishment of a Syngeneic Tumor Model to Evaluate Means to Improve Radioimmunotherapy. Clinical Cancer Research 2005;11:7104s-7108s.

I

Abbas et al. EJNMMI Research 2011, 1:18
http://www.ejnmmires.com/content/1/1/18

EJNMMI Research
a SpringerOpen Journal

ORIGINAL RESEARCH Open Access

Experimental α-particle radioimmunotherapy of breast cancer using ^{227}Th-labeled p-benzyl-DOTA-trastuzumab

Nasir Abbas[1*], Helen Heyerdahl[1], Øyvind S Bruland[2,3], Jørgen Borrebæk[5], Jahn Nesland[4] and Jostein Dahle[1]

Abstract

Background: The aim of the present study was to explore the biodistribution, normal tissue toxicity, and therapeutic efficacy of the internalizing low-dose rate alpha-particle-emitting radioimmunoconjugate ^{227}Th-trastuzumab in mice with HER2-expressing breast cancer xenografts.

Methods: Biodistribution of ^{227}Th-trastuzumab and ^{227}Th-rituximab in nude mice bearing SKBR-3 xenografts were determined at different time points after injection. Tumor growth was measured after administration of ^{227}Th-trastuzumab, ^{227}Th-rituximab, cold trastuzumab, and saline. The toxicity of ^{227}Th-trastuzumab was evaluated by measurements of body weight, blood cell, and clinical chemistry parameters, as well as histological examination of tissue specimens.

Results: The tumor uptake reached peak levels of 34% ID/g (4.6 kBq/g) 3 days after injection of 400 kBq/kg of ^{227}Th-trastuzumab. The absorbed radiation dose to tumor was 2.9 Gy, while it was 2.4 Gy to femur due to uptake of the daughter nuclide ^{223}Ra in bone; the latter already explored in clinical phases I and II trials without serious toxicity. A significant dose-dependent antitumor effect was observed for dosages of 200, 400, and 600 kBq/kg of ^{227}Th-trastuzumab but no effect of 400 and 600 kBq/kg ^{227}Th-rituximab (non-tumor binding). No serious delayed bone marrow or normal organ toxicity was observed, but there was a statistical significant reduction in blood cell parameters for the highest-dose group of ^{227}Th-trastuzumab treatment.

Conclusion: Internalizing ^{227}Th-trastuzumab therapy was well tolerated and resulted in a dose-dependent inhibition of breast cancer xenograft growth. These results warrant further preclinical studies aiming at a clinical trial in breast cancer patients with metastases to bone.

Keywords: alpha radiation, radioimmunotherapy, SKBR-3, trastuzumab, thorium-227

Background

Metastatic breast cancer patients have poor prognosis despite recent therapeutic advances [1]. The human epidermal growth factor receptor-2 (HER-2/neu) is a transmembrane receptor tyrosine kinase that is over-expressed in 25% to 30% of metastatic breast cancers and associated with more aggressive disease [2]. Trastuzumab (Herceptin®) is a humanized monoclonal antibody (mAb) directed against this antigen and shows clinical activity in women both with HER2/neu-overexpressing primary and metastatic breast cancer [3].

Tumor cell-targeted alpha emitters have the potential to improve therapy of hematological malignancies and micrometastatic disease. Alpha particles have a short path length (50 to 80 μm) and high linear energy transfer (LET approximately 100 keV/μm) and, thus, deliver a high amount of DNA-damaging energy to cells in close vicinity of their decay. However, no alpha-emitting radioimmunoconjugate (RIC) has reached phase III clinical trial yet due to poor physical or chemical characteristics, supply limitations, and high production costs for the most promising alpha emitters [4]. Recently, we have suggested ^{227}Th as a novel radionuclide for alpha-particle

* Correspondence: nasir.abbas@rr-research.no
[1]Department of Radiation Biology, Institute for Cancer Research, Oslo University Hospital, Montebello, 0310 Oslo, Norway
Full list of author information is available at the end of the article

radioimmunotherapy (RIT), as this radionuclide can be produced in clinically relevant amounts from β-decay of the long-term generator ^{227}Ac [5,6]. ^{227}Ac can be produced by thermal neutron irradiation of ^{226}Ra in a nuclear reactor. The yield of ^{227}Ac after purification is relatively high and ^{226}Ra is highly available, making the process cost efficient. ^{227}Ac has a half-life of 21.8 years and thus, would serve as a generator nuclide for ^{227}Th production for decades [7].

Thorium-227 decays via its alpha- and beta-emitting daughters ^{223}Ra, ^{219}Rn, ^{215}Po, ^{211}Pb, ^{211}Bi, and ^{207}Tl to stable 207 Pb. The long half-life of ^{227}Th ($T_{1/2}$ = 18.7 days) permits the tumor targeting and normal tissue clearance of a ^{227}Th-labeled RIC to occur before larger amounts of the daughter nuclide ^{223}Ra is generated. Upon decay, ^{223}Ra will detach from the antibody. Importantly, clinical trials have not shown worrisome toxicity of ^{223}Ra injected as a therapy for prostate cancer bone metastases [8,9]. Previously, we have shown that ^{227}Th conjugated to the monoclonal antibody rituximab was effective in treatment of mice with lymphoma xenografts and had a relatively low normal tissue toxicity [7,10,11].

The conjugation of trastuzumab with different alpha-particle-emitting radionuclides, i.e., ^{211}At, ^{225}Ac, and ^{213}Bi, has already been investigated by other groups [12-16]. The purpose of the present study was to determine the biodistribution, therapeutic effect, and toxicity of the low-dose rate alpha-particle-emitting RIC ^{227}Th-trastuzumab on HER2-expressing SKBR-3 xenografts. *In vitro* experiments have shown internalization of the ^{227}Th-trastuzumab/HER2 complex, retention of ^{227}Th, and a high toxic effect against single tumor cells [17]. The increased cytotoxic effect created by alpha particles may offer the opportunity to both improve the overall response rate of the trastuzumab treatment and also to treat patients with a lower HER2 expression.

Material and methods

Production of ^{227}Th and radiolabeling of monoclonal antibodies

^{227}Ac was produced through thermal neutron irradiation of ^{226}Ra followed by β^- decay of ^{227}Ra ($T_{1/2}$ = 42.2 min) to ^{227}Ac [18]. ^{227}Th was selectively retained from a ^{227}Ac decay mixture in 7 M HNO_3 by anion exchange chromatography [19].

Radiolabeling of trastuzumab (Herceptin®, Hoffmann-La Roche, Basel, Switzerland) and rituximab (MabThera, Hoffmann-La Roche) with ^{227}Th was performed at Algeta ASA, Oslo, Norway. The antibodies were conjugated with p-SCN-Bn-DOTA at pH 9 (sodium borate buffer) at 37°C over night. The number of DOTA molecules per antibody was approximately four as determined by LC/MS analysis. The conjugate was purified with a spin filter (Amicon, Millipore, USA) using 0.9% NaCl as running buffer removing daughter nuclides and non-chelated ^{227}Th. The purified antibody was distributed to microcentrifuge tubes (1 mg/tube) and freeze dried to keep a larger batch under stable conditions over a long period of time. The freeze-dried conjugate was dissolved in sodium acetate buffer pH 5.5 and added about 4 MBq of newly purified ^{227}Th in 0.01 M HCl. The reaction was done over night at 42°C in a thermomixer (Eppendorf, Hamburg, Germany). The chelate was purified on a NAP5 column (GE Healthcare, Little Chalfont, UK) using PBS as running buffer. The specific activity was 1000-1600 kBq/mg with regard to ^{227}Th.

Immunoreactivity

The immunoreactive fraction (IRF) of the radioimmunoconjugate ^{227}Th-trastuzumab was estimated by measuring the cell bound activity in a one point assay. SKOV-3 cells (2×10^7 cells/ml) in 200 μl PBS were used. Four million SKOV-3 cells in one vial of cells were blocked by incubating with 150 μg/ml cold trastuzumab for 15 min at 37°C. The cells in another vial were not blocked. About 500 cpm of ^{227}Th-trastuzumab was added to each vial and the cells were incubated for 2 h before washing and measurement of radioactivity with an automated gamma counter (Wizard, Packard Instrument Co., Downers Grove, IL, USA). IRF was 70% to 90%.

Animals

All procedures and experiments involving animals in this study were approved by the National Animal Research Authority and carried out according to the European Convention for the Protection of Vertebrates used for Scientific Purposes. The animals were maintained under pathogen-free conditions. Food and water were supplied *ad libitum*. Eight to 12 weeks old, institutionally bred female Balb/C nu/nu (NCR) mice, with an average weight of 20 to 27 g at the start of study, were used. Mice were anesthetized with subcutaneous injection of 0.05 ml Zoletil® mix (Virbac, Carros Cedex, France) before HER-2-positive breast cancer (SKBR-3) tumor fragments from xenografted animals (1 × 1 × 1 mm) were implanted subcutaneously. The xenografted tumor line originated from HER-2-positive breast cancer (SKBR-3) cells from American Type Culture Collection (Manassas, VA). Mice with growing tumors of diameters between 4 and 8 mm were included in the experiments. Mice were killed by cervical dislocation.

Biodistribution of ^{227}Th-labeled antibodies

The conjugates ^{227}Th-trastuzumab and ^{227}Th-rituximab were administered by tail vein injection of 100 μl (15 kBq) solution to each animal. For each conjugate and time point, a total of four to six animals were autopsied. Tumor and organs were measured for radioactivity content and

weighed. Samples of the injectates (10%) were used as references in the measurement procedure.

Thorium-227 and ^{223}Ra were measured using a solid-state photon well detector (GCW6021, Canberra, Meridan, CT, USA) coupled to a digital gamma ray spectrometer and analyzed using the computer software Apex™ version 1 (Canberra). For ^{227}Th, the 236 keV (abundance 17.6%) and 256 keV (abundance 9.5%) γ-ray lines were used and for ^{223}Ra the 154 keV (abundance 5.7%), 269 keV (abundance 13.9%), 324 keV (abundance 4%), and 338 keV (abundance 2.8%) γ-ray lines were used.

Calculation of absorbed dose

The total number of disintegrations, i.e., the cumulated activity, in various tissues from the time of injection of the preparation until no activity was left in the body was estimated by calculation of the area under the activity concentration versus time curves (AUC). For ^{227}Th-labeled antibodies, the absorbed radiation doses were calculated assuming dose contributions coming only from α-particle emissions with a mean α-energy (E_α) of 5.9 MeV for ^{227}Th and 26.4 MeV for ^{223}Ra with its daughters in equilibrium, and that there was a 100% absorption of the absorbed dose from the α-particle within a tissue, i.e., absorbed fraction equal to unity ($\phi = 1$). For α-particle radiation uniform distribution of radionuclides in the various tissues as well as no cross irradiation was assumed. Thus, the total absorbed dose to each organ was estimated by: Dose = $AUC_0^\infty \cdot E_\alpha$ (^{227}Th) + $AUC_0^\infty \cdot E_\alpha$ (^{223}Ra + daughters). Also for blood, the absorbed dose was calculated assuming 100% absorption of the α-particles, i.e., $\phi = 1$. This was obviously a simplification since in the capillaries there will probably be escape of α-particles beyond the blood.

Therapeutic studies

Mice were injected with a single dose of NaCl (control; $n = 10$), 20 μg ($n = 5$), 100 μg ($n = 6$), or 250 μg ($n = 5$) of cold trastuzumab; 200 kBq/kg ($n = 10$), 400 kBq/kg ($n = 11$), and 600 kBq/kg ($n = 12$) of ^{227}Th-trastuzumab; and 400 kBq/kg ($n = 9$) and 600 kBq/kg ($n = 10$) ^{227}Th-rituximab in 100 μl solution. Tumor growth and mouse weight were assessed three times a week in the first week before injection and the 3 weeks after injection; thereafter, weight, growth, and survival were assessed twice a week. Caliper measurements of perpendicular tumor diameters were used to estimate tumor volume by assuming ellipsoid shape. Mice with tumor diameter larger than 20 mm were killed. Mantley Cox log rank test was used to test for significant differences in surviving fraction of mice, which is defined as the fraction of mice that did not have to be sacrificed due to tumor diameter above 20 mm.

Evaluation of toxicity

Toxicity was evaluated in all treatment groups except ^{227}Th-rituximab. Approximately 100 to 200 μl of blood was collected from the vena saphena lateralis in 500 μl EDTA-coated tubes (Microtainer K2E tubes, Becton, Dickinson, NJ, USA) for blood cell counting. Blood samples were taken before and at 3, 6, and 8 to 10 weeks after start of the study. For control, a group of ten mice without tumor was injected with NaCl and sampled at the same time points for blood cell count. While for clinical chemistry data, the samples from this control group were taken after 8 weeks. Blood cells were counted in an automatic blood counter (Scil Vet ABC, Horiba ABX, Montpellier, France). In addition, when mice were sacrificed due to tumor size or weight loss, blood samples were collected by heart puncture into EDTA-coated tubes and also lithium heparin-coated tubes (Microtainer LH tubes, Becton, Dickinson) for analysis of clinical chemistry parameters. Clinical chemistry strips were used to assess the serum aspartate aminotransferase (AST), alanine aminotransferase (ALT), alkaline phosphatase (ALP), and urea level (Reflotron, Roche Diagnostics GmbH, Mannheim, Germany). Full blood samples (30 μl) were analyzed by a clinical chemistry analyzer (Reflovet, Roche Diagnostics).

At the end of the study, the lung, heart, kidney, spleen, small intestine, large intestine, liver, femur, skull, and tumor were fixed with formalin, cut in 5-μm slices, stained with hematoxylin and eosin, and analyzed by a pathologist to detect any pathological changes. Slides from cold trastuzumab and ^{227}Th-trastuzumab groups were compared to the slides of control groups.

Autoradiography

Mice bearing tumor xenografts were injected with 15 kBq of ^{227}Th-trastuzumab, corresponding to approximately 600 kBq/kg. Four animals were sacrificed by cervical dislocation 4 and 8 days after injection. Tumors were removed and immediately frozen in liquid nitrogen. Tissue sections of thickness 5 μm were used for exposure of Kodak Biomax MR-1 single-sided emulsion or Kodak Medical General Purpose Blue x-ray film (Eastman Kodak Company, Rochester, NY, USA). Films were exposed for 6 to 11 days at -80°C prior to development. Film patterns were compared to hematoxylin and eosin (H/E)-stained tissue sections.

Results

Biodistribution and dosimetry of ^{227}Th -trastuzumab and ^{227}Th-rituximab

The *in vivo* biodistribution profiles of ^{227}Th-trastuzumab, ^{227}Th-rituximab, and the daughter nuclide ^{223}Ra in nude mice with SKBR-3 xenografts at different time points after administration are shown in Figure 1. The

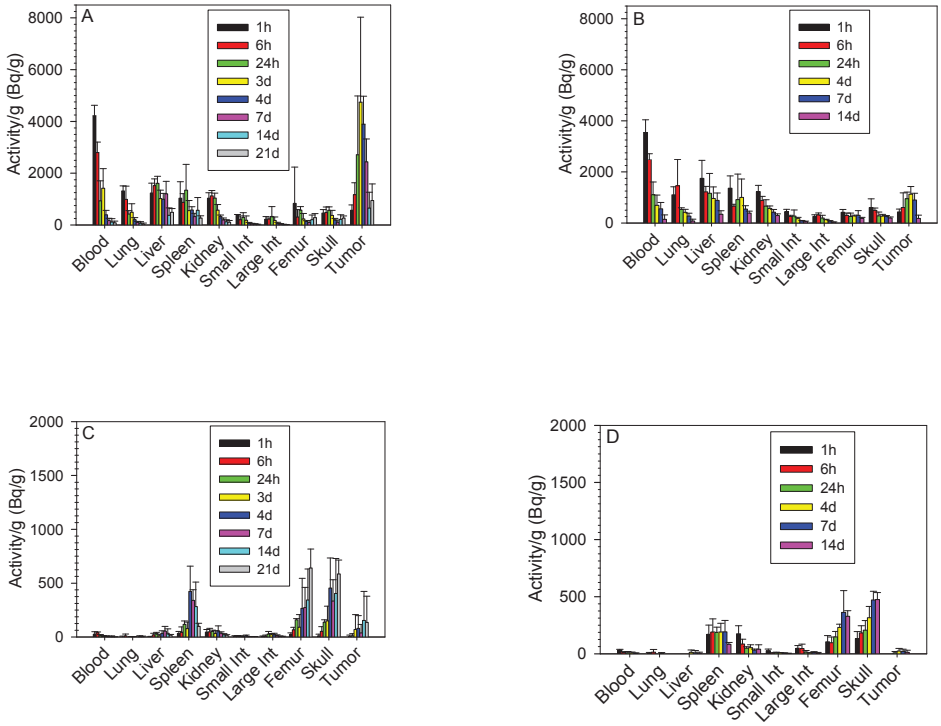

Figure 1 Biodistribution of ^{227}Th-conjugates and ^{223}Ra in mice with SKBR-3 xenografts. Biodistribution profile of ^{227}Th-trastuzumab (**a**) and daughter nuclide ^{223}Ra (**c**) after administration of ^{227}Th-trastuzumab, and biodistribution of ^{227}Th-rituximab (**b**) and daughter nuclide ^{223}Ra (**d**) after administration ^{227}Th-rituximab, in mice bearing SKBR-3 xenografts. The measured ^{227}Th activities were normalized to an injection of 400 kBq/kg bodyweight. Values are mean ± SD. *N* = 6 for each time point except at day 3, where *N* = 5.

maximum uptake of ^{227}Th-trastuzumab in tumor (4.6 kBq/g) occurred 3 days after injection (Figure 1a). There was a large difference between the amount of activity in tumor and in normal organs for ^{227}Th-trastuzumab. The uptake of non-tumor binding ^{227}Th-rituximab (Figure 1b) in tumor was significantly lower than the uptake of ^{227}Th-trastuzumab (Figure 1a). The ^{227}Th daughter nuclide ^{223}Ra was mainly localized to bone (femur and skull) but there were also some retention of ^{223}Ra in spleen, kidneys, and in tumor (Figure 1c, d).

The absorbed radiation dose in tumor was 2.9 ± 0.8 Gy for ^{227}Th-trastuzumab (Figure 2a) and 0.7 ± 0.1 Gy for ^{227}Th-rituximab (Figure 2b); both normalized to injections of 400 kBq/kg. Radiation doses were less than 2 Gy for all organs for both RICs, except for femur (2.4 ± 0.6 Gy) and skull (2.7 ± 0.6 Gy) in mice treated with ^{227}Th-trastuzumab.

Therapeutic efficacy

Growth of SKBR-3 tumor xenografts in mice treated with alpha-particle-emitting ^{227}Th-trastuzumab was compared with cold trastuzumab, non-tumor binding ^{227}Th-rituximab, as well as saline (controls; Figure 3). There was a large variability in tumor growth within treatment groups. Table 1 shows growth delays calculated from average tumor growth curves. The mean tumor growth in mice treated with cold trastuzumab (20, 100, and 250 μg/mice or approximately 0.8, 4, and 10 mg/kg body weight) or 400 and 600 kBq/kg ^{227}Th-rituximab was similar to the growth of the untreated controls. The dosage groups for cold trastuzumab and for ^{227}Th-rituximab in Table 1 and Figure 3b, c were pooled since there was no difference between them. For 200 and 400 kBq/kg ^{227}Th-trastuzumab, some of the tumors responded well to the treatment, while others did not (Figure 3d, e). The average delays to grow to a normalized tumor volume of 500 mm^3 were 7 and 23 days, respectively (Table 1). For 600 kBq/kg ^{227}Th-trastuzumab, all tumors responded to the treatment (Figure 3f) and the average growth delay to reach a tumor volume of 500 mm^3 was 45 days (Table 1).

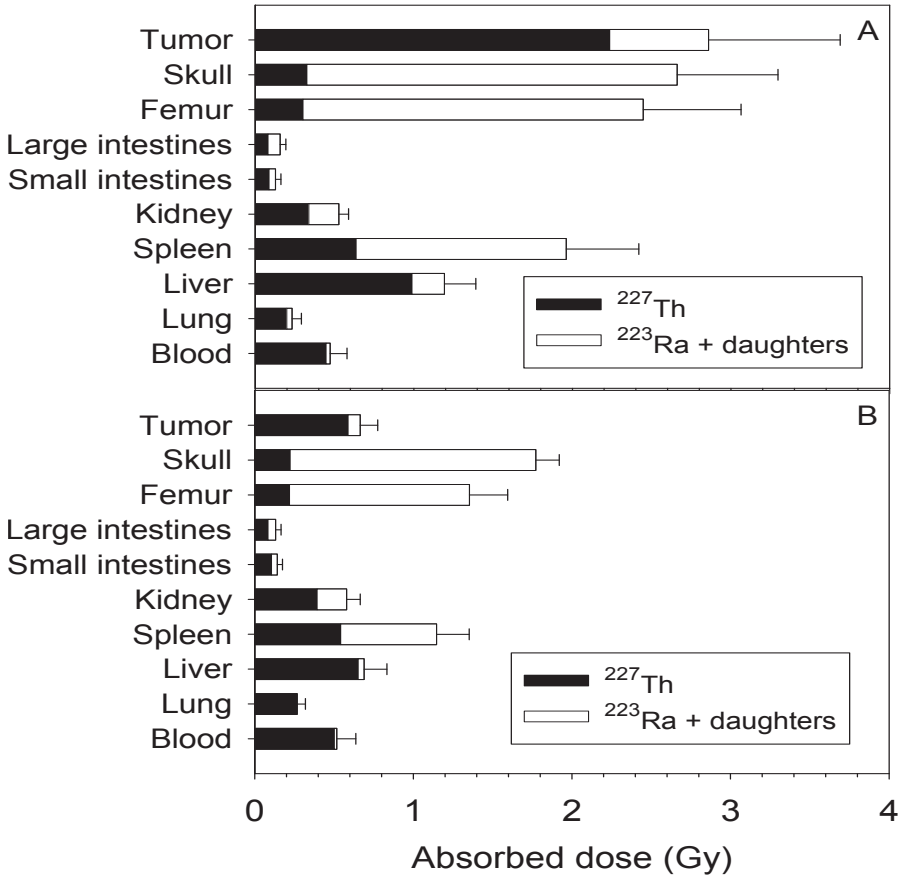

Figure 2 Absorbed radiation doses to normal tissues and tumor xenografts. Absorbed radiation dose in tumor and normal organs of mice injected with ^{227}Th-trastuzumab (**a**) or ^{227}Th-rituximab (**b**). Cumulated activities were calculated from biodistribution curves and multiplied with the mean energy of α-particles from ^{227}Th, ^{223}Ra, and daughters. Biodistribution data of ^{227}Th-trastuzumab and ^{227} Th-rituximab were normalized to 400 kBq/kg bodyweight.

The surviving fraction of the different dosages of ^{227}Th-trastuzumab was not significantly different from each other ($p > 0.05$), but there was a significant difference in survival between the ^{227}Th-trastuzumab treatment groups and control groups (NaCl and trastuzumab; $p < 0.001$) (Figure 4a). Mean and median survival times were significantly different for mice in the dosage groups 400 and 600 kBq/kg ^{227}Th-trastuzumab as compared to mice in the NaCl (control) group ($p < 0.05$; Table 2). None of the dosages of cold trastuzumab had an effect on survival ($p = 0.40$). Hence, the data were pooled into one group. The survival of mice treated with non-tumor-binding ^{227}Th-rituximab was not significantly different from the survival of the control group ($p > 0.6$; Figure 4b). In addition, no significant differences ($p > 0.05$) in mean and median survival times between control and ^{227}Th-rituximab treatment groups were observed (Table 2).

Toxicity of ^{227}Th-trastuzumab

White blood cell (WBC), platelet cell (PLT) counts, and clinical chemistry parameters of control mice and mice treated with ^{227}Th-trastuzumab are shown in Figures 5 and 6. Figure 5a, b shows WBC and PLT counts of individual mice as well as mean values at 0, 3, 6, and 9 weeks time points from each treatment groups. In the control groups mice without tumor was also included in order to get measurements at longer follow-up. The WBC count was significantly lower in the control (NaCl) group at

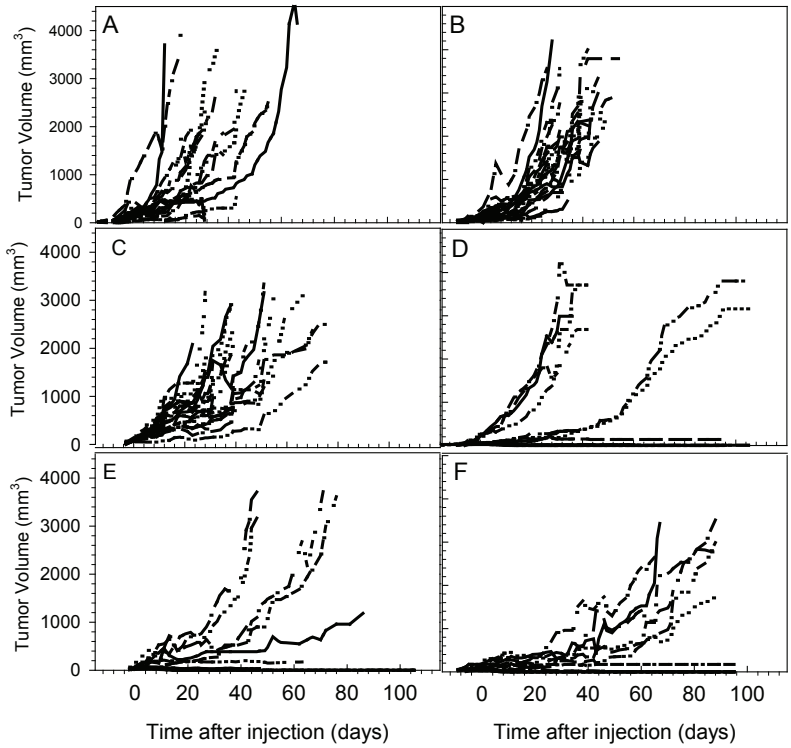

Figure 3 Effects of ^{227}Th-based RIT on growth of individual SKBR-3 tumor xenografts. Individual tumor growth after treatment with NaCl (**a**); 20, 100, and 250 μg cold trastuzumab (**b**); ^{227}Th-rituximab at dosage of 400 and 600 kBq/kg (**c**); 200 kBq/kg (**d**); 400 kBq/kg (**e**) and 600 kBq/kg (**f**) of ^{227}Th-trastuzumab. *N* = 9 to 19.

time 0 as compared to 3 weeks after injection. WBC decreased significantly for treatment with 400 kBq/kg ($p < 0.001$, *t* test) and 600 kBq/kg ($p < 0.001$, *t* test) of ^{227}Th-trastuzumab as compared to WBC in the cold trastuzumab group and control mice after 3 weeks (Figure 5a) but not as compared with the 0 time point. After 6 weeks, only the 600 kBq/kg ^{227}Th-trastuzumab group was significantly different from control ($p = 0.008$, *t* test).

No significant difference in PLT count was found for the 200 kBq/kg ^{227}Th-trastuzumab treatment group when compared to control at any time point (Figure 5b). The PLT count was significantly lower for the 400 kBq/kg ($p = 0.017$, *t* test) and 600 kBq/kg (p = 0.003, *t* test) ^{227}Th-trastuzumab treatments as compared to control after 3 weeks. At 6 weeks, the PLT counts had recovered. However, at 9 weeks, the PLT count was significantly

Table 1 Growth inhibition for tumor volume of 500 and 1,000 mm^3 after treatment

Treatment	Dosage	500 mm^3		1,000 mm^3	
		Days[a]	Growth delay[b]	Days	Growth delay
NaCl		15 ± 7	0 ± 10	25 ± 7	0 ± 11
Trastuzumab (pooled)	20 - 250 μg	15 ± 7	0 ± 11	23 ± 8	-2 ± 12
^{227}Th-rituximab	400 and 600 kBq/kg	15 ± 8	-3 ± 11	27 ± 10	2 ± 11
^{227}Th-trastuzumab	200 kBq/kg	22 ± 8	7 ± 11	32 ± 8	7 ± 12
^{227}Th-trastuzumab	400 kBq/kg	38 ± 8	23 ± 10	70 ± 10	45 ± 12
^{227}Th-trastuzumab	600 kBq/kg	60 ± 7	45 ± 7	90 ± 10	65 ± 7

[a]The number of days to reach the chosen tumor volume. [b]Growth delay = days (treatment) - days (NaCl).

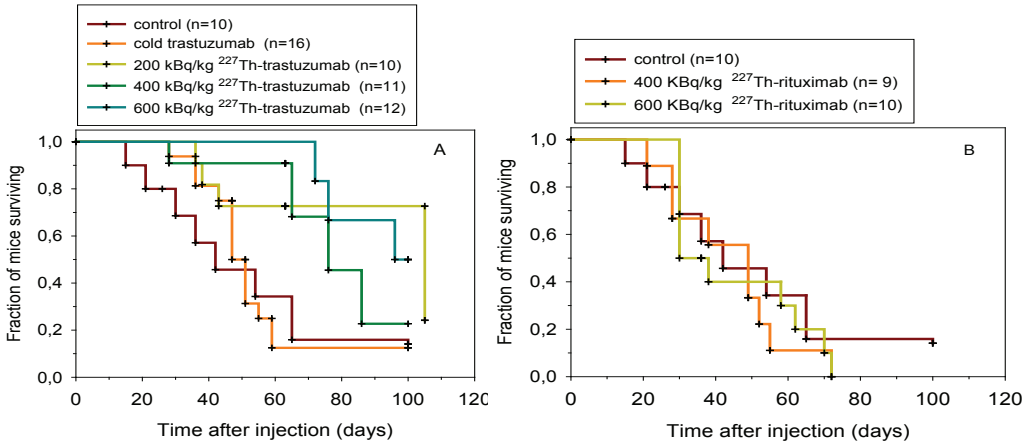

Figure 4 Effects of ^{227}Th-based RIT on survival of mice with SKBR-3 tumor xenografts. Survival of mice after intravenous injection of NaCl, 20,100, and 250 μg cold trastuzumab, and 200, 400, and 600 kBq/kg ^{227}Th-trastuzumab (**a**), or 400 and 600 kBq/kg ^{227}Th-rituximab (**b**).

lower than the control for the 400 kBq/kg ^{227}Th-trastuzumab group (p = 0.038, t test) and for the cold trastuzumab group (p < 0.001, t test) as compared to control mice.

Urea, AST, ALT, and ALP levels in blood from control mice were compared with blood from mice treated with cold trastuzumab, 200, 400, and 600 kBq/kg of ^{227}Th-trastuzumab (Figure 6a, b, c, d). Urea levels were within the normal range and were not significantly different from control. One mouse in each RIT group and one control mouse showed high ALT levels, i.e., above normal range. Another mouse treated with 200 kBq/kg ^{227}Th-trastuzumab group had a very high AST levels as compared to mice in all other treatment groups. Large variations in ALP levels were observed among all treatment groups but were within the normal range. Therapy related pathological changes were not observed in any organ upon histological examination.

Figure 7 shows no morphological differences in normal bone marrow for a mouse treated with NaCl (Figure 7a) and a mouse treated with 600 kBq/kg of ^{227}Th-trastuzumab up to 72 days (Figure 7b). Body weights of animals were measured throughout the study but no significant differences between the treatment groups were observed (data not shown).

Autoradiography

Autoradiography of SKBR-3 tumor xenografts showed that the distribution patterns of radioactivity after injection of 600 kBq/kg of ^{227}Th-trastuzumab were inhomogeneous (Figure 8). The smallest of the tumors analyzed showed highest concentration of radioactivity present as a rim corresponding to areas with viable tumor tissue close to the well perfused connective tissue capsule surrounding the tumor (Figure 8a). The tumor in Figure 8b had localized hotspots. On the corresponding H/E-stained tissue section, the hotspots with high ^{227}Th-trastuzumab uptake matched areas with high density of blood vessels and/or large blood vessels, with areas of necrotic tissue and loosely bound cells in between. A similar correspondence was also seen in tissue sections taken at later time points (Figures 8c, d).

Table 2 Mean and median survival times for all treatment groups

Treatment	Dosage	Mean ± standard error	Median ± standard error	Number of mice
NaCl		52 ± 10	42 ± 13	10
Trastuzumab (Pooled)	20 - 250 μg	54 ± 5	47 ± 2	16
^{227}Th-rituximab	400 kBq/kg	44 ± 5	49 ± 8	9
^{227}Th- rituximab	600 kBq/kg	47 ± 5	36 ± 3	10
^{227}Th-trastuzumab	200 kBq/kg	39 ± 2	38 ± 2	10
^{227}Th-trastuzumab	400 kBq/kg	87 ± 7*	63 ± 3*	11
^{227}Th-trastuzumab	600 kBq/kg	95 ± 3*	96 ± 3*	12

*Significant difference between control and therapy.

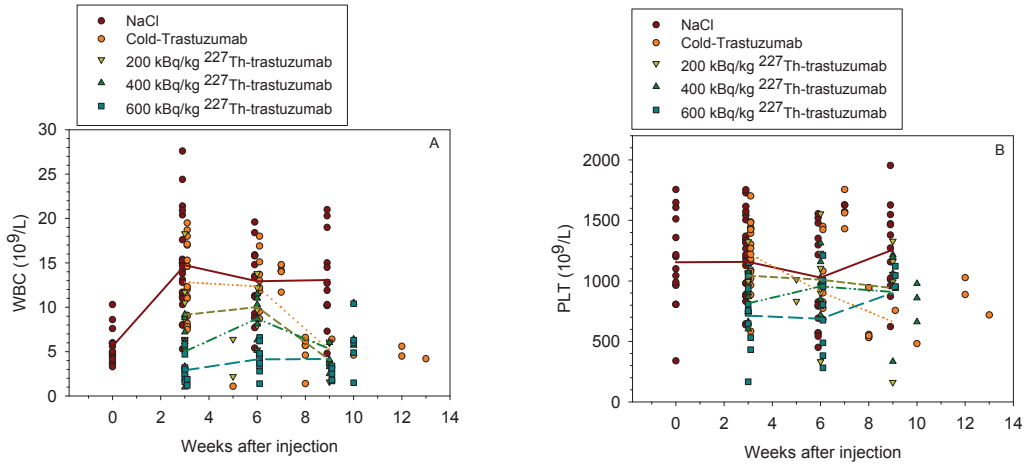

Figure 5 Blood cell counts after ^{227}Th-trastuzumab therapy. Assessment of bone marrow toxicity estimated by white blood cell counts (**a**) and platelet counts (**b**) as a function of time after administration of NaCl, cold trastuzumab, and 200, 400, and 600 kBq/kg of ^{227}Th-trastuzumab. Line graphs shows means of each treatment group.

Discussion

The present study of alpha-particle-emitting ^{227}Th-trastuzumab showed a significant dose-dependent inhibition of tumor growth of human SKBR-3 breast cancer xenografts in mice, leading to long-term survival with low toxicity.

In RIT with ^{227}Th the distribution of free daughter nuclides also has to be considered, as the daughter nuclide ^{223}Ra detaches from the DOTA-trastuzumab construct upon alpha-particle emission from ^{227}Th. The biodistribution study showed that ^{223}Ra re-localized to bone and to spleen. It should be noticed that the 18.7-day half-life of ^{227}Th allows for excretion of a large fraction of ^{227}Th-trastuzumab before ^{223}Ra is formed. The uptake in spleen was probably related to mouse-specific calcification of the spleen [20]. Radium-223 has a half-life of 11.4 days and is excreted from the blood via the intestines with a major part of the ^{223}Ra ending up in the hydroxyapatite of bone [8,20,21]. The half-lives of the ^{223}Ra-daughters are in the millisecond to minute range. They are therefore likely to contribute mainly to the absorbed radiation dose in the vicinity of the site of ^{223}Ra decay. Thus, as shown in Figure 2 the absorbed doses to bone were comparable to the doses in tumor.

Microautoradiography studies of ^{227}Th-rituximab have shown that there probably is a contribution to the bone marrow absorbed dose from ^{223}Ra and daughters on the bone surface [11]. One could suspect that localization in bone would give a high contribution to bone marrow toxicity, but clinical studies of ^{223}Ra have shown that it is well tolerated by breast and prostate cancer patients [8], with data from repeated dosing suggesting no more damage on red bone marrow compared to placebo [9]. This lack of toxicity is probably due to the short path length of alpha emission, as previous data have shown that the beta-emitter strontium-89 is strikingly more toxic, although presumably localizing in an identical way in bone tissue [20]. Therefore, we suggest that localization of small amounts of ^{223}Ra in bone tissue would be acceptable. Furthermore, because of the long half-life of ^{227}Th and internalization of HER-2 antigen after binding to ^{227}Th- trastuzumab complex much of the ^{227}Th will be excreted or internalized before ^{223}Ra is formed and thereby reducing relocalization of ^{223}Ra to bone. We also suggest that an optimized chelator will reduce the small amounts of free ^{227}Th, indicated by the present biodistribution data.

No severe bone marrow toxicity was observed in this study even when therapeutically effective amounts were administered. A dosage of 600 kBq/kg of ^{227}Th-rituximab is equal to an absorbed radiation dose in tumor of around 1 Gy. One could expect a small therapeutic effect of this dose since there was a significant therapeutic effect of 200 kBq/kg (1.45 Gy) of ^{227}Th-trastuzumab. However, there was no therapeutic effect of even the highest dosage of ^{227}Th-rituximab, showing that the antibody has to bind to the cells to get the emitted alpha particles close enough to the tumor cell nucleus. This is in analogy with the lack of bone marrow toxicity, discussed above, i.e., the low bone marrow toxicity might be due to

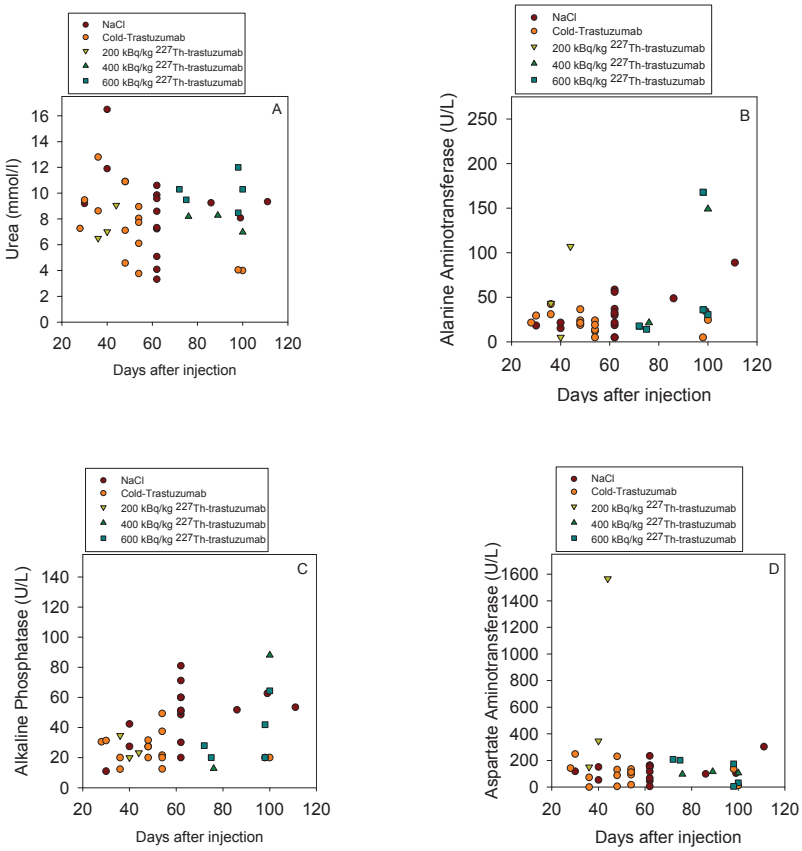

Figure 6 Assessment of liver and kidney functions after ^{227}Th-trastuzumab therapy. Measurement of urea (**a**), ALT (**b**), ALP (**c**), and AST (**d**) concentration in blood of mice with time after administration of NaCl, cold trastuzumab, 200, 400, and 600 kBq/kg of ^{227}Th-trastuzumab.

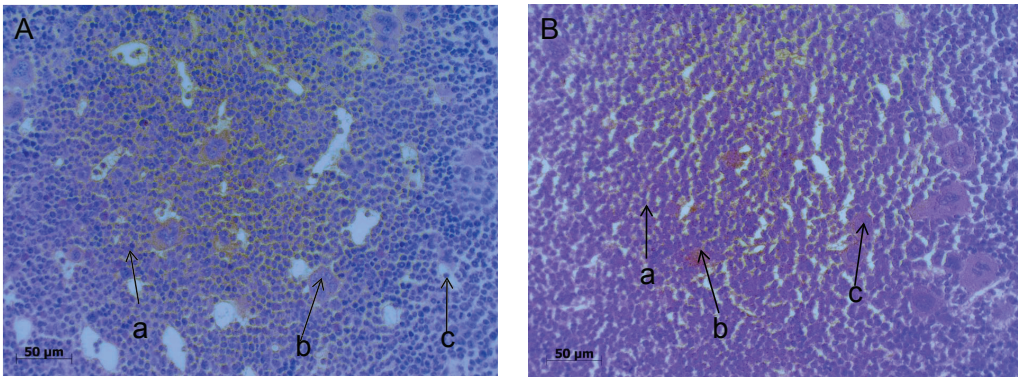

Figure 7 Histological examination of bone marrow after ^{227}Th-trastuzumab therapy. Histological microscopy images of bone marrow in femur of mice after administration of NaCl (**a**) or 600 kBq/kg ^{227}Th-trastuzumab (**b**) showing islands of haemopoetic cells composed of blood cells in various stages of maturation (arrow a), a great population of nucleated blood cells (arrow b), and blood vessels (arrow c).

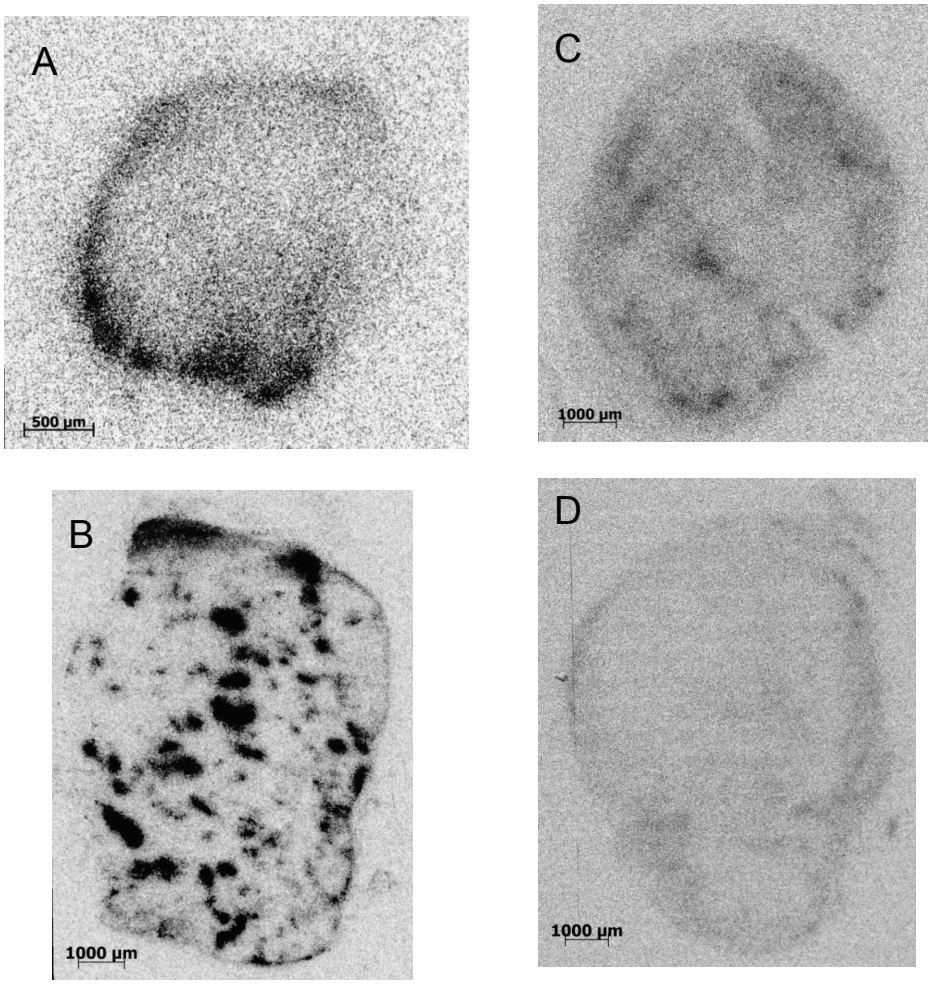

Figure 8 Autoradiography images after ^{227}Th-trastuzumab therapy. Autoradiography images of the radioactivity distribution in 5-µm-thick frozen tissue sections from four different SKBR-3 human tumor xenografts in athymic nude mice following injection of 600 kBq/kg of ^{227}Th-trastuzumab. Tumors in mages (**a**) and (**b**) were resected 4 days post injection, while (**c**) and (**d**) were removed 8 days post injection. $N = 4$.

the lack of binding of ^{227}Th-trastuzumab or ^{223}Ra to bone marrow cells.

In the present study, the tumor volumes were 8 to 16 times larger than the size of micrometastases (< 2 mm in diameter) in breast cancer patients. However, in a previous study we treated single SKBR-3 cells and achieved up to two log reduction in clonogenic survival and growth inhibition [17]. Therefore, one relevant clinical setting for ^{227}Th-trastuzumab might be adjuvant treatment of breast cancer patients with micrometastases. Due to the ^{223}Ra (daughter) affinity to bone, patients with a high risk of developing bone metastasis might be an intriguing application [22,23].

There was a dosage-dependent increase in tumor growth inhibition but not for survival. This may be related to individual differences in tumor vascularization and the presence of necrosis. In the 200 kBq/kg group we observed a variable therapeutic effect, while in the 400 and 600 kBq/kg groups we got a more prominent and similar therapeutic effect.

Radiolabeled antibody therapy for solid tumor has been less successful as compared to hematological tumors. The

reasons are that the solid tumors are generally less sensitive to radiation and are more difficult to target due to macromolecule transport barriers, e.g., vascular supply limitation, high interstitial pressure, and vascular permeability limitation. Targeted delivery of high LET α-particles after administration of ^{227}Th-trastuzumab may not be the only reason behind the successful growth inhibition of SKBR-3 tumor xenografts. The autoradiography images indicated that ^{227}Th-trastuzumab in some tumors, were located close to the tumor vasculature. Targeting the tumor vasculature or vasculature near the tumor cells with α-emitting radionuclides has previously been shown to yield a therapeutic effect on solid tumors [24,25].

The tumors treated in the present study were much larger than the range of alpha particles. However, the autoradiogaphy images indicated hot spots of ^{227}Th-trastuzumab activity in perfused areas within the tumor xenografts, which might result in destruction of the blood vessels and eradication of tumors due to lack of nutrients. Furthermore, there was also some retention of free ^{223}Ra in tumor. This is a small ion with several α-emitting daughter radionuclides that might surmount the macromolecular transport barriers of solid tumors and result in high LET α-irradiation of tumor cells not reached by the larger molecule ^{227}Th-trastuzumab. Thus, the antitumor effect might have been a combined effect of tumor cell kill by both ^{227}Th-trastuzumab, ^{223}Ra, and daughters and destruction of the blood vessels that delivers nutrients and oxygen to the tumor cells.

At two samplings, the dosage-dependent decrease in the WBC count was significantly lower for mice in one or both of the two highest dosages groups compared to control mice; both for the 400 and 600 kBq/kg ^{227}Th-trastuzumab groups at 3 weeks after injection, and for the 600 kBq/kg^{227}Th-trastuzumab at 6-week time points. However, the blood values were within the normal physiological range for nude mice for all dosages of ^{227}Th-trastuzumab. Furthermore, the most striking change in the WBC count is the increase for the control group from 0 to 3, 6, and 9 weeks. If the WBC count at 3, 6, and 9 weeks are compared with the WBC count of the control at 0 weeks there is no significant difference. The reason for this increase is unknown, but it might be related to an undetected infection in one cage of the control mice. Therefore, we conclude that the ^{227}Th-trastuzumab treatment had no pathological effect on the WBC count.

There was a dosage-dependent decrease in PLT count at 3 weeks after injection, but the PLT count had recovered after 6 weeks. At the 9-week time point, the PLT count was significantly lower than the control for the 400 kBq/kg ^{227}Th-trastuzumab group and the cold trastuzumab group. However, this decrease was probably related to a combination of biological variation and the low number of mice in these two groups (5 and 1, respectively). It should also be pointed out that control mice without tumor xenografts were used in order to get blood samples for the controls at the later time points.

Liver enzymes and urea levels in the blood did not show any dose-dependent changes following injection of ^{227}Th-trastuzumab with levels in the highest dosage group similar to that of control. Other treatment groups showed random increase or decrease of some enzymes when compared with control. This may be related to one mouse within each group with very high value of the parameter in question. Since there were no dose-dependent changes and since there were no significant changes between the control and the 600 kBq/kg group for any parameters, these changes might be due to other factors than the ^{227}Th-trastuzumab treatment.

In conclusion, ^{227}Th-trastuzumab inhibits growth of breast cancer xenografts in a dose-dependent manner. Possibly due to the longer half-life, single dosing was efficacious; not excluding that improved efficacy might be obtained with multiple doses, as has been shown clinically with a more short-lived alpha emitter [9]. The limited toxicity of the treatment was mainly related to reversible bone marrow depression. Further preclinical studies of ^{227}Th-trastuzumab involving mice with breast cancer micrometastases and, if possible, metastasis to bone are warranted.

Acknowledgements

The authors are grateful to Katrine B. Melhus, Camilla Mollatt, and Anne. K. Hjelmerud of Norwegian Radium Hospital, and Åsmund Larsen and Ellen M. Brevik of Algeta ASA, for technical assistance. We thank Lars Abrahamsen and Thomas Ramdahl at Algeta ASA for valuable comments on the manuscript.

Author details

[1]Department of Radiation Biology, Institute for Cancer Research, Oslo University Hospital, Montebello, 0310 Oslo, Norway [2]Faculty of Medicine, University of Oslo, P.O. Box 1074 Blindern, 0316 Oslo, Norway [3]Department of Oncology, The Norwegian Radium Hospital, Oslo University Hospital, Montebello, 0310 Oslo, Norway [4]Department of Pathology, Oslo University Hospital, Montebello, 0310 Oslo, Norway [5]Algeta ASA, Kjelsås, 0411 Oslo, Norway

Authors' contributions

NA designed and performed the invivo studies and carried out interpretation and analysis of data including dosimetry calculation and writing of manuscript. JB performed radiolabeling and contributed in manuscript writing. JN and NA carried out histopathological studies of slides. HH carried out the autoradiography studies including interpretation and analysis of these data, and contributed to performing experiments and writing of parts of the manuscript. ØSB contributed to the study design, interpretation and analyses of data as well as writing of the manuscript. JD contributed to the study design, interpretation and analyses of data, writing the manuscript as well as performing experiments and dosimetry calculations. All authors read and approved the final manuscript.

Competing interests

JB is an employee of Algeta ASA which owns the patents for using ^{227}Th in radioimmunotherapy. JD and OSB own a small amount of shares in Algeta ASA.

Received: 30 May 2011 Accepted: 24 August 2011
Published: 24 August 2011

References

1. Steger GG, Abrahamova J, Bacanu F, Brincat S, Brize A, Cesas A, Cufer T, Dank M, Duchnowska R, Eniu A, Jassem J, Kahan Z, Matos E, Padrik P, Plate S, Pokker H, Purkalne G, Timcheva C, Tzekova V, Vyzula R, Zielinski CC: **Current standards in the treatment of metastatic breast cancer with focus on Lapatinib: a review by a Central European Consensus Panel.** *Wien Klin Wochenschr* 2010, **122**:368-379.
2. Cianfrocca M, Goldstein LJ: **Prognostic and predictive factors in early-stage breast cancer.** *Oncologist* 2004, **9**:606-616.
3. Spector NL, Blackwell KL: **Understanding the mechanisms behind trastuzumab therapy for human epidermal growth factor receptor 2-positive breast cancer.** *J Clin Oncol* 2009, **27**:5838-5847.
4. Tolmachev V, Carlsson J, Lundqvist H: **A limiting factor for the progress of radionuclide-based cancer diagnostics and therapy–availability of suitable radionuclides.** *Acta Oncol* 2004, **43**:264-275.
5. Dahle J, Borrebaek J, Melhus KB, Bruland OS, Salberg G, Olsen DR, Larsen RH: **Initial evaluation of ^{227}Th-p-benzyl-DOTA-rituximab for low-dose rate alpha-particle radioimmunotherapy.** *Nucl Med Biol* 2006, **33**:271-279.
6. Larsen RH, Borrebaek J, Dahle J, Melhus KB, Krogh C, Valan MH, Bruland OS: **Preparation of TH227-labeled radioimmunoconjugates, assessment of serum stability and antigen binding ability.** *Cancer Biother Radiopharm* 2007, **22**:431-437.
7. Dahle J, Borrebaek J, Jonasdottir TJ, Hjelmerud AK, Melhus KB, Bruland OS, Press OW, Larsen RH: **Targeted cancer therapy with a novel low-dose rate alpha-emitting radioimmunoconjugate.** *Blood* 2007, **110**:2049-2056.
8. Nilsson S, Larsen RH, Fossa SD, Balteskard L, Borch KW, Westlin JE, Salberg G, Bruland OS: **First clinical experience with alpha-emitting radium-223 in the treatment of skeletal metastases.** *Clin Cancer Res* 2005, **11**:4451-4459.
9. Nilsson S, Franzen L, Parker C, Tyrrell C, Blom R, Tennvall J, Lennernas B, Petersson U, Johannessen DC, Sokal M, Pigott K, Yachnin J, Garkavij M, Strang P, Harmenberg J, Bolstad B, Bruland OS: **Bone-targeted radium-223 in symptomatic, hormone-refractory prostate cancer: a randomised, multicentre, placebo-controlled phase II study.** *Lancet Oncol* 2007, **8**:587-594.
10. Dahle J, Bruland OS, Larsen RH: **Relative biologic effects of low-dose-rate alpha-emitting 227Th-rituximab and beta-emitting 90Y-tiuexetan-ibritumomab versus external beam X-radiation.** *Int J Radiat Oncol Biol Phys* 2008, **72**:186-192.
11. Dahle J, Jonasdottir TJ, Heyerdahl H, Nesland JM, Borrebaek J, Hjelmerud AK, Larsen RH: **Assessment of long-term radiotoxicity after treatment with the low-dose-rate alpha-particle-emitting radioimmunoconjugate (227)Th-rituximab.** *Eur J Nucl Med Mol Imaging* 2010, **37**:93-102.
12. Ballangrud AM, Yang WH, Palm S, Enmon R, Borchardt PE, Pellegrini VA, McDevitt MR, Scheinberg DA, Sgouros G: **Alpha-particle emitting atomic generator (Actinium-225)-labeled trastuzumab (herceptin) targeting of breast cancer spheroids: efficacy versus HER2/neu expression.** *Clin Cancer Res* 2004, **10**:4489-4497.
13. Borchardt PE, Yuan RR, Miederer M, McDevitt MR, Scheinberg DA: **Targeted actinium-225 *in vivo* generators for therapy of ovarian cancer.** *Cancer Res* 2003, **63**:5084-5090.
14. Palm S, Back T, Claesson I, Danielsson A, Elgqvist J, Frost S, Hultborn R, Jensen H, Lindegren S, Jacobsson L: **Therapeutic efficacy of astatine-211-labeled trastuzumab on radioresistant SKOV-3 tumors in nude mice.** *Int J Radiat Oncol Biol Phys* 2007, **69**:572-579.
15. Boskovitz A, McLendon RE, Okamura T, Sampson JH, Bigner DD, Zalutsky MR: **Treatment of HER2-positive breast carcinomatous meningitis with intrathecal administration of alpha-particle-emitting (211)At-labeled trastuzumab.** *Nucl Med Biol* 2009, **36**:659-669.
16. Milenic DE, Brady ED, Garmestani K, Albert PS, Abdulla A, Brechbiel MW: **Improved efficacy of alpha-particle-targeted radiation therapy: dual targeting of human epidermal growth factor receptor-2 and tumor-associated glycoprotein 72.** *Cancer* 2010, **116**:1059-1066.
17. Heyerdahl H, Krogh C, Borrebaek J, Larsen A, Dahle J: **Treatment of HER2-expressing breast cancer and ovarian cancer cells with alpha particle-emitting 227Th-trastuzumab.** *Int J Radiat Oncol Biol Phys* 2011, **79**:563-570.
18. Henriksen G, Hoff P, Alstad J, Larsen RH: **^{223}Ra for endoradiotherapeutic applications prepared from an immobilized ^{227}Ac/^{227}Th source.** *Radiochim Acta* 2001, **89**:661-666.
19. Henriksen G, Bruland OS, Larsen RH: **Thorium and actinium polyphosphonate compounds as bone-seeking alpha particle-emitting agents.** *Anticancer Res* 2004, **24**:101-105.
20. Henriksen G, Fisher DR, Roeske JC, Bruland OS, Larsen RH: **Targeting of osseous sites with alpha-emitting 223Ra: comparison with the beta-emitter 89Sr in mice.** *J Nucl Med* 2003, **44**:252-259.
21. Henriksen G, Breistol K, Bruland OS, Fodstad O, Larsen RH: **Significant antitumor effect from bone-seeking, alpha-particle-emitting (223)Ra demonstrated in an experimental skeletal metastases model.** *Cancer Res* 2002, **62**:3120-3125.
22. Liepe K: **Alpharadin, a 223Ra-based alpha-particle-emitting pharmaceutical for the treatment of bone metastases in patients with cancer.** *Curr Opin Investig Drugs* 2009, **10**:1346-1358.
23. Zimskind PD, SURVER JM: **Metastasis to bone from carcinoma of the breast.** *Clin Orthop* 1958, **11**:202-216.
24. Thorpe PE, Burrows FJ: **Antibody-directed targeting of the vasculature of solid tumors.** *Breast Cancer Research and Treatment* 1995, **36**:237-251.
25. Kennel SJ, Mirzadeh S, Eckelman WC, Waldmann TA, Garmestani K, Yordanov AT, Stabin MG, Brechbiel MW: **Vascular-targeted radioimmunotherapy with the alpha-particle emitter 211At.** *Radiat Res* 2002, **157**:633-641.

doi:10.1186/2191-219X-1-18
Cite this article as: Abbas *et al.*: Experimental α-particle radioimmunotherapy of breast cancer using ^{227}Th-labeled p-benzyl-DOTA-trastuzumab. *EJNMMI Research* 2011 **1**:18.

II

III

Comparing high LET ^{227}Th-trastuzumab and low LET ^{177}Lu-trastuzumab in mice with HER-2 Positive SKBR-3 Xenografts

Authors and Affiliations

Nasir Abbas*[1], Helen Heyerdahl[1], Øyvind S. Bruland[2, 3], Ellen Mengshoel Brevik[4], Jostein Dahle[1]

[1]Department of Radiation Biology, Institute for Cancer Research, Oslo University Hospital, The Norwegian Radium Hospital, Oslo, Norway; [2]Faculty of Medicine, University of Oslo, Box 1074 Blindern, 0316 Oslo, Norway; [3]Department of Oncology, Oslo University Hospital, The Norwegian Radium Hospital, Oslo, Norway; [4]Algeta ASA, 0411 Oslo, Norway.

Key Words: alpha radiation; beta radiation; ^{227}Th; ^{177}Lu; trastuzumab; radioimmunotherapy; RBE, SKBR-3;

*Corresponding Author: Nasir Abbas, email: nasir.abbas@rr-research.no tel: +4792422841

Abstract:

The aim of the present study was to compare the biodistribution, normal tissue toxicity and therapeutic effect of the alpha-particle emitting ^{227}Th-trastuzumab and the beta-particle emitting ^{177}Lu-trastuzumab in mice with HER2-expressing SKBR-3 breast cancer xenografts.

Methods: Biodistributions of the two radioimmunoconjugates were determined at different time points after i.v. injection. Inhibition of tumor growth was measured after single injection of ^{227}Th-trastuzumab (200, 400, 600 or 1000 kBq/kg), ^{177}Lu-trastuzumab (40 or 200 MBq/kg) or saline. The toxicity profiles were compared by measurements of body weight, clinical chemistry and hematological parameters, as well as histological examination of tissue specimens.

Results: 400 kBq/kg of ^{227}Th-trastuzumab and 40 MBq/kg of ^{177}Lu-trastuzumab both resulted in an absorbed radiation dose to tumor of approximately 3 Gy. A significant anti-tumor effect and increase in survival was observed at injected dosages of 400-1000 kBq/kg of ^{227}Th-trastuzumab and 200 MBq/kg of ^{177}Lu-trastuzumab as compared to the saline control. When compared at the same therapeutic effect level (100 % prolonged growth delay as compared to control) the absorbed radiation dose of ^{227}Th-trastuzumab was 3 times lower than with ^{177}Lu-trastuzumab, which indicates that the relative biological effect (RBE) was 2.8 times higher for ^{227}Th-trastuzumab than for ^{177}Lu-trastuzumab. In contrast, when compared at the same temporary decrease of WBC count (50 % decrease in number of white blood cells as compared to control), the increase in growth delay was 3 times longer with ^{177}Lu-trastuzumab than with ^{227}Th-trastuzumab, which indicate that the therapeutic index was three times higher for ^{177}Lu-trastuzumab than for ^{227}Th-trastuzumab.

Conclusion: In this xenograft model the RBE was higher for ^{227}Th-trastuzumab than for ^{177}Lu-trastuzumab, while the therapeutic index of ^{177}Lu-trastuzumab was superior to that of ^{227}Th-trastuzumab.

Introduction:

Radioimmunotherapy (RIT) with beta particle emitting anti-CD20 ^{90}Y-labeled ibritumomab-tiuxetan, Zevalin® and ^{131}I-labeled tositumomab, Bexxar®, is an approved treatment for non-Hodgkin lymphoma. However, the use of RIT is still limited, probably due to alternative non-radioactive therapies, reimbursement issues, high treatment cost and administration procedures [1,2]. Treatment related bone marrow toxicity appears to be the dose limiting factor for Zevalin and Bexxar [3].

The development of alpha-particle emitting RIT has been halted by lack of radionuclides with adequate physical and radiobiological properties and high cost for the most promising radionuclides [4]. While beta particles deposit only 0.01- 0.1 keV/μm of energy per distance travelled, alpha particles deposit 25-230 keV/μm. The latter are therefore suitable for tumors with a diameter of less than 200 μm while beta emitters can be used for tumors up to 2-10 mm [5]. Because of the relatively long range of beta particles, cross radiation of neighbouring cells is an important mechanism of action using beta-RIT, while alpha-RIT is more dependent on a homogeneous tumor uptake.

Thorium-227 is a novel radionuclide for alpha-RIT that can be produced in clinically relevant amounts from beta-decay of the long-term generator ^{227}Ac [6,7]. The decay chain of ^{227}Th (^{227}Th → ^{223}Ra → ^{219}Rn→ ^{215}Po → ^{211}Pb → ^{211}Bi → ^{207}Tl → ^{207}Pb) emits 5 alpha and 2 beta particles. The relatively long half-life of ^{227}Th ($T_{½}$ = 18.7 days) provides time for tumor cell targeting and excretion of non-bound RICs (^{227}Th-conjugates) before large amounts of the daughter nuclide ^{223}Ra is generated.

The beta-emitter ^{177}Lu ($T_{1/2}$ = 6.7 days) has been successfully tested for beta-RIT in several clinical trials [8,9]. It can be produced by direct neutron activation of ^{176}Lu, or via beta decay of reactor-produced ^{177}Yb [10,11]. Lutetium-177 might be used in RIT of smaller sized

tumors because the energy of the beta particle is relatively low (resulting in shorter range in tissue) compared to other beta-emitters used for RIT [11].

One quarter of breast cancer patients overexpresses human epidermal growth factor receptor-2 (HER-2/neu) both at their primary and distant tumor sites [12]. The anti-HER-2 humanized antibody trastuzumab (Herceptin®) is approved for patients with HER-2 overexpressing breast cancer; both in the adjuvant and metastatic setting [13]. Patients with high HER-2 overexpression respond best to trastuzumab [14]. Use of trastuzumab as a carrier for either alpha- or beta-emitting radionuclides may enhance the effect of the treatment and may also enable treatment of patients with lower HER-2 overexpression [15].

Recently, ^{227}Th- and ^{177}Lu-labeled trastuzumab has been evaluated and showed promising results [16–20]. In the present study we have compared their therapeutic effects and toxicities in nude mice bearing breast cancer xenografts (SKBR-3).

Material and methods:

Radiolabeling of ^{227}Th and ^{177}Lu

Radiolabeling of trastuzumab (Roche, Basel, Switzerland) with ^{227}Th was performed at Algeta ASA (Oslo, Norway). The *p*-SCN-Bn-DOTA (Macrocyclics Inc., Dallas, TX) was conjugated to trastuzumab, and the conjugate DOTA-Bn-trastuzumab was used in the following ^{227}Th chelation reaction. The detailed conjugation and radiolabeling methods have previously been described [17].

Radiolabeling of trastuzumab with ^{177}Lu (Perkin Elmer, Shelton, CT) was performed at the Norwegian Radium Hospital. Freeze-dried DOTA-Bn-trastuzumab was dissolved in (10 mg/ml) ammonium acetate buffer (pH 5) (VWR International, Leuven, Belgium).185 MBq ^{177}Lu was added to 0.5 mg DOTA-Bn-trastuzumab and the reaction was done by shaking at 42 ºC for one hour. The RIC was purified twice on a 10 DG column (Bio-Rad Laboratories, USA) using PBS (PAA Laboratories GmbH, Pasching, Austria) added 5 mM EDTA (Sigma-Aldrich Co., 3050 Spruce Street, St. Louis) and 0.25 % foetal calf serum (FCS) (PAA Laboratories GmbH, Pasching, Austria) as running buffer.

Immunoreactivity and specific activity

The estimation of immunoreactive fraction (IRF) of ^{227}Th-trastuzumab was done by measuring the cell bound activity in a one point binding assay. Two vials with SKOV-3 cell concentrations up to 2×10^7 cells/mL in 200 µL PBS were used. In one vial, four million cells were blocked with 0.1 mg trastuzumab for 15 minutes at 37 ºC. The four million cells in the other vial were not blocked. About 500 cpm (5-9 ng) of ^{227}Th-trastuzumab was added to each vial and the cells were incubated for 2 hours at 37 ºC before washing and measuring radioactivity using an automated gamma counter (Wizard, Packard Instrument Co., Downers

Grove, IL). The IRF of ^{227}Th-trastuzumab was 62-90 %. The specific activity of ^{227}Th-trastuzumab was 1000-1600 kBq/kg [17].

A modified Lindmo method [21] was used to determine the immunoreactive fraction (IRF) of ^{177}Lu-trastuzumab. Cell concentrations of up to 3 x 10^9 cells/ml were used; one vial of each concentration was blocked with 0.5 mg trastuzumab for 10 minutes at 4 ºC and 2-10 ng ^{177}Lu-trastuzumab was added. After incubation with shaking at 4 ºC for 1.5-2 hours, the cells were washed twice and cells, supernatant and wash were counted in a gamma counter (Cobra-gamma, Packard Instrument Co. Downers Grove, IL). For ^{177}Lu-trastuzumab, the specific activity was 100-125 MBq/mg and the IRF was 90-94 %.

Animals

Eight to 12 weeks old female Balb/C nu/nu (NCR) mice (institutionally bred), with an average weight of 19-25 g, were used in the study. Subcutaneous injection of 0.05 ml Zoletil® mix (Virbac, Carros Cedex, France) was used for anaesthesia before HER-2 positive breast cancer (SKBR-3) tissue was implanted subcutaneously. Tumor xenografts were originated from human breast cancer cells from the American Type Culture Collection (ATCC, Manassas, VA, USA). The animals were maintained under pathogen-free conditions, and food and water were supplied ad libitum. Mice with growing tumor of diameters between 4 and 8 mm were included in the experiments. The mice were killed by cervical dislocation.

Ethics information

Procedures and experiments involving animals in this study were approved by the National Animal Research Authority (Permit ID: 2202) and carried out according to the European Convention for the Protection of Vertebrate Animals used for Experimental and other Scientific Purposes.

Biodistribution of ^{227}Th and ^{177}Lu labeled trastuzumab

^{227}Th-trastuzumab (10 kBq) or ^{177}Lu-trastuzumab (1 MBq) (100 µl) was injected into mice via the tail vein. For each conjugate and time point a total of 4 to 6 animals were autopsied. Radioactivity content and weight of tissues were measured.

Thorium-227 and ^{223}Ra were measured using a solid-state photon well germanium detector (GCW6021, Canberra, Meriden, CT) coupled to a digital gamma ray spectrometer and analyzed using the computer software Apex™ version 1 (Canberra). For ^{227}Th, the 236 keV (abundance 17.6 %) and 256 keV γ-ray (abundance 9.5 %) lines were used and for ^{223}Ra the 154 keV (abundance 5.7 %), 269 keV (abundance 13.9 %), 324 keV (abundance 4 %) and 338 keV (abundance 2.8 %) γ-ray lines were used [17].

The ^{177}Lu-trastuzumab samples were measured with a calibrated gamma detector (Cobra-gamma). Samples of the injectates (10 %) were used as references in the measurement procedure.

Calculation of dose

The total number of disintegrations in various tissues from the time of injection of the preparation until no significant activity was left in the body was estimated by calculation of the area under the activity concentration versus time curves (AUC).

The absorbed radiation dose and dose rate for ^{227}Th-trastuzumab [17] were calculated assuming dose contributions only from α-particle emissions with a mean α-energy (Eα) of 5.9 MeV for ^{227}Th and 26.4 MeV for ^{223}Ra with daughters in equilibrium [22]. It was assumed that there was a 100 % uniform absorption of the α-dose within a tissue and the probability of cross irradiation between adjacent organs was not taken into consideration.

The absorbed radiation dose and dose rate for ^{177}Lu-trastuzumab was calculated assuming dose contributions only from β-particle emissions with a mean energy of 134.2 keV

[23]. It was assumed that the absorbed fraction and cross irradiation ($AF(W_T)$) of β-particles in the organs varied according to Table 13 in Miller et al.[24].

Thus the total dose to each organ could be estimated by Eq 1 and 2:

Dose (^{227}Th-trastuzumab) = $AUC_0^{\infty} \cdot E\alpha$ (^{227}Th) + $AUC_0^{\infty} \cdot E\alpha$ (^{223}Ra+daughters) (1) [17]

Dose (^{177}Lu-trastuzumab) = $AUC_0^{\infty} \cdot E_\beta$ (^{177} Lu).AF (W_T) (2)

Therapeutic studies

Mice were injected i.v. with sterile filtered solutions of NaCl (control), 200, 400, 600 or1000 kBq/kg of ^{227}Th-trastuzumab, or 40 or 200 MBq/kg of ^{177}Lu-trastuzumab in 100 µl PBS. Tumor growth and mouse weight were assessed 3 times during the week before injection and in the first 3 weeks after injection; thereafter, weight, growth and survival were assessed 2 times a week. Mice with tumor diameter larger than 20 mm were sacrificed.

Calculation of relative biological effect

The number of days after injection of RICs needed for the tumor to reach the normalized tumor volume (NTV) of 500 mm^3 and 1000 mm^3 was determined for each treatment and cumulative absorbed radiation doses to tumor were calculated for these time points. Treatment–induced percent increase in number of days to grow to 500 mm^3 and/or 1000 mm^3 were plotted against the cumulative absorbed radiation dose. The doses needed to induce a 50 % increase or 100 % increase in the number of days to grow to 500 mm^3 and/or 1000 mm^3 were determined. Relative Biological Effect (RBE) was calculated by dividing the dose for ^{227}Th-trastuzumab by the dose for ^{177}Lu-trastuzumab.

Toxicity evaluation

Kidney function and liver enzyme activity, blood cell counts and histopathological changes were assessed. Approximately 100-200 µl blood was collected from the vena saphena lateralis in 500 µl EDTA-coated tubes (Microtainer K2E tubes, Becton, Dickinson, NJ) for blood counting. Blood samples were taken the day before injection and at 3, 6, 9 and 12 weeks after start of the study. In addition, when the mice had to be killed due to tumor size or weight loss, blood samples were collected by heart puncture and added to EDTA-coated tubes and to lithium coated tubes (Microtainer LH tubes, Becton, Dickinson) for analysis of clinical chemistry parameters. Blood cells were counted in an automatic blood counter (Scil Vet abc blood machine, Horiba group, Montpellier, France). Clinical chemistry strips were used to assess the serum aspartate aminotransferase (AST), alanine aminotransferase (ALT), alkaline phosphatase (ALP) and urea level (Reflotron, Roche Diagnostics GmbH, Mannheim, Germany). Blood serum samples (30 µl) were analyzed by serum analyzer (Reflovet, Roche, Diagnostics).

The lungs, heart, kidneys, spleen, small intestine, large intestine, liver, femur, skull and tumor were fixed with formalin, cut in 5 µm slices, stained with hematoxylin and eosin and analyzed to detect pathological changes.

Statistical analysis

Statistical analysis of the survival experiments was done using Mantley Cox log-rank test by SPSS version 16. Student t-test was used to determine significance, $p \leq 0.05$.

Results:

Biodistribution

Table 1 and 2 show the biodistribution of ^{227}Th-trastuzumab and ^{177}Lu-trastuzumab, respectively. The blood levels were 27 ± 3 % ID/g and 25 ± 1 % ID/g one hour after injection of ^{227}Th-trastuzumab and ^{177}Lu-trastuzumab, respectively. The maximum decay-adjusted uptake of ^{227}Th-trastuzumab in tumor (34 ± 25 % ID/g) occurred 3 days after injection. Upon injection of ^{227}Th-trastuzumab the ^{223}Ra content is very low, for instance only 26 Bq/g in the blood 1 h after injection of 400 kBq/kg ^{227}Th-trastuzumab [17]. However, as ^{227}Th decays the amount of ^{223}Ra increases, and ^{223}Ra is either excreted, taken up by bone or retained in the tumor. After 21 days the uptake in femur and skull was 642 Bq/g and 586 Bq/g and the content of ^{223}Ra in tumor was 135 Bq/g [17]. The maximum decay-adjusted uptake of ^{177}Lu-trastuzumab in tumor (40 ± 18 % ID/g) occurred 7 days after injection. There were no statistically significant differences in uptake of ^{227}Th-trastuzumab and ^{177}Lu-trastuzumab in other organs for the 24 h, 4 day and 7 day time points. In other studies the peak levels of ^{177}Lu-trastuzumab in SKBR-3 tumor xenografts and ^{177}Lu-pertuzumab in SKOV-3 tumors were achieved 3 days after administration [16,25].

Figure 1A and B show the absorbed dose rate in the blood, femur and tumor after injection of 400 kBq/kg ^{227}Th-trastuzumab and 40 MBq/kg ^{177}Lu-trastuzumab, respectively. The dose rate was calculated assuming dose contribution only from alpha particles from ^{227}Th, ^{223}Ra and daughters. Absorbed dose rate decreased rapidly for blood while increased for tumor in the first 24 hours after injection for both RICs. In tumor tissue the absorbed dose rate increased gradually for ^{227}Th-trastuzumab injection and more rapidly for ^{177}Lu-trastuzumab. The apparent difference in timing for peak dose rate was not statistically significant. Tumor dose rate for ^{177}Lu-trastuzumab was almost similar from 24 h to 7 days time points (Figure 1B). Maximum dose rate in tumor was 413 ± 273 mGy/day for 400

kBq/kg ^{227}Th-trastuzumab. The absorbed dose rate in femur increased to its maximum level (257 ± 65 mGy/day) at 21 days after ^{227}Th-trastuzumab injection due to relocalization of ^{223}Ra to femur, introducing a dose contribution from both ^{223}Ra and its daughters. Maximum dose rate in tumor was 357 ± 213 mGy/day for 40 MBq/kg ^{177}Lu-trastuzumab.

Therapeutic effects

Growth of SKBR-3 tumor xenografts in mice treated with different dosages of alpha-particle emitting ^{227}Th-trastuzumab was compared with different dosages of beta-particle emitting ^{177}Lu-trastuzumab and with saline as control (Figure 2 and Table 3). Dose dependent growth inhibition of SKBR-3 tumor xenografts was observed for both ^{227}Th-trastuzumab and ^{177}Lu-trastuzumab. 400 kBq/kg ^{227}Th-trastuzumab and 40 MBq/kg ^{177}Lu-trastuzumab both resulted in an absorbed dose of approximately 3 Gy to tumor. However, the tumor growth in mice treated with 400 kBq/kg ^{227}Th-trastuzumab (2.9 Gy to tumor) was considerably inhibited and the average delay to grow to a tumor volume of 500 mm^3 was 23 ± 10 days in comparison to the control. The tumor growth was not affected by 40 MBq/kg ^{177}Lu-trastuzumab (3 Gy to tumor), however a significant anti-tumor effect was observed after injection of 200 MBq/kg ^{177}Lu-trastuzumab (16 Gy to tumor). Hence, growth delay to reach a tumor volume of 500 mm^3 was 4 ± 11 days, 45 ± 7 days, and 38 ± 8 days for 200 kBq/kg, 600 kBq/kg and 1000 kBq/kg of ^{227}Th-trastuzumab, respectively, while it was 74 ± 9 days after 200 MBq/kg ^{177}Lu-trastuzumab injection (Figure 2 and Table 3). The tumor volume for each treatment group was normalized to the same tumor volume at the time of injection.

Survival of mice treated with 200, 400, 600 and 1000 kBq/kg ^{227}Th -trastuzumab and 200 MBq/kg ^{177}Lu-trastuzumab was significantly longer than observed in untreated control ($p < 0.05$) (Figure 3). No significant difference in survival of mice was observed between 40 MBq/kg ^{177}Lu-trastuzumab and control groups ($p > 0.05$).

Relative biological effectiveness

The percent increase in number of days to reach a tumor volume of 500 mm^3 and 1000 mm^3 was plotted against the cumulative radiation dose for the corresponding time (Figure 4A and B). Two levels of biologic effects; 50 % and 100 % increase in the number of days to reach the chosen normalized tumor volume, were used as end points for calculation of RBE. RBE was 2.8 for 100 % increase and 2.2 for 50 % increase in the number of days to grow to 500 $mm^3$and RBE was 2.5 for 100 % and 2.2 for 50 % increase in the number of days to grow to 1000 mm^3.

Toxicity of the treatments

Leukocyte and platelet counts in all treatment groups remained within normal physiological range for NCR nude mice [26] with a transient decrease of leukocyte count, between 3 to 9 weeks after the start of treatment while platelets remained unaffected (Figure 5A and B). This transient decrease of WBC counts after higher dosage administration was statistically significant in comparison to control ($p < 0.05$). This short time reduction of WBC count was less after ^{177}Lu-trastuzumab (200 MBq/kg) than the highest dosages of ^{227}Th-trastuzumab (600 and 1000 kBq/kg) (Figure 5A). Similar decrease of WBC counts was seen for 200 MBq/kg ^{177}Lu-trastuzumab and 400 kBq/kg ^{227}Th-trastuzumab (Figure 5A), both giving a 50 % decrease in the number of white blood cells after 3 weeks. However, ^{177}Lu-trastuzumab was 3 times more efficient in inhibiting tumor growth than ^{227}Th-trastuzumab at these dosages (200 MBq/kg ^{177}Lu-trastuzumab and 400 kBq/kg ^{227}Th-trastuzumab), which indicates that although the RBE was higher for ^{227}Th-trastuzumab, the therapeutic index was higher for ^{177}Lu-trastuzumab.

Bone marrow morphology after administration of ^{227}Th-trastuzumab (200, 400, 600 and 1000 kBq/kg), 40 MBq/kg and 200 MBq/kg of ^{177}Lu-trastuzumab was analyzed and compared to the control. No pathological findings in hematopoietic tissue (bone marrow)

were seen in this study even at highest therapeutic dosages of both RICs (data not shown). Blood urea level (BUL), and activity of alanine aminotransferase (ALT), alkaline phosphatase (ALP) and aspartate aminotransferase (AST) were found to be within the normal physiological range of these parameters in NCR Nude mice for all treatments [26] (data not shown). Weight loss was not observed in any of the treatment groups compared to control except for 1000 kBq/kg ^{227}Th-trastuzumab. In this group, 5 mice out of 8 had to be killed due to weight loss (data not shown). In this study, weight loss was considered if mice losses weight either more than 15 % (for 1000 kBq/kg ^{227}Th-trastuzumab) or 20 % (for rest of the treatment groups) from maximum tumor free body weight.

Discussion:

The aim of the present study was to compare the biodistribution, normal tissue toxicity and therapeutic effect of the alpha-particle emitting ^{227}Th-trastuzumab and the beta-particle emitting ^{177}Lu-trastuzumab in mice with HER2-expressing SKBR-3 breast cancer xenografts. Based on the temporary decrease in WBC count, the therapeutic index was higher for ^{177}Lu-trastuzumab compared to ^{227}Th-trastuzumab. In contrast, the high LET emitting ^{227}Th-trastuzumab was 2.8 fold more efficacious against SKBR-3 tumors compared to the low LET emitting ^{177}Lu-trastuzumab when compared at the same relatively low dose to tumor (3 Gy). No severe bone marrow or normal organ toxicities were seen in this study after administration of both RICs. However, a mild and transient WBC reduction was seen with ^{227}Th-trastuzumab.

Injection of 200 MBq/kg ^{177}Lu-trastuzumab or 400 kBq/kg ^{227}Th-trastuzumab resulted in similar reduction of WBC count at 3 weeks time point. The therapeutic efficacy of 200 MBq/kg ^{177}Lu-trastuzumab was three times higher than for 400 kBq/kg ^{227}Th-trastuzumab. These results can be expected because the absorbed radiation dose to the tumor was 5.3 times higher for 200 MBq/kg ^{177}Lu-trastuzumab than for 400 kBq/kg ^{227}Th-trastuzumab (16 vs 3 Gy). A similar therapeutic effect was also seen with 200 MBq/kg ^{177}Lu-pertuzumab in mice with SKOV-3 xenografts [25].

Tumors treated in the present study were much larger (4-8 mm) than considered ideal for short ranged alpha particle ^{227}Th-trastuzumab and more suitable for ^{177}Lu-trastuzumab, which may partly explain the difference in therapeutic index. Short ranged ^{227}Th-trastuzumab therapy is suitable for small sized tumors (less than 200 μm) and due to cross fire and long range, ^{177}Lu-trastuzumab would be suitable for larger sized tumors. Therefore, it can be anticipated that the therapeutic index in humans would have been higher for ^{227}Th-

trastuzumab than for ^{177}Lu-trastuzumab because of small micrometastatic lesions resulting in more even dose distribution.

Administration of 600 and 1000 kBq/kg ^{227}Th-trastuzumab resulted in modest and temporary decrease of WBC, possibly due to bone localization of ^{223}Ra and its daughters, slightly more than seen after 200 MBq/kg of ^{177}Lu-trastuzumab. Radium-223, generated from ^{227}Th decay, could have been produced either from tumor cell-internalized [18] or tumor cell bound ^{227}Th-trastuzumab in the tumor tissue.

A dosage of 40 MBq/kg of ^{177}Lu-trastuzumab and 400 kBq/kg of ^{227}Th- trastuzumab resulted in the same absorbed radiation dose to the tumor (3 Gy). 40 MBq/kg ^{177}Lu-trastuzumab neither inhibited the tumor growth nor improved the survival of mice, while 400 kBq/kg ^{227}Th-trastuzumab improved survival by 166 % and growth inhibition by 253 %. Interestingly, slightly higher dosage (74 MBq/kg) of ^{177}Lu-d9MAb used for treatment of mice with intraperitoneal gastric carcinoma cells (HSC45-M2) have been shown to result in prolongation of survival [27]. The difference in the tumor model and mode of administration (i.p. vs i.v.) of ^{177}Lu- d9MAb could explain the different results.

The RBE of high LET emitting ^{227}Th-trastuzumab was 2.8 fold higher than for the low LET emitting ^{177}Lu-trastuzumab. Similar results were also obtained in our previous study; administration of low dose ^{227}Th-rituximab was more effective per dose unit as compared to both low LET RIT and X-radiation [28].

No severe bone marrow or normal organ toxicity was seen in this study after administration of both RICs. However, a mild toxic effect of transient WBC reduction was seen with ^{227}Th-trastuzumab. The low bone marrow toxicity of ^{227}Th-trastuzumab could be due to the short range of alpha particles from ^{227}Th, ^{223}Ra and daughters. With similar localization to bone, the long range beta-emitter Strontium-89 has been found to be more toxic than the short range ^{223}Ra [29]. The long half life of ^{227}Th and ^{227}Th-trastuzumab

internalization, after binding to HER2, results in either excretion or internalization of larger amounts of ^{227}Th before ^{223}Ra is generated, which might reduce its localization to bone. A recently conducted and reviewed phase III trial [30,31] with other clinical studies [29,32] have also shown that ^{223}Ra is well tolerated by breast and prostate cancer patients. These clinical results show that the accumulation of small amounts of ^{223}Ra in the bone marrow is tolerable and is also compatible with our previous data in animal model [33].

Conclusion: At the same, relatively low absorbed radiation dose, the alpha-particle emitting ^{227}Th-trastuzumab was 3 times more efficient in inhibiting tumor growth than the beta-particle emitting ^{177}Lu-trastuzumab. However, at the same level of transient reduction in WBC count ^{177}Lu-trastuzumab was almost 3 times more efficient in inhibiting tumor growth than ^{227}Th-trastuzumab.

Acknowledgements

The authors are thankful to Jahn Nesland for reading histopathological slides. We are grateful to Katrine B. Melhus, Camilla Mollatt and Anne. K. Hjelmerud, Norwegian Radium Hospital, and Åsmund Larsen and Jørgen Borrebæk Algeta ASA, for technical assistance. We also thank Lars Abrahamsen at Algeta ASA for valuable comments on the manuscript.

References

1. Pouget JP, Navarro-Teulon I, Bardies M, Chouin N, Cartron G, Pelegrin A, Azria D (2011) Clinical radioimmunotherapy--the role of radiobiology. Nat Rev Clin Oncol 8: 720-734.

2. Schaefer NG, Huang P, Buchanan JW, Wahl RL (2011) Radioimmunotherapy in non-Hodgkin lymphoma: opinions of nuclear medicine physicians and radiation oncologists. J Nucl Med 52: 830-838.

3. Barbet J, Chatal JF (2011) The best radionuclide for radioimmunotherapy of small tumors: beta- or alpha-emitter? Eur J Nucl Med Mol Imaging 38: 271-273.

4. Dahle J, Abbas N, Bruland ØS, Larsen RH (2011) Toxicity and relative biological effectiveness of alpha emitting radioimmunoconjugates. Current Radiopharmaceuticals 4: 321-328.

5. Karagiannis TC (2007) Comparison of different classes of radionuclides for potential use in radioimmunotherapy. Hell J Nucl Med 10: 82-88.

6. Dahle J, Borrebaek J, Melhus KB, Bruland OS, Salberg G, Olsen DR, Larsen RH (2006) Initial evaluation of ^{227}Th-p-benzyl-DOTA-rituximab for low-dose rate alpha-particle radioimmunotherapy. Nucl Med Biol 33: 271-279.

7. Larsen RH, Borrebaek J, Dahle J, Melhus KB, Krogh C, Valan MH, Bruland OS (2007) Preparation of TH227-labeled radioimmunoconjugates, assessment of serum stability and antigen binding ability. Cancer Biother Radiopharm 22: 431-437.

8. Bander NH, Milowsky MI, Nanus DM, Kostakoglu L, Vallabhajosula S, Goldsmith SJ (2005) Phase I Trial of 177Lutetium-Labeled J591, a Monoclonal Antibody to Prostate-Specific Membrane Antigen, in Patients With Androgen-Independent Prostate Cancer. Journal of Clinical Oncology 23: 4591-4601.

9. Stillebroer AB, Zegers CML, Boerman OC, Oosterwijk E, Mulders PFA, O'Donoghue JA, Visser EP, Oyen WJG (2012) Dosimetric Analysis of 177Lu-cG250 Radioimmunotherapy in Renal Cell Carcinoma Patients: Correlation with Myelotoxicity and Pretherapeutic Absorbed Dose Predictions Based on 111In-cG250 Imaging. Journal of Nuclear Medicine 53: 82-89.

10. Dvorakova Z, Henkelmann R, Lin X, Turler A, Gerstenberg H (2008) Production of 177Lu at the new research reactor FRM-II: Irradiation yield of 176Lu(n,gamma)177Lu. Appl Radiat Isot 66: 147-151.

11. Schmitt A, Bernhardt P, Nilsson O, Ahlman H, Kolby L, Schmitt J, Forssel-Aronsson E (2003) Biodistribution and dosimetry of 177Lu-labeled [DOTA0,Tyr3]octreotate in male nude mice with human small cell lung cancer. Cancer Biother Radiopharm 18: 593-599.

12. Carlsson J, Nordgren H, Sjostrom J, Wester K, Villman K, Bengtsson NO, Ostenstad B, Lundqvist H, Blomqvist C (2004) HER2 expression in breast cancer primary tumours and corresponding metastases. Original data and literature review. Br J Cancer 90: 2344-2348.

13. Pegram M, Liao J (2012) Trastuzumab Treatment in Multiple Lines: Current Data and Future Directions. Clinical Breast Cancer 12: 10-18.

14. Spector NL, Blackwell KL (2009) Understanding the mechanisms behind trastuzumab therapy for human epidermal growth factor receptor 2-positive breast cancer. J Clin Oncol 27: 5838-5847.

15. Milenic DE, Wong KJ, Baidoo KE, Nayak TK, Regino CA, Garmestani K, Brechbiel MW (2010) Targeting HER2: a report on the in vitro and in vivo pre-clinical data supporting trastuzumab as a radioimmunoconjugate for clinical trials. MAbs 2: 550-564.

16. Rasaneh S, Rajabi H, Babaei MH, Daha FJ (2010) 177Lu labeling of Herceptin and preclinical validation as a new radiopharmaceutical for radioimmunotherapy of breast cancer. Nucl Med Biol 37: 949-955.

17. Abbas N, Heyerdahl H, Bruland O, Borrebaek J, Nesland J, Dahle J (2011) Experimental alpha-particle radioimmunotherapy of breast cancer using 227Th-labeled p-benzyl-DOTA-trastuzumab. EJNMMI Research 1: 18. 10.1186/2191-219X-1-18.

18. Heyerdahl H, Krogh C, Borrebaek J, Larsen A, Dahle J (2011) Treatment of HER2-expressing breast cancer and ovarian cancer cells with alpha particle-emitting 227Th-trastuzumab. Int J Radiat Oncol Biol Phys 79: 563-570.

19. Rasaneh S, Rajabi H, Babaei MH, Daha FJ, Salouti M (2009) Radiolabeling of trastuzumab with 177Lu via DOTA, a new radiopharmaceutical for radioimmunotherapy of breast cancer. Nucl Med Biol 36: 363-369.

20. Rasaneh S, Rajabi H, Hossein BM, Johari DF (2010) Toxicity of trastuzumab labeled 177Lu on MCF7 and SKBr3 cell lines. Appl Radiat Isot 68: 1964-1966.

21. Lindmo T, Bunn PA, Jr. (1986) Determination of the true immunoreactive fraction of monoclonal antibodies after radiolabeling. Methods Enzymol 121: 678-691.

22. Institute for Transuranium Elements KG (2000) Nuclide Explorer 2000, version 1.00 [computer program]. European Communities 2000.

23. Erwin WD, Groch MW, Macey DJ, DeNardo GL, DeNardo SJ, Shen S (1996) A radioimmunoimaging and MIRD dosimetry treatment planning program for radioimmunotherapy. Nucl Med Biol 23: 525-532.

24. Miller WH, Hartmann-Siantar C, Fisher D, Descalle MA, Daly T, Lehmann J, Lewis MR, Hoffman T, Smith J, Situ PD, Volkert WA (2005) Evaluation of beta-absorbed fractions in a mouse model for 90Y, 188Re, 166Ho, 149Pm, 64Cu, and 177Lu radionuclides. Cancer Biother Radiopharm 20: 436-449.

25. Persson M, Gedda L, Lundqvist H, Tolmachev V, Nordgren H, Malmstrom PU, Carlsson J (2007) [177Lu]pertuzumab: experimental therapy of HER-2-expressing xenografts. Cancer Res 67: 326-331.

26. Moore DM (2000) Heamtology of the Mouse (Mus musculus). In: Feldman BF, Zinkl JG, Jain NC, editors. Chalm's Veterinary Hematology. Philadelphia: Lippincott, Williams & Wilkins. pp. 1219-1224.

27. Seidl C, Zockler C, Beck R, Quintanilla-Martinez L, Bruchertseifer F, Senekowitsch-Schmidtke R (2011) 177Lu-immunotherapy of experimental peritoneal carcinomatosis shows comparable effectiveness to 213Bi-immunotherapy, but causes toxicity not observed with 213Bi. Eur J Nucl Med Mol Imaging 38: 312-322.

28. Dahle J, Bruland OS, Larsen RH (2008) Relative biologic effects of low-dose-rate alpha-emitting 227Th-rituximab and beta-emitting 90Y-tiuexetan-ibritumomab versus external beam X-radiation. Int J Radiat Oncol Biol Phys 72: 186-192.

29. Nilsson S, Larsen RH, Fossa SD, Balteskard L, Borch KW, Westlin JE, Salberg G, Bruland OS (2005) First clinical experience with alpha-emitting radium-223 in the treatment of skeletal metastases. Clin Cancer Res 11: 4451-4459.

30. Parker C, Heinrich D, O'Sullivan JM, Fossa S, Chodacki A, Demkow T, Cross A, Bolstad B, Garcia-Vargas J, Sartor O (2011) Overall Survival Benefit of Radium-223 Chloride (Alpharadin) in the Treatment of Patients with Symptomatic Bone Metastases in Castration-resistant Prostate Cancer (CRPC): a Phase III Randomized Trial (ALSYMPCA). European Journal of Cancer 47, Supplement 2: 3. doi: 10.1016/S0959-8049(11)70100-9.

31. Sartor O, Hoskin P, Bruland OS (2012) Targeted radio-nuclide therapy of skeletal metastases. Cancer Treat Rev .

32. Nilsson S, Franzen L, Parker C, Tyrrell C, Blom R, Tennvall J, Lennernas B, Petersson U, Johannessen DC, Sokal M, Pigott K, Yachnin J, Garkavij M, Strang P, Harmenberg J, Bolstad B, Bruland OS (2007) Bone-targeted radium-223 in symptomatic, hormone-refractory prostate cancer: a randomised, multicentre, placebo-controlled phase II study. Lancet Oncol 8: 587-594.

33. Abbas N, Bruland ØS, Brevik EM, Dahle J (9000) Preclinical evaluation of 227Th-labeled and 177Lu-labeled trastuzumab in mice with HER-2-positive ovarian cancer xenografts. Nuclear Medicine Communications Publish Ahead of Print.

Figure Legends

Figure 1. Absorbed radiation dose rates

Dose rates to blood, tumor and femur after injections of 400 kBq/kg ^{227}Th-trastuzumab (A) and 40 MBq/kg ^{177}Lu-trastuzumab (B). Error bars represent SD.

Data for ^{227}Th-trastuzumab has previously been published [17] except 1000 kBq/kg ^{227}Th-trastuzumab (accepted for publication in PLoS ONE).

Figure 2. Normalized average tumor volumes versus time after treatment

Normalized mean tumor size versus time after a single injection of saline (n = 23), 200 kBq/kg (n = 10), 400 kBq/kg (n = 11), 600 kBq/kg (n =12) and 1000 kBq/kg (n = 8) ^{227} Th-trastuzumab and 40 MBq/kg (n = 10) and 200 MBq/kg (n = 9) ^{177}Lu-trastuzumab.

Error bars represent SE. The tumor sizes were not removed from the calculation of mean tumor volume when the mice were killed. Data for ^{227}Th-trastuzumab therapy has previously been published [17] except 1000 kBq/kg ^{227}Th-trastuzumab (accepted for publication in PLoS ONE).

Figure 3. Survival of mice with tumor xenografts

Survival of mice after a single injection of saline (n = 23), 200 kBq/kg (n = 10), 400 kBq/kg (n = 11), 600 kBq/kg (n =12) and 1000 (n = 8) kBq/kg ^{227} Th-trastuzumab and 40 MBq/kg (n = 10) and 200 MBq/kg (n = 9) ^{177}Lu-trastuzumab. Median survival times of treated mice were compared using Kaplan Meier log-rank test.

Mice with tumor diameter greater than 20 mm were killed. Data for ^{227}Th-trastuzumab has previously been published [17] except 1000 kBq/kg ^{227}Th-trastuzumab (accepted for publication in PLoS ONE).

Figure 4. Treatment induced growth delay

Percent increase in number of days to reach a normalized tumor volume of 500 mm^3 (A) and 1000 mm^3 (B) for ^{227}Th-trastuzumab and ^{177}Lu-trastuzumab.

Data for ^{227}Th-trastuzumab therapy has previously been published [17] except 1000 kBq/kg ^{227}Th-trastuzumab (accepted for publication in PLoS ONE).

Figure 5. Bone marrow toxicity

Bone marrow toxicity assessment in the form of white blood cell (A) and platelet count (B) analysis as function of time after injection of NaCl, 200 kBq/kg, 400 kBq/kg, 600 kBq/kg and 1000 kBq/kg of ^{227}Th-trastuzumab and 40 MBq/kg and 200 MBq/kg of ^{177}Lu-trastuzumab. Error bars represent SD. Data for ^{227}Th-trastuzumab toxicity has previously been published [17] except 1000 kBq/kg ^{227}Th-trastuzumab (accepted for publication in PLoS ONE).

Tables

Table 1. Biodistribution of ^{227}Th-trastuzumab (% ID/g)

	1 h	6 h	24 h	3 days	4 days	7 days	14 days	21days
Blood	27 ± 3*	6 ± 13	5 ± 5	10 ± 4	3 ± 1	2 ± 1	1 ±1	1 ± 1
Lungs	8 ± 1	6 ± 5	2 ± 1	3 ± 2	1 ± 0	1 ± 0	1 ± 1	0 ± 0
Liver	8 ± 3	9 ± 6	8 ± 5	6 ± 1	7 ± 3	7 ± 6	5 ± 3	7 ± 2
Spleen	7 ± 4	5 ± 4	6 ± 7	4 ± 2	4 ± 2	2 ± 1	7±5	4 ± 1
Kidneys	7 ± 1	7 ± 4	5 ± 3	4 ± 1	2 ± 0	1 ± 1	2 ± 0	2 ± 1
S.int.	2 ± 0	1 ± 1	1 ± 1	1 ± 1	0 ± 0	0 ± 0	0 ± 0	0 ± 0
L.int.	1 ± 0	1 ± 1	2 ± 2	1 ± 0	0 ± 0	0 ± 0	0 ± 0	0 ± 0
Femur	5 ± 10	2 ± 2	3 ± 2	2 ± 1	1 ± 0	1 ± 0	3±2	4 ± 2
Skull	3 ± 1	3 ± 2	3 ± 2	2 ± 1	2 ±0	0 ± 0	3±2	4 ± 1
Tumor	4 ± 2	7 ± 5	14 ± 14	34 ± 25	24±14	17 ± 11	14±8	13 ±9

*: Data are presented as % of injected dose (mean ± SD)

Data for ^{227}Th-trastuzumab biodistribution (kBq/kg) has previously been presented in (Abbas et al. 2011).

Table 2. Biodistribution of ^{177}Lu-trastuzumab (% ID/g)

Time	1 h	6 h	24 h	4 days	7 days	14 days
Blood	25 ± 1*	19 ± 4	9 ± 5	6 ± 3	5 ± 2	1 ± 0
Lungs	6 ± 1	8 ± 3	4 ± 1	3 ± 1	2 ± 1	0 ± 0
Liver	9 ± 1	9 ± 2	12 ± 4	8 ± 2	7 ± 2	5 ± 2
Spleen	7 ± 0	5 ± 1	9 ± 6	6 ± 1	5 ± 2	3 ± 1
Kidneys	5 ± 0	5 ± 1	3 ± 1	3 ± 1	2 ± 0	1 ± 0
Sm.int.	2 ± 1	2 ± 0	2 ± 1	1 ± 0	1 ± 0	0 ± 0
Lg.int.	1 ± 0	2 ± 0	1 ± 0	1 ± 0	1 ± 0	0 ± 0
Femur	2 ± 0	2 ± 0	2 ± 0	1 ± 0	1 ± 0	1 ± 0
Skull	2 ± 0	2 ± 0	2 ± 1	2 ± 1	1 ± 1	0 ± 0
Tumor	4 ± 0	10 ± 4	21 ± 13	27 ± 15	40 ± 18	2 ± 4

*: Data are presented as % of injected dose (mean ± SD).

Table 3. Time for tumor to reach a volume of 500 mm^3 and 1000 mm^3 after treatment with ^{227}Th-trastuzumab and ^{177}Lu-trastuzumab

		Tumor Volume (500 mm^3)		Tumor Volume (1000 mm^3)	
Treatment	Dosage	Days	Growth Delay ¶	Days	Growth Delay¶
NaCl		15 ± 7	0 ± 10	24 ± 7	0 ± 10
^{227}Th-trastuzumab**	200 kBq/kg	19 ± 8	4 ± 11	33 ± 8	9 ± 11
^{227}Th-trastuzumab**	400 kBq/kg	38 ± 8	23 ± 10	70 ± 10	46 ± 11
^{227}Th-trastuzumab**	600 kBq/kg	60 ± 7	45 ± 7	81 ± 10	57 ± 10
^{227}Th-trastuzumab	1000 kBq/kg	53 ± 8	38 ± 8	Did not reach	> 170 ± 10*
^{177}Lu-trastuzumab	40 MBq/kg	16 ± 7	1 ± 8	24 ± 9	0 ± 9
^{177}Lu-trastuzumab	200 MBq/kg	89 ± 9	74 ± 9	Did not reach	> 90 ± 10*

¶: Growth delay in days to reach a mean tumor size of 500 mm^3 and 1000 mm^3 after i.v. administration of NaCl, ^{227}Th-trastuzumab and ^{177}Lu-trastuzumab compared to the control group injected NaCl.

*: Mice treated with ^{177}Lu-trastuzumab and ^{227}Th-trastuzumab did not reach the 1000 mm^3 after 90 and 170 days, respectively.

**: Data for ^{227}Th-trastuzumab has previously been presented in (Abbas et al.2011) except 1000 kBq/kg ^{227}Th-trastuzumab (accepted for publication in PLoS ONE).

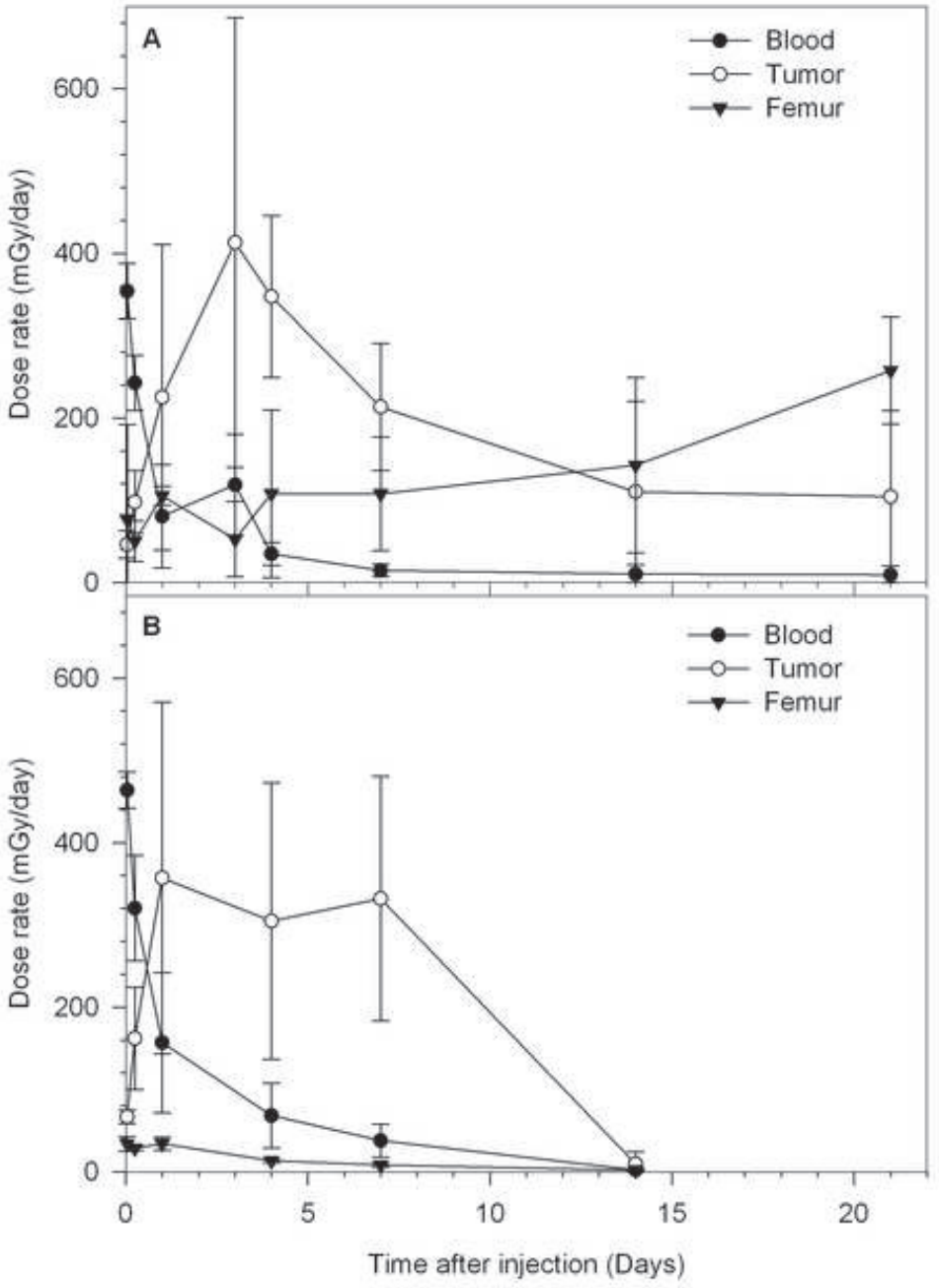
A
B
Blood
Tumor
Femur
Dose rate (mGy/day)
0
200
400
600
0
5
10
15
20
Time after injection (Days)

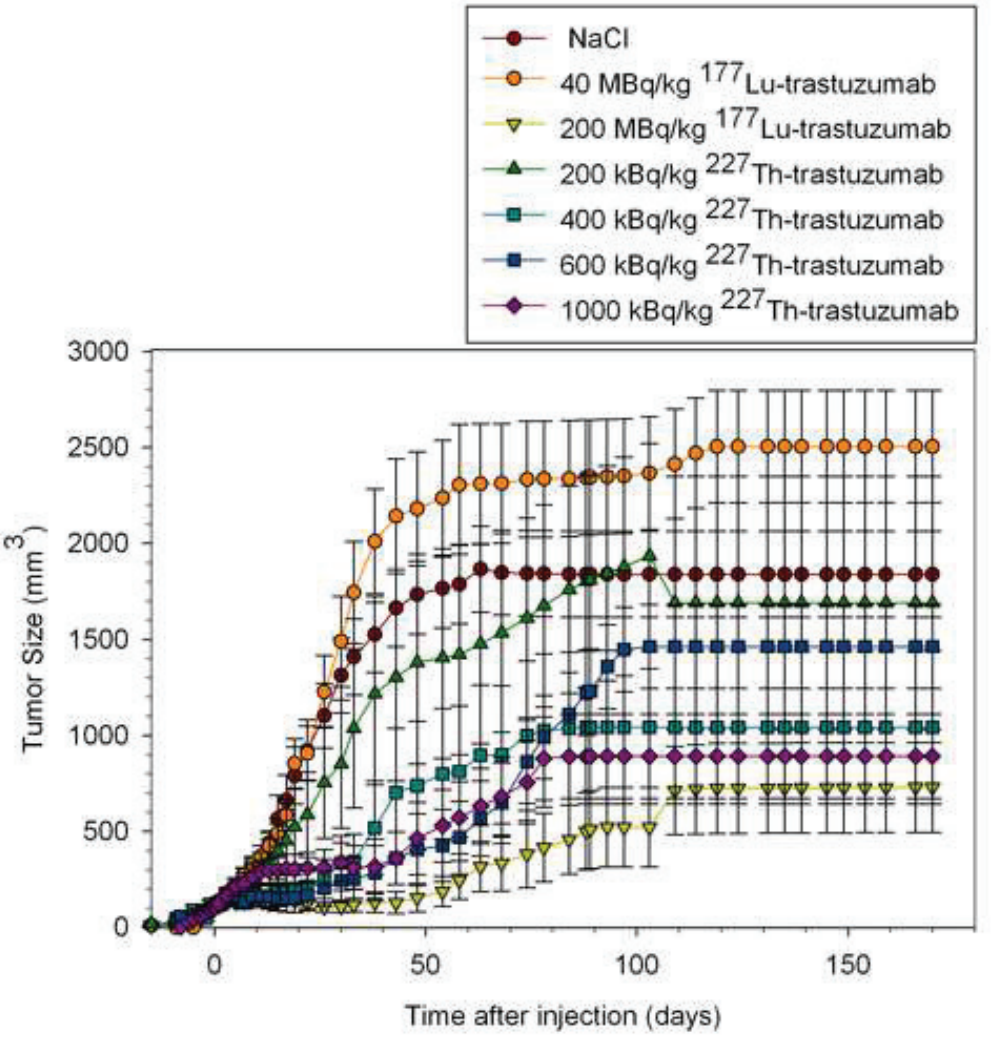
NaCl
40 MBq/kg 177Lu-trastuzumab
200 MBq/kg 177Lu-trastuzumab
200 kBq/kg 227Th-trastuzumab
400 kBq/kg 227Th-trastuzumab
600 kBq/kg 227Th-trastuzumab
1000 kBq/kg 227Th-trastuzumab
Tumor Size (mm3)
3000
2500
2000
1500
1000
500
0
0
50
100
150
Time after injection (days)

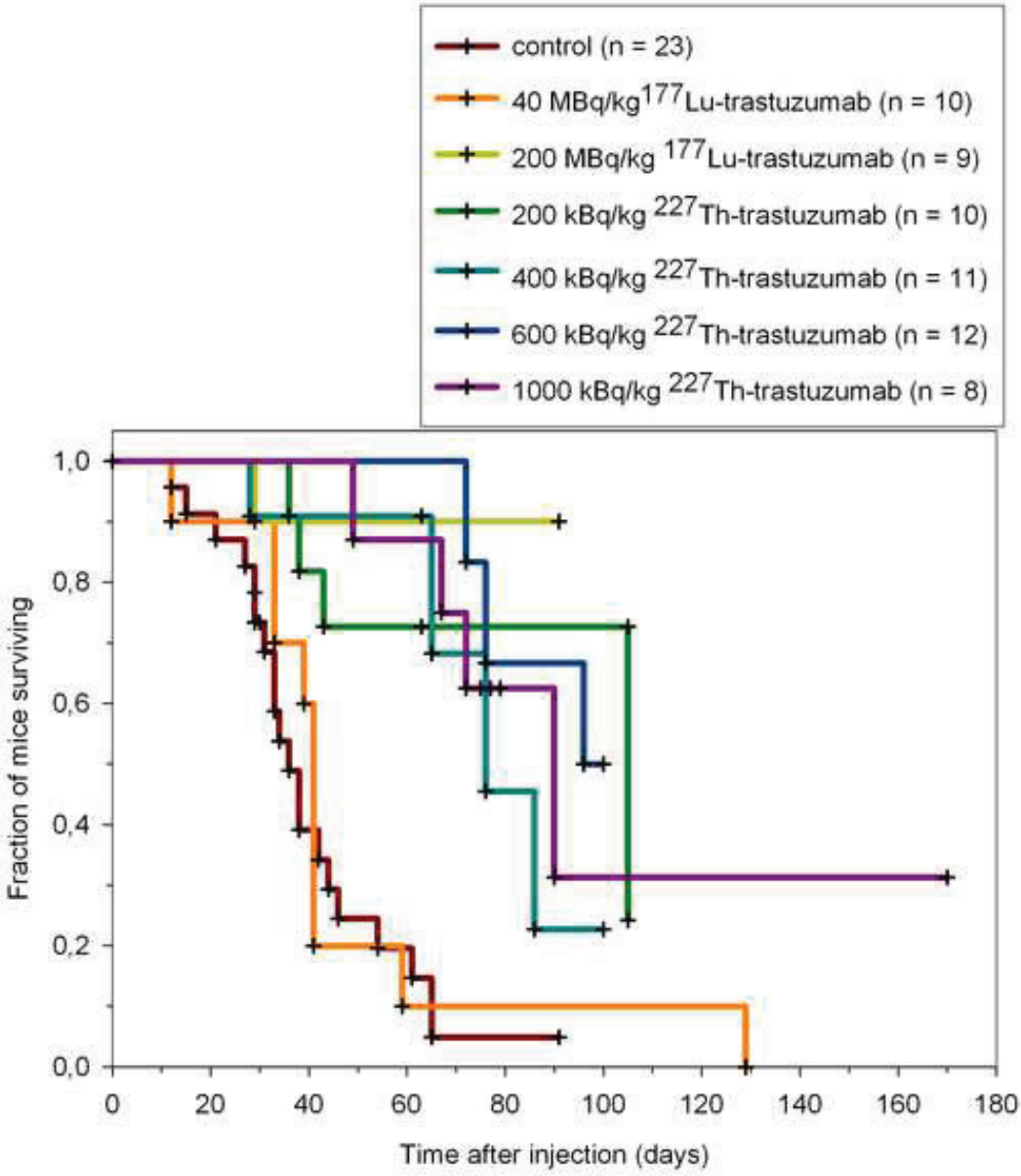
control (n = 23)
40 MBq/kg 177Lu-trastuzumab (n = 10)
200 MBq/kg 177Lu-trastuzumab (n = 9)
200 kBq/kg 227Th-trastuzumab (n = 10)
400 kBq/kg 227Th-trastuzumab (n = 11)
600 kBq/kg 227Th-trastuzumab (n = 12)
1000 kBq/kg 227Th-trastuzumab (n = 8)
Fraction of mice surviving
1,0
0,8
0,6
0,4
0,2
0,0
0
20
40
60
80
100
120
140
160
180
Time after injection (days)

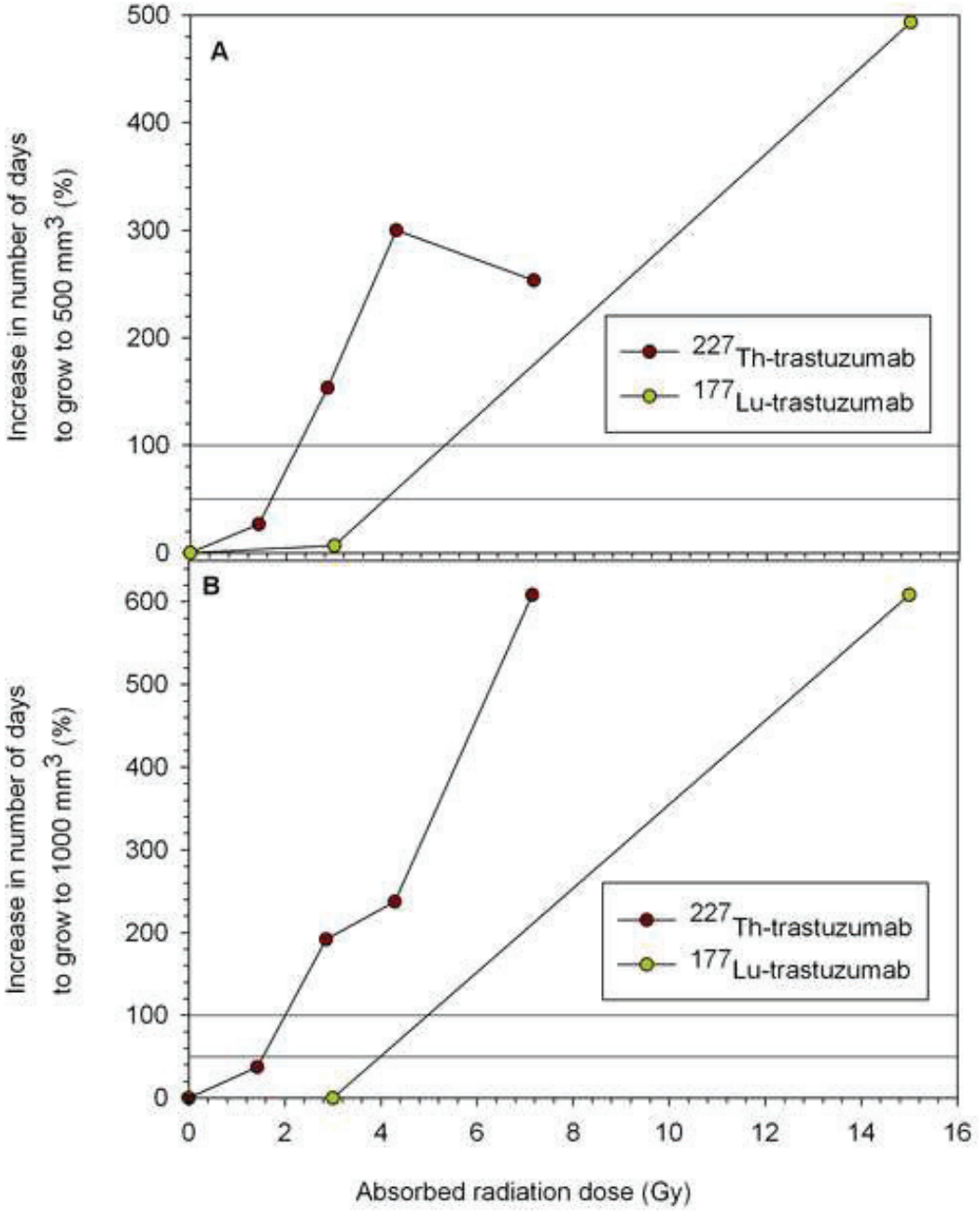
A
B
Increase in number of days to grow to 500 mm3 (%)
Increase in number of days to grow to 1000 mm3 (%)
227Th-trastuzumab
177Lu-trastuzumab
Absorbed radiation dose (Gy)
0
100
200
300
400
500
600
2
4
6
8
10
12
14
16

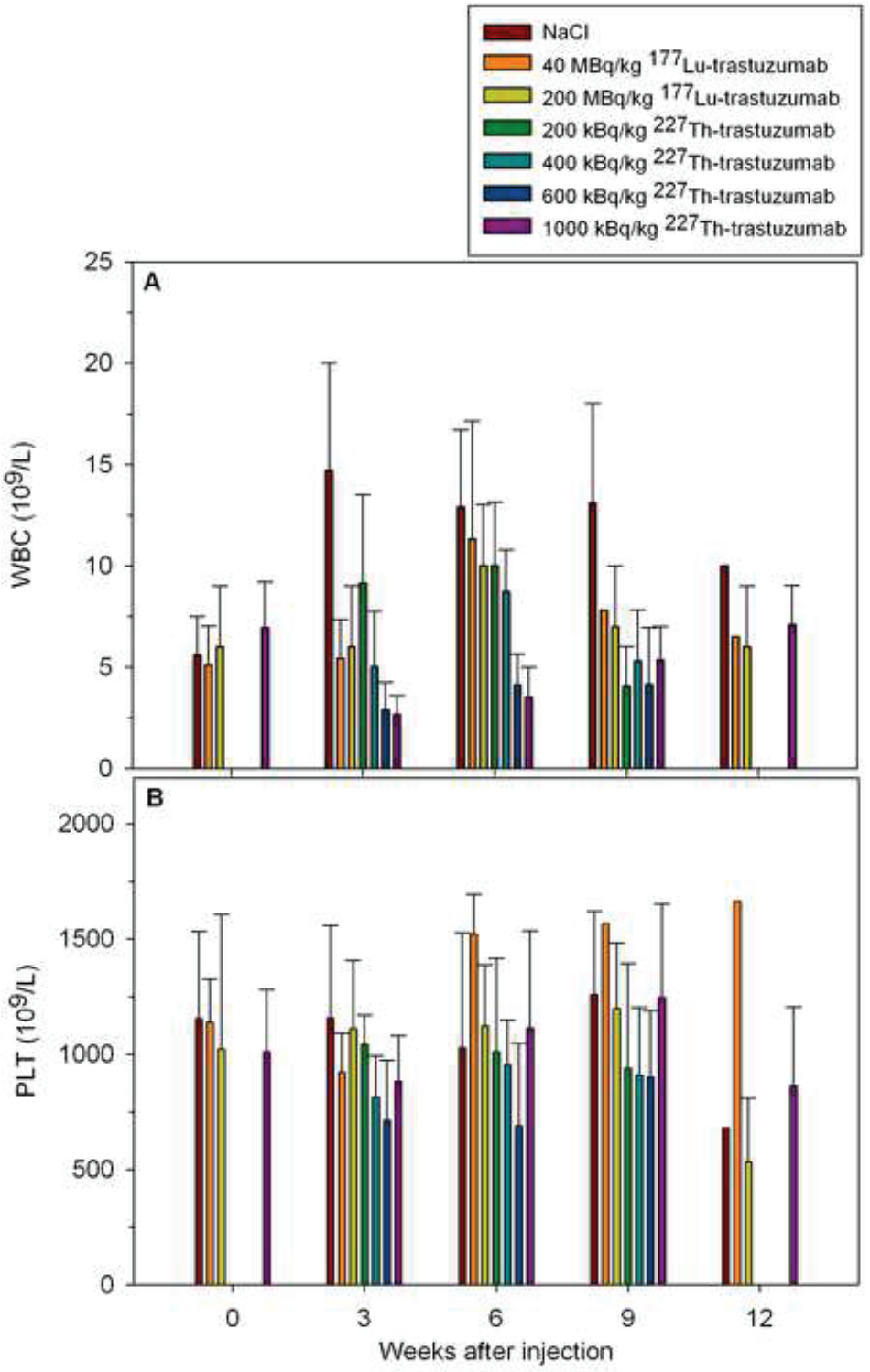
NaCl
40 MBq/kg 177Lu-trastuzumab
200 MBq/kg 177Lu-trastuzumab
200 kBq/kg 227Th-trastuzumab
400 kBq/kg 227Th-trastuzumab
600 kBq/kg 227Th-trastuzumab
1000 kBq/kg 227Th-trastuzumab
A
B
WBC (10^9/L)
PLT (10^9/L)
0
5
10
15
20
25
500
1000
1500
2000
0
3
6
9
12
Weeks after injection